The Role of Hypoxia-Regulated microRNA in Cancer

Thesis submitted by
Robert Iain McCormick
Brasenose College

For the degree of
Doctor of Philosophy
Department of Medical Oncology
Hilary Term 2011
University of Oxford

Supervisor: Professor Adrian L. Harris

Acknowledgements

I would like to thank all the institutions who provided the financial support to make this work possible. These include the Oxford Health Services Research Committee (OHSRC), The Royal College of Surgeons of England (RCSeng), the Urological Foundation (UF), and Urology Cancer Research and Education (UCARE).

I am grateful to David Cranston for his guidance in helping me to choose a research institution and supervisor, and the opportunities he opened for me.

The greatest thanks must go to my supervisor, Professor Adrian Harris. His knowledge, enthusiasm and advice have guided and inspired me during my time in his laboratory. I would also like to thank all the members of his lab, and the collaborators who worked on this project with us.

Abstract

MicroRNAs (miRNAs) are short, non-coding RNA sequences which regulate gene expression. Regulation is mediated primarily through binding to complementary sites in their un-translated regions which leads to mRNA degradation or translational repression. Hypoxia is a known feature of many tumours, and increased hypoxia is associated with poor prognosis. Hypoxia leads to the up-regulation of many genes involved in a variety of functions including angiogenesis, a shift to glycolytic metabolism, and cell proliferation. This is mediated by the heterodimeric transcription factor HIF (hypoxia inducible factor), which is stabilised in hypoxia. In normoxia, the von-Hippel Lindau protein (VHL) targets HIF for degradation. Mutation in the VHL gene, as is frequently seen in clear cell renal cell cancer (CCRCC), results in constitutive over-expression of HIF and its gene targets, leading to a pro-angiogenic and pro-tumourigenic state. This thesis examined the expression of hypoxia-regulated miRNAs in cancer. The principal aims were to determine gene targets of miR-210, and to explore the effects of its over-expression and knock-down, both *in vitro* and *in vivo*. The expression of hypoxia-regulated miRNAs was examined in clinical renal tumour samples with matched normal tissue controls, and correlated with VHL mutation status.

It was found that miR-210 targeted the iron sulphur cluster homologue (ISCU) gene, and was responsible for much of its down-regulation in hypoxia. Knock-down of ISCU had consequences on cell metabolism, in particular involving mitochondrial function and iron metabolism. miR-210 was found to be highly over-expressed in clear cell renal tumours (CCRCC), with greater expression seen in tumours with VHL mutations. miR-210 over-expression was also observed in papillary renal tumours, but to a lesser extent than in CCRCCs. miR-210 expression appeared to be correlated with reduced stage and grade, and improved survival. ISCU protein expression in CCRCCs was determined by immunohistochemistry, which showed that its expression correlated negatively with miR-210 expression, suggesting a functional role of miR-210 *in vivo*.

Submitted for the degree of D. Phil in Medical Oncology by:
Robert Iain McCormick
Brasenose College, University of Oxford
Hilary Term 2011

Supervisor: Professor Adrian L. Harris
Department of Medical Oncology
Weatherall Institute of Molecular Medicine,
John Radcliffe Hospital, Headington, OX3 9DS

List of Tables

Table	Legend	Page
1-1	The types of mutations found in different VHL disease types	18
2-1	Reagent for annealing oligonucleotides in Block-It protocol	40
2-2	Ligation reagents for Block-It protocol	41
2-3	Fugene6 protocol reagent ratios for transfection	42
2-4	PAGE resolving gel reagents	50
2-5	PAGE stacking gel reagents	50
2-6	IHC primary antibodies	52
2-7	cDNA synthesis for miRNA qRT-PCR	54
2-8	Run settings for miRNA cDNA synthesis	54
2-9	Pooled primer cDNA synthesis reagents for miRNA qRT-PCR	55
2-10	Run settings for pooled primer miRNA cDNA synthesis	55
2-11	qRT-PCR mastermix reagents for miRNA analysis	56
2-12	Run settings for miRNA qRT-PCR	56
2-13	cDNA synthesis for mRNA qRT-PCR	57
2-14	Run settings for cDNA synthesis for mRNA qRT-PCR	57
2-15	Mastermix for mRNA qRT-PCR	58
2-16	Run settings for mRNA qRT-PCR	59
3-1	The mRNA targets for miR-210 predicted by the PicTar algorithm	68
3-2	The mRNA targets for miR-210 predicted the TargetScan algorithm	69
3-3	Genes down-regulated in hypoxia ranked by the degree of rescue in expression by miR-210 knock-down	79
6-1	Distribution of histological subtypes and VHL mutations in 58 renal tumour samples	131
6-2	The frequence of different types of VHL mutations in the CCRCC tumours	132
6-3	miRNAs up- and down-regulated in the absence of VHL	146

List of figures

Figure	Legend	Page
1-1	The interaction of HIF-1 and the hallmarks of cancer	9
1-2	The structure of the HIF-1α and HIF-1β proteins	13
1-3	The regulation of PHDs and HIF	16
1-4	The pri-miRNA transcript is processed in the nucleus by the drosha-DGCR8 complex to a ~70 nucleotide pre-miRNA	25
2-1	Block-It vector diagram	43
2-2	pBabe vector diagram	44
3-1	The TargetScan algorithm finds complementary sequences in the UTRs to a miRNA, and scores the target based on conservation across species and the negative free energy of duplex binding	65
3-2	Effect of hypoxia on miR-210 expression in MCF7 and MDA-MB-231 cell lines.	67
3-3	Effect of anti-210 on miR-210 expression in MCF7 cells.	71
3-4	The effect of anti-210 on miR-21	72
3-5	Effect of anti-210 on interferon-responsive genes in normoxia	73
3-6	The effect of anti-210 on HIF, CA9, and PDK1 expression.	74
3-7	Effect of anti-210 on LDHA and B	75
3-8	MPTX1 was poorly expressed in MCF7 cells	76
3-9	The effect of hypoxia on NPTX1 expression	76
3-10	The response of ACVR1B to hypoxia and miR-210 knockdown	77
4-1	Structure of Iron-Sulphur clusters	84
4-2	MCF7 cells were transfected with anti-ctrl, anti-210 or mimic-210, and cultured in hypoxia for 48 hours	88
4-3	Immunoblot for ISCU, Tom20 and beta actin in MCF7 cells following incubation with mimic-210 or siISCU.	90
4-4	The effect of concentration of transfection reagents on ISCU expression	91
4-5	Rescue of ISCU expression in hypoxia with anti-210	92
4-6	The effect of miR-210 in ISCU on PC3 cells	93
4-7	The effect of miR-210 on ISCU in SCC25 cells	93
4-8	Effect of hypoxia and miR-210 on PEO1 cells	94
4-9	Effect of miR-210 on aconitase expression	96
4-10	Intracellular iron staining of HCCT116 cells transfected with with siISCU or mimic-210 in normoxia	98
4-11	The relationship of hypoxia and miR-210 with ISCU, and the physiological consequences to the cell	103
5-1	RNA absorbance in fractionated RNA	105
5-2	Constitutive over-expression of miR-210 in MCF7 and MDA-MB-231 cell lines using pBabe vectors	107
5-3	Effect of miR-210 over-expression on cell proliferation	108
5-4	Effect of miR-210 in MDA-231 cells in serum-free medium	109
5-5	Effect of miR-210 over-expression in MCF7 cells in serum-free medium	109
5-6	Xenograft experiments with MCF7 and MDA-231 cells	112
5-7	Expression of miR-210 in xenografts post sacrifice	113
5-8	Immunohistochemistry of paraffin-embedded sections of	115

	xenograft tumours	
5-9	miR-210 in serum of xenograft mice	116
5-10	Polysomal fractionation work-flow	117
5-11	miR-210 expression in input samples for fractionation	118
5-12	The UV absorbance graph for the sucrose gradients following ultracentrifugation	119
5-13	Beta actin expression in the polysomal fraction	120
6-1	HIF expression in VHL- and VHL+ RCC4 cells cultured in normoxia or 0.1%O_2	126
6-2	miR-210 expression in RCC4 cells in normoxia or 0.1% O_2 for 24 hours	127
6-3	miR-210 expression in VHL+ and VHL- 786-O cells cultured in normoxia or 0.1% O_2 for 24 hours	128
6-4	Expression of HIF-2 in VHL+ and VHL- 786-O cells with scr or siHIF-2 transfections, cultured in normoxia or 0.1% O_2 for 24 hours	129
6-5	Effect of siHIF-2α on miR-210 expression	129
6-6	Chip-seq data for 786-O cells	130
6-7	The distribution of histological subtypes in 58 renal tumour samples	131
6-8	The distribution of VHL mutations in the 43 CCRCC tumours	132
6-9	Frequency and location of VHL gene mutations	133
6-10	Graph showing expression of miR-210 in normal tissue and different renal tumour histological subtypes	134
6-11	Expression of miR-210 in normal tissue and CCRCCs	135
6-12	Correlation of VHL and miR-210 RNA expression	136
6-13	Combined data of CCRCCs from Fig. 12 and 30 additional tumours	137
6-14	CA9 expression in VHL mut-ve tumours v smut+ve tumours	138
6-15	CA9 expression vs miR-210 expression	139
6-16	miR-210 expression in low grade and high grade CCRCCs	140
6-17	miR-210 expression in early stage RCCs and late stage	140
6-18	miR-210 expression in CCRCCs and patient survival	141
6-19	Typical appearances of IHC staining for Ki67 on the CCRCC TMAs, showing PIS scores ranging from 2-24	142
6-20	Relationship of miR-210 expression to Ki67 expression determined by IHC in the CCRCC TMAs	143
6-21	Relationship of miR-210 expression to exonic location of the VHL mutations	144
6-22	Relationship of VHL mutation type to miR-210 expression	145
6-23	miR-148a expression in CCRCC and papillary tumours	147
6-24	miR-148a expression and tumour stage/grade	148
6-25	miR-2100 expression in CCRCCs and papillary tumours	149
6-26	miR-100 expression in CCRCCs and tumour stage/grade	150
6-27	Expression of miR-503 -193 and -424 in renal cortex and tumours	151
6-28	ISCU expression in CCRCC renal tumours and renal cortex measured by qRT-PCR	152
6-29	ISCU expression in low- and high-grade/stage tumours, measured by qRT-PCR	153

6-30	The histological appearances in normal renal cortex and CCRCC tumours of ISCU PIS scores 0-8	154
6-31	Mean PIS scores of ISCU in normal renal cortex and tumours in TMAs	155
6-32	Relationship of ISCU expression to miR-210 expression	156
6-33	ISCU expression in tumours with or without VHL mutations	157
6-34	ISCU PIS in CCRCCs and papillary tumours	157
6-35	Distribution of HIF-1 and HIF-2 staining in the CCRCC TMAs	158
6-36	Representative TMA scores stain for VHL by IHC with PIS scores form 0-300	159
6-37	VHL protein expression and miR-210 / CA9 expression	160
6-38	miR-210 expression and E2F3/GH2AX PIS	161
6-39	miR-210 expression pre- and post-nephrectomy	163

Contents

1. Introduction 6

1.1. Cancer 6

1.2. The hypoxic tumour microenvironment 8

1.3. The Hypoxia-Inducible Factors 10

1.4. Cellular oxygen sensing and control of HIF activity 13

1.5. The von Hippel Lindau Protein 16

1.5.1. Ubiquitin-mediated proteolysis 16

1.5.2. Von Hippel-Lindau syndrome 17

1.6. The consequences of HIF-α over-expression 18

1.7. HIF-independent roles of VHL 20

1.7.1. Extracellular matrix 20

1.7.2. E-cadherin and β-catenin 20

1.7.3. Transcription factor sequestration 21

1.8. microRNAs 22

1.8.1. Discovery of miRNAs 22

1.8.2. microRNA structure, processing and function 22

1.8.2.1. Translational regulation and mRNA degradation 26

1.8.2.2. Translational inhibition 27

1.8.2.3. mRNA degradation and P-bodies 28

1.8.2.4. Translational stimulation by miRNAs 30

1.8.3. microRNA in development and differentiation 30

1.8.4. microRNAs and cancer 32

1.8.4.1. microRNAs as tumour suppressors 33

1.8.4.2. microRNAs as oncogenes 34

1.9. Hypothesis and aims of this thesis 34

CHAPTER 2 36

Materials and methods 36

2.1 Cell culture and procedures 36

2.1.1 Cell lines 36

2.1.2 Cell passage 37

2.1.3 Cell counting 37

2.1.4 Cell freezing and storage 37

2.1.5 Exposure of cells to hypoxic conditions 38
2.2 Cell Transfection 38
2.2.1 Transient transfection of cells with microRNA mimics and inhibitors 38
2.2.2 Block-It shRNA system 39
2.2.3 Stable up-regulation of miR-210 in cancer cells 43
2.3 RNA extraction 44
2.3.1 RNA extraction from monolayer cell cultures 44
2.3.2 Extraction of purified microRNA for microarrays 45
2.3.3 Extraction of RNA and DNA from tissue samples 46
2.3.3.1Tissue homogenisation 46
2.3.3.2 RNA extraction 46
2.3.3.3 DNA extraction from tumour samples 46
2.4 Protein extraction, quantification, and expression analysis 47
2.4.1 Protein extraction from monolayer cultures 47
2.4.1 Western blotting (Polyacrylamide gel electrophoresis) 48
2.4.2 Immunohistochemistry on paraffin-embedded tissues 52
2.5 RNA expression analysis 53
2.5.1 Quantitative Real-Time PCR for *microRNA* 53
2.5.1.1 cDNA synthesis 53
2.5.1.2 Synthesis of cDNA using pooled primers 54
2.5.1.3 qRT-PCR 56
2.5.2 Quantitative Real-Time PCR for *messengerRNA* 57
2.5.2.1 cDNA synthesis 57
2.5.2.2 qRT-PCR 58
2.5.3 Microarray expression profiling 59
2.5.3.1 Hybridization, and labelling 59
2.6 Polysomal Fractionation 61
2.6.1 Preparation of sucrose gradients 61
2.6.2 Preparation of cell extract 62
2.6.3 Size Fractionation of RNA 62
2.7 Xenograft experiments 63
CHAPTER 3 – Results 64
Identifying hypoxia-regulated miRNAs and their targets in human cancer cell lines 64

3.1 Introduction 64
3.1.1 Microarrays as screening tools 64
3.1.2 miRNA target prediction 65
3.2 In vitro studies of miR-210 66
3.2.1 Identifying hypoxia-regulated miRNA 66
3.2.2 miR-210 is up-regulated in hypoxia in MCF7 and MDA-MB-231 cell lines 67
3.2.3 Computational prediction of miR-210 targets 68
3.2.3.1 *In silico* search 68
3.3 Investigating potential miR-210 targets using miRNA knockdown 70
3.3.1 Validation of antimiR-210 70
3.3.2 miR-210 inhibitors specifically knocked down miR-210 71
3.3.3 Anti-210 does not induce an interferon response 72
3.4 Searching for predicted targets using anti-miR-210 73
3.4.1 Anti-210 does not directly affect hypoxic HIF induction 73
3.4.2 Neuronal Pentraxin 1 75
3.4.3 Activin Receptor Type-1B 77
3.4.4 NDUFA4 and other investigated targets 77
3.5 Use of anti-210 to look for miR-210 targets with microarrays 78
3.7 Discussion 80
CHAPTER 4 - Results 84
ISCU target validation 84
4.1 Introduction 84
4.1.1 Iron Sulphur Clusters 84
4.1.2 Biological functions of iron-sulphur clusters 85
4.1.3 ISCU and the biogenesis of iron-sulphur clusters 85
4.1.4 Iron sulphur clusters in human disease 86
4.1.5 Rationale for selection of ISCU as a potential miR-210 target 86
4.2 ISCU is down-regulated by hypoxia and miR-210 87
4.2.1 miR-210 targets both cytosolic and mitochondrial ISCU 88
4.2.2 Knockdown of ISCU by miR-210 is dose-dependent 90
4.5 miR-210 down-regulates ISCU in multiple cell lines 92
4.5.1 anti-210 and mimic-210 in PC3 cell lines 92
4.5.2 anti-210 and mimic-210 in SCC25 cell lines 93

4.5.3 miR-210 knocks down ISCU in PEO1 cell lines 94
4.6 miR-210 inhibits ISCU mRNA expression 95
4.7 miR-210 over-expression reduces aconitase activity, but not protein expression 95
4.8 Iron studies 97
4.9 miR-210 increases free radical and lactate production in normoxia and hypoxia 98
4.10 Discussion 99
4.10.1 miR-210 and mitochondrial function 101
CHAPTER 5 – Results 104
Experiments using constitutive miR-210 over-expression 104
5.1 Introduction 104
5.1.1 Polysomal Fractionation 104
5.2 Generation of constitutively over-expressing miR-210 cells 106
5.3 The effect of miR-210 over-expression on proliferation in vitro 107
5.4 MCF7 and MDA-231 Xenograft Work 110
5.4.1 Experimental design 110
5.4.2 Tumour proliferation 111
5.4.3 Validation of miR-210 expression 113
5.4.4 Immunohistochemistry on formalin-fixed tumours 113
5.4.5 miR-210 in serum 115
5.5 Polysomal fractionation 116
5.5.1 Validation experiments 117
5.5.2 Microarray results 120
5.6 Discussion 121
CHAPTER 6 - Results 125
miRNA studies in clinical samples 125
6.1 Introduction 125
6.2 126
VHL regulation of miR-210 in renal cancer cell lines 126
6.2.1 miR-210 is up-regulated in RCC4 cell lines 126
6.2.2 miR-210 is up-regulated in 786-O cells lacking HIF-1α 127
6.2.3 HIF-2 regulates miR-210 in 786-O cells 128
6.3 VHL mutations in renal tumour samples 130

6.3.1 Sequencing of renal tumours for VHL mutations 131
6.4 miR-210 expression in renal tumours 133
6.4.1 miR-210 is up-regulated in renal tumours 133
6.4.2 Degree of miR-210 expression is associated with VHL mutation status 134
6.4.3 CA9 expression correlates with VHL mutation status and miR-210 expression in CCRCCs 137
6.4.4 miR-210 correlation with tumour grade and stage 139
6.4.5 141
miR-210 and survival 141
6.4.6 miR-210 expression correlates negatively with Ki-67 expression 142
6.4.7 miR-210 expression and mutation type and location 143
6.5 Expression of other VHL-regulated miRNAs in renal tumours 145
6.5.1 miR-148a is down-regulated in renal tumours 146
6.5.2 miR-100 is down-regulated in renal tumours 148
6.5.3 Expression of other miRNAs in renal tumours 150
6.6 ISCU mRNA expression in renal tumours 152
6.6.1 ISCU protein is down-regulated in tumours and correlates with VHL mutation status 153
6.7 Characterization of CCRCCs using IHC and tissue microarrays 158
6.7.1 VHL protein expression 159
6.7.2 TMA staining for E2F3 and GH2AX 160
6.8 miR-210 expression in the serum of patients pre- and post nephrectomy 162
6.9 Discussion 163
CHAPTER 7 172
Conclusions and future work 172
7.1 Conclusions 172
7.2 Future work 175
References 176

1. Introduction

1.1. Cancer

Cancer is common, affecting one in three people in their lives, and being the cause of death in one in six people. It is predominantly a disease of the elderly, with 74% of cancers arising in those over the age of 60.(*1*) Growth, maintenance and repair of tissue in the body relies on a delicate balance of cell growth and death, mediated by signalling systems leading to promotion of cell growth, inhibition of cell growth, or cell death. Certain tissues in the body, for example the skin and the intestine, have a very high turnover of cells, which are constantly shed and require replacing. In contrast, many tissues, such as the liver, are relatively stable and only replicate when necessary, for example following tissue damage. Still other tissues, such as muscle, have limited ability to undergo cell division, and enlarge primarily by hypertrophy.(*2*)

Cancer is the result of failure of cell cycle control, leading to excess cell proliferation and (usually) tumour formation. It is the disruption of genes which are instrumental in this control, which leads to cancer. Three broad categories of genes exist which have the potential to induce cancer when mutated: proto-oncogenes, tumour suppressor genes and caretaker genes. Proto-oncogenes usually promote cell division and growth. Mutations of proto-oncogenes can occur which cause them to exert excessive growth-promoting effects, either due to an over-active product or a high copy number of the gene being produced. An example of this is activation of the RAS oncogene, which promotes oncogenesis through two major signalling pathways: the Raf/MEK/ERK pathway(*3*) and the

PI3-kinase pathway.(*4*) This results in increased potential for cell proliferation, migration and invasion. Tumour suppressor genes are those with growth suppressing effects in the normal cell. An example is p53, which is a transcription factor whose targets include pro-apoptotic genes BAX, BID, PUMA and NOXA. Inactivating mutation of p53 therefore confers an anti-apoptotic, pro-proliferative state(*5*). The third category of genes important in tumorigenesis is the caretaker group of genes, which are responsible for maintaining the integrity of the genome. BRCA1 is one of the best-known examples of such a gene. It is mutated in 50% of inherited breast cancers, and loss of its function in DNA-break repair results in increased numbers of chromosomal aberrations, and increased sensitivity to DNA-damaging agents such as radiation. Mutation in BRCA1 or BRCA2 confers a significantly increased risk of breast and ovarian cancer in affected individuals.(*6*)

It is exposure of cells to carcinogens over their lifetime which leads to the onset of cancer through the induction of mutations in the DNA. Unrepaired mutations affecting the function of key regulatory proteins will increase the risk of cancer developing. However, cancer frequently results from an accumulation of mutations, rather than simply one. Knudson famously proposed his two hit hypothesis in 1971, stating that inactivating mutations in one allele of the RB gene in retinoblastoma must be followed by a second mutation in the remaining normal allele in order for retinoblastoma to occur. In those with a dominant inherited mutation of one allele of the RB gene, retinoblastoma was common due to the fact that only one mutation of the remaining allele was necessary to induce cancer, and these patients frequently suffer multifocal disease.(*7*) A well known model is that of the adenoma-carcinoma sequence, in which mutations in a number of genes cause progression from normal tissue, through to benign

polyps, and ultimately resulting in a malignant colorectal tumour. In this model, the first mutation occurs in the APC tumour suppressor gene, followed by the RAS oncogene. Two further mutations of the tumour suppressor TP53 results in a dysplastic polyp which, with further mutations or aberrations, results in a tumour with invasive and ultimately metastatic potential.(*8*)

In 2000, Robert Weinberg summarised the 'hallmarks of cancer' as cell populations exhibiting six key features. These are: the ability to evade apoptosis, self-sufficiency in growth signals, insensitivity to growth signals, sustained angiogenesis, limitless replicative potential, and the ability to invade tissues and metastasize.(*9*) (Fig. 1-1) These features will be covered in the context of hypoxia in the following sections of this introduction.

1.2. The hypoxic tumour microenvironment

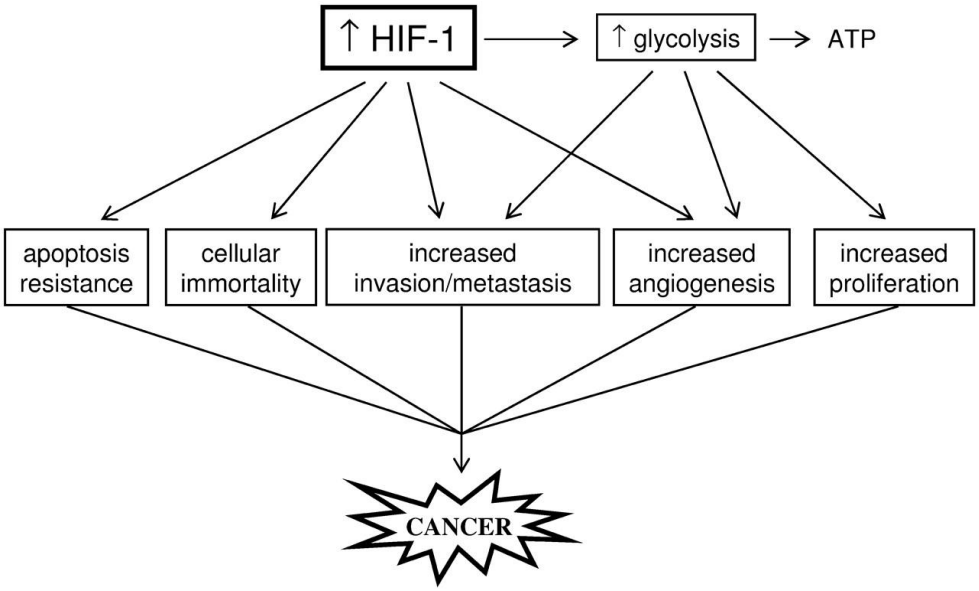


Figure 1-1. The interaction of HIF-1 and the hallmarks of cancer. (10)

The concentration of oxygen to which cells in the human body are exposed ranges from about 21% (which corresponds to a partial pressure of oxygen (pO_2) of about 150mmHg) to about 1% at the cortico-medullary junction in the kidney.(*11*) Solid tumours are characteristically hypoxic compared to most tissues, though the pattern of hypoxia is usually heterogeneous.(*12*) This was demonstrated in cervical and breast cancer using needle oxygen-sensing electrodes. Vaupel and colleagues showed that cervical cancers had mean and median pO2 values of 16 and 10mmHg respectively, compared with normal cervix with pO2s of 40 and 42mmHg respectively.(*13, 14*)

More hypoxic tumours have been shown to be more radio-resistant. Radiotherapy relies on molecular oxygen to create free radicals, and thus induce DNA damage. The dose required to achieve a given biological effect is 3 times higher in the absence of oxygen. Additionally, hypoxic cells are more likely to be in a quiescent state or in G1 of the cell cycle, during which they are relatively radio-resistant.(*15*)

Hypoxia-induced resistance has been described with agents such as cyclophosphamide, carboplatin and doxorubicin.(*16, 17*) This has been ascribed to hypoxic inhibition of cell proliferation, the decreased hypoxic cytotoxicity of some agents, and tissue acidosis. .(*16*) In addition, the delivery of cytotoxic agents (often due to poor vascular supply) to hypoxic regions, and thus cellular drug uptake, is poor.(*18*) In general, greater tumour hypoxia confers a worse prognosis. Hockel *et al* showed that tumour hypoxia in cervical cancer, defined as a median tumour pO2 <10mmHg, was a strong predictor of poor outcome in terms of overall and disease free survival in advanced cervical cancer. The poor

outcome was irrespective of treatment modality (radiotherapy or surgery).(*19*) Studies of HIF expression and hypoxia-regulated gene expression in breast cancer show a strong correlation with expression of these genes and poor prognosis.(*20, 21*)

The diffusion distance of oxygen is a crucial factor in tissue oxygenation, and is a limiting factor for tumour development. Typically, tumours are unable to grow to a diameter of greater than 1-2mm without developing additional vasculature, at which point their rate of proliferation will be balanced by the rate of cell death.(*22*) Tumour oxygenation is affected by a number of factors. The first is the availability of haemoglobin in the blood supply and its saturation with oxygen – a haemoglobin level of <8g/dL confers significantly more hypoxia to tumour cells.(*23*) Many tumour vessels do not carry blood cells; in particularly hypoxic arterioles, erythrocytes become stiff leading to increased blood viscosity and further reducing flow. The density, geometry and calibre of blood vessels are critical in tumour oxygenation. Tumour cells too distant from a blood vessel will become hypoxic, and shunt vessels can divert blood away from certain areas of the tumour. Tumours with low density, chaotically organised vasculature of small calibre will have greater hypoxia. It is important to note that tumour hypoxia is a dynamic, cycling process, caused by a variety of factors including vascular remodelling, compression of vessels by tumour growth, and angiogenic responses induced by hypoxia inducible factors.(*24*)

1.3. The Hypoxia-Inducible Factors

Cells undergo a number of significant proteomic and metabolic changes in response to hypoxia. A critical mediator of this response is the role of

transcription factors called the hypoxia inducible factors (HIF). HIF is a heterodimeric basic helix-loop-helix-PAS transcription factor consisting of a HIF-1α subunit bound to the aryl hydrocarbon receptor nuclear translocator (ARNT), also known as HIF-1β. The PAS domain is a protein region, about 130 residues in length, originally named after certain proteins it occurs in (**P**eriod, **A**RNT, **S**ingle-minded).(*25*) HIF-1α was discovered following research in to erythropoietin (EPO), whose expression at RNA level had been noted to increase dramatically after a 1 hour exposure to hypoxia.(*26*) Deletion of a DNA fragment of the 3' end and flanking region of the EPO gene was found to completely eliminate hypoxia responsiveness,(*27*) demonstrating typical features of a eukaryotic enhancer.(*28-30*) Further mutagenesis studies of the so-called hypoxia-inducing element, followed by electophoretic mobility shift assays, identified a bound nuclear factor which was termed hypoxia-inducible factor 1 (HIF-1).(*31*) Elimination of hypoxia-induced HIF-1 binding was noted in the presence of cyclohexamide, an inhibitor of protein synthesis, indicating that *de novo* synthesis of HIF-1 is required. Metabolic inhibitors of transcription (actinomycin D) and protein phosphorylation (2-aminopurine) also reduced HIF-1 binding, suggesting these processes are also required.(*32*)

HIF-1α protein is inversely correlated with oxygen concentration, and its expression increases dramatically between 6% O_2 and 0.5% O_2. In contrast, HIF-1β displays only a modest increase under hypoxic conditions, suggesting that the HIF-1α subunit concentration is the key mediator of transcription factor activity. The fact that HIF-1β expression appears constitutively higher than HIF-1α and that its expression is relatively stable under hypoxia, fits with its role as a subunit shared among other bHLH-PAS proteins.(*33*)

HIF-1 was cloned and found to be a heterodimer of two basic helix-loop-helix PAS proteins (alpha and beta). It was found that HIF-1β was identical to ARNT (aryl hydrocarbon receptor nuclear translocator), which is essential for the xenobiotic response of organisms to certain environmental hydrocarbons. The importance of the ARNT heterodimer was demonstrated in ARNT deficient cell clones (c4 murine hepatoma line), which failed to undergo increased HIF-1 DNA binding in the presence of elevated levels of HIF-1α.(*34*)

A bHLH-PAS protein was identified which had significant sequence homology to HIF-1α, and formed a functional heterodimer with ARNT. This molecule, originally called endothelial Pas-protein 1 (EPAS1), was later termed HIF-2α. HIF-2α was found to bind to hypoxia-responsive elements with similar sequence specificity to HIF-1α/ARNT, but its distribution within tissues was found to be different. Although most tissues in the body express both HIF-1α and HIF-2α mRNA, is enriched in endothelial cells and highly vascular organs.(*35*) A third HIF-α protein, HIF-3α, has also been described, but there is little data on this protein to date.

The HIF-α/HIF-β dimer binds to a DNA motif (R-CGTG), which is identical for both HIF-1α and HIF-2α. The HIF-α molecules contain two transactivation domains: the internal N-terminal activating domain (NAD) and the carboxy-terimnal activating domain (CAD). (Fig. 1-2) These regions are necessary for the activity of HIF as a transcription factor through recruitment of other proteins necessary for transcription initiation.(*36*)

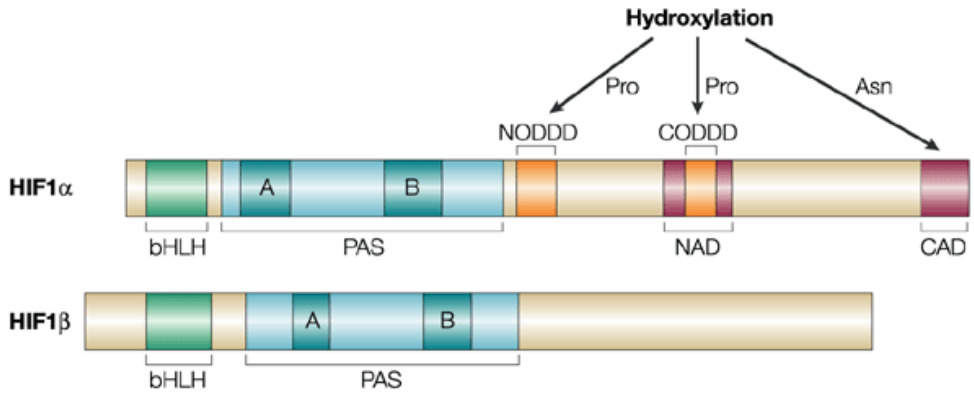


Figure 1-2. The structure of the HIF-1α and HIF-1β proteins. Both contain basic helix-loop-helix (bHLH) and PAS domains. The HIF-1α molecule can be hydroxylated at the amino-terminal oxygen-dependent degradation domain (NODDD) or the carboxy-terminal oxygen-dependent degradation domain (CODDD), by prolyl hydroxylases (Pro), resulting in binding to VHL. Hydroxylation of an asparigine (Asn) residue at the c-terminal end can also occur. The c- and n-terminal transactivating domains (CAD and NAD) are responsible for the transcription initiating activity of the HIF heterodimers by recruiting transcriptional coactivators to create an initiation complex. Schofield et al. (37)

1.4. Cellular oxygen sensing and control of HIF activity

When there is plentiful oxygen supply, HIF-α becomes hydroxylated at two highly conserved proline residues located near the NTAD region. This is mediated by members of the proline hydroxylase (PHD) group of proteins, which simultaneously convert one molecule of 2-oxoglutarate to succinate with the release of one molecule of carbon dioxide figure. Hydroxylation of the residues Pro 402 and Pro 564 creates a binding site for the tumour-suppressor protein, von Hippel Lindau (VHL), which is a ubiquitin ligase complex. Binding of HIF-α to VHL results in ubiquitination and subsequent rapid degradation of the HIF molecule within minutes. Another protein involved in HIF regulation is Factor Inhibiting HIF (FIH), which hydroxylates an asparigine residue (Asp 903) within the CTAD domain of HIF-α. This results in a conformational change, preventing the binding of HIF to the transcriptional activators p300/CBP, thus leading to the inactivation, rather than the destruction of HIF. FIH is active at lower

concentrations than the PHDs, and has a greater effect in inhibiting HIF-1α than HIF-2α. Thus, in conditions of moderate hypoxia, the effect (of these proteins at least), should be to inhibit predominantly HIF-1α without the destruction of the HIF-β molecules. The PHDs are known to exist in three isoforms, which have different predominance in different cell types. PHD2 is the most abundant enzyme of the three in normoxic conditions. PHD2 and 3 both show up-regulation in hypoxia in many cell lines. The apparent importance of PHD2 has been demonstrated in that siRNA to PHD2 resulted in over-expression of HIF target genes, whereas suppression of PHDs 1 and 3 did not. This could, however, perhaps be explained by the fact the PHD2 is in much greater abundance than the other two isoforms.(*38, 39*) Knockout mouse models of $PHD2^{-/-}$ showed embryonic lethality, whereas PHD1 and 3 knockouts did not.(*40*) Additionally, conditional knockout of PHD3 in mice resulted in polycythaemia, whereas knockout of PHD1 or 3 did not. A double knockout ($PHD1^{-/-}$ and $PHD3^{-/-}$) did result in polycythaemic mice, however.

The role of PHDs in regulating HIF expression appears to extend beyond the variable of cellular oxygen concentration alone. As previously mentioned, PHD expression itself can vary, and often with hypoxia. Additional mechanisms of PHD expression exist – for example, PHD1 expression has been reported to be induced by oestrogens.(*41*) Higher constitutive expression of PHDs would confer a lower constitutive level of HIF, and vice versa. The PHDs also require ferrous iron, ascorbate (*42*) and 2-oxoglutarate to catalyse their reaction, and thus the availability of these substrates will affect HIF degradation. This explains why HIF expression is sensitive to iron chelators – removal of available iron results in reduced PHD activity and accumulation of HIF. Addition of iron results in accumulation of HIF, but only in the presence of an intact PHD system and an

intact VHL-ubiquitination pathway. It has been observed that fumarate and succinate inhibit hydroxylase activity, perhaps due to the increase of these molecules affecting flux through the Citric Acid Cycle, of which they are substrates downstream of 2-oxoglutarate.(*43*)

It has been demonstrated that increased levels of reactive oxygen species (ROS) can result in the accumulation of non-hydroxylated HIF-α. This suggests that increased ROS leads to inhibition of the PHDs, thus preventing recognition by VHL and subsequent ubiquitination and degradation. It is not certain what the source of the ROS is, but it could be the result of reduced mitochondrial oxygen use.(*44*) Nitric oxide (NO) may also play a role in HIF regulation. It has been shown to reduce PHD activity in normoxia, but paradoxically prevents the stabilization of HIF-α in hypoxia. It has been postulated that this is due to NO binding to and inactivating cytochrome c in the mitochondria, resulting in reduced oxygen consumption by the organelle.(*45*)

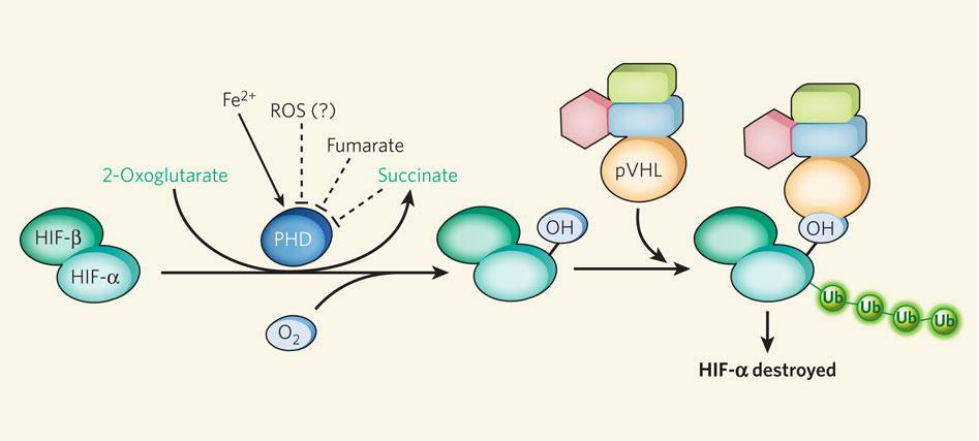


Figure 1-3. The regulation of PHDs and HIF. In normoxia, HIF-α subunits are hydroxylated by PHD enzymes and bind to VHL, resulting in ubiquitination and eventual proteasomal degradation. Iron increases PHD activity, whereas ROS, fumarate and succinate inhibit PHD activity, promoting HIF-α stabilisation. Kaelin et al (46)

In summary, HIF activity is controlled by the activity of PHD through the availability of oxygen, iron and substrates of the Citric acid cycle. Expression of the PHD proteins is also a factor in HIF degradation, and this is subject to further levels of control.

1.5. The von Hippel Lindau Protein

The von Hippel Lindau gene (VHL) encodes a 213 amino acid protein which forms the substrate-recognition unit of a ubitquitin ligase complex. It has two major structural domains – the larger β-domain contains a discrete binding-pocket which forms hydrogen bonds with hydroxylated (but not non-hydroxylated), HIF-α.(*47, 48*) The smaller α-domain binds to Elongin C and Elongin B, a heterotrimeric structure known as the VCB complex which is resistant to proteasomal degradation.(*49*) The VCB complex binds to CUL2 which, along with NEDD8, RBX1, and E2, form the active E3 ubiquitin ligase complex. Reviewed in (*50*). In the presence of oxygen, HIF-α is hydroxylated by PHD enzymes and binds to the VHL component of this complex. This results in the attachment of multiple ubiquitin molecules, which target it for rapid proteasomal degradation.

1.5.1. Ubiquitin-mediated proteolysis

Proteasomal degradation is a regulatory system controlling the amount of a variety of proteins within cells. This process is thought to have roles in cell-cycle progress, signal transduction, transpcriptional regulation, receptor down-regulation and endocytosis. Examples of proteins regulated in this fashion include IκBα, β-catenin and p53. During this process, ubiquitin is first activated by ATP to form a high energy thiol ester intermediate with an E1 ubiquitin-activating enzyme. The Ubiquitin molecule is then transferred to the active site of a

ubiquitin-conjugating enzyme E2.(*51*) In the case of HIF-α ubiquitination, the VCB complex acts as the E3 substrate-recognition module.(*50*) On binding of the substrate to E3, E2 transfers ubiquitin to a lysine residue in the targeted substrate forming a covalent bond. Polyubiquitinated proteins are recognised and subsequently degraded by the 26s proteasome.(*51*)

1.5.2. Von Hippel-Lindau syndrome

The importance of the VHL tumour suppressor protein can be appreciated in patients suffering with VHL syndrome. This is a rare, dominantly-inherited syndrome caused by inherited mutations of the VHL gene and occurs in 1:36000 individuals.(*52*) Mutation or loss of the remaining normal allele can result in tumour formation. Depending on the type of VHL mutation, sufferers may develop clear cell renal cell cancer, phaeochromocytomas, retinal or central nervous system haemangioblastomas, amongst other tumours types and sites of disease. The syndrome has near 100% penetrance, with a mean onset of disease occurring at 26 years of age.(*50*) Several types of VHL disease have been characterised, based on mutation types, and are given in Table 1-1.

The consequences of VHL inactivation can be explained by the de-repression of HIF-α, as described above, in addition the dysregulated HIF- and hypoxia-independent functions of VHL as described in the next section.

VHL disease type	Tumour types occurring			Commonly associated VHL germline mutations
	HB	RCC	Phaeo	
Type 1	+	+	-	Deletions and truncations
Type 2A	+	-	+	Missense Tyr98His and Tyr112His
Type 2B	+	+	+	Missense
Type 2C	-	-	+	Missense Leu188Val, Val84Leu, Ser80Leu

Table 1-1. The types of mutations found in different VHL disease types, and the tumour types that characterise them. Abbreviations: Hb – hameangioblastoma; RCC – renal cell cancer; Phaeo – Phaeochromocytoma. (50)

1.6. The consequences of HIF-α over-expression

Tumours are often hypoxic, and the degree of hypoxia correlates positively with increased HIF-α expression negatively with prognosis. There is increasing evidence that HIF over-expression is a contributory factor in the pathogenesis of cancers, as opposed to simply a marker caused by aggressive tumours outgrowing their blood supplies and leading to increased intratumoural hypoxia.(*53*) HIF-1α has been implicated in the Warburg effect, whereby tumours demonstrate a shift towards anaerobic glycolysis instead of oxidative phosphorylation. Transcription targets of HIF-1 such as lactate dehydrogense A (LDHA), Hexokinase 2 (HK2), pyruvate kinase M2 (PKM2), and pyruvate dehydrogenase kinase 1 (PDK1) are involved in this process. PDK1 deactivates pyruvate dehydrogenase, which converts pyruvate to acetyl co-A which is the key substrate in the citric acid cycle

– the driving force for oxidative phosphorylation. This forces the cell to generate energy by the conversion of pyruvate to lactate, which is facilitated by increased levels of LDHA. Increased levels of Carbonic Anhydrase 9 (CA9) may help to protect the cell from the increased production of acidic lactate, while increased expression of Glucose transporter 1 (GLUT1) facilitates entry of more glucose in to the cell.(*54*)

Many HIF targets have now been described. One of the most studied is Vascular Endothelial Growth Factor (VEGF), which has an important role in angiogenesis. Targets such as platelet derived growth factor (PDGF), Transforming Growth Factor-α or β (TGFα/β) are pro-proliferative, matrix metalloproteinase 1 (MMP1) facilitate invasion of tumours in to the extracellular space.(*55*) HIF-2α, although very similar in structure to HIF-1α, is now known to have distinct targets. For example erythropoietin (EPO), which promotes the formation of red blood cells in the marrow (erythropoiesis), is known to be a HIF-2 target. Additionally, evidence is emerging that the pattern of HIF-1 vs HIF-2 expression in tumours is important. For example, it has been shown that over-expression of HIF-2α, but not HIF-1α, is sufficient to override the tumour suppressor function of VHL in xenograft studies.(*56*) Gordan *et el* found that pVHL-deficient clear cell renal cell carcinomas expressing only HIF-2α displaced enhanced transcriptional activity of the c-Myc oncoprotein, whereas tumours expressing HIF-1 appear to inhibit Myc. Although HIF-2 does not regulate glycolytic gene expression as above, it is known to increase expression of the stem cell factor Oct-4. It also promotes proliferation by increasing c-Myc activity, resulting in increased activity of cyclin D2 and E2F1, along with repression of the pro-apoptotic p21 and p27.(*57*)

1.7. HIF-independent roles of VHL

1.7.1. Extracellular matrix

Although HIF degradation is the most well-known example of VHL function, several other proteins are known to bind to VHL, suggesting a role for VHL in other molecular mechanisms. Fibronectin is a crucial component of the extracellular matrix, and has many roles, including cell adhesion and differentiation. Altered fibronectin expression or function has been implicated in oncogenesis.(*58*) Ohh *et al* found that fibronectin co-immunoprecipitated with VHL, and that $VHL^{-/-}$ mouse embryos exhibited failure of assembly of normal extracellular fibronectin matrix, in contrast to the $VHL^{+/+}$ embryos, which were normal. There were similar findings in $VHL^{-/-}$ renal cell tumours which showed loss of fibronectin matrix assembly in comparison to the tumours with intact VHL. They found that VHL co-immunoprecipitated with fibronectin, and physically interacts with fibronectin in intact cells.(*52*) Mutations in the VHL gene appear to universally impair its binding to fibronectin.(*59*) It has been shown that altered fibronectin matrix construction in VHL mutants is independent of HIF-1,(*60*) and that impaired fibronectin assembly occurs even in VHL mutants with preserved HIF-1 regulation activity.(*61*) The above evidence points to an important role for VHL in roles other than HIF regulation alone. Grosfeld *et al* showed that VHL binds to hydroxylated fibrillar collagen IV, but not folded collagen triple helix, providing further evidence of the role of VHL in normal extracellular matrix modelling.(*62*)

1.7.2. E-cadherin and β-catenin

Epithelial cells organised in a polarized fashion rely on intercellular junctions to maintain their structure. A key component of these junctions is E-cadherin whose

expression is associated with normal differentiation of mesenchymal cells in to tubular epithelial cells in the adult nephron. Loss of E-cadherin expression is associated with epithelial to mesenchymal transition and increased oncogenic potential.(*63*) It has been shown that loss of E-cadherin occurs due to HIF-α up-regulation as a result of VHL inactivation or loss, although there are conflicting reports as to whether this is a HIF-1α exclusive mechanism, or one dependent on both HIF-1 and 2.(*64, 65*) Loss of E-cadherin may have implications in the Wnt signalling system, due to dissociation of β-catenin from the cadherin-catenin complex. Increased free catenin would be able to bind to T-cell factor and translocate to the nucleus, resulting in increased transcription of pro-proliferative genes. (*66*) Dysregulated β-catenin has been associated with defective primary cilia function and the development of cystic kidney disease.(*67*)

1.7.3. Transcription factor sequestration

VHL has been shown to bind the transcriptional activator Specificity Protein 1 (SP1), likely resulting in a sequestration of SP1 from the nucleus. This negative regulation of SP1 activity has been proposed as a direct means by which VHL down-regulates VEGF.(*68*) Down-regulation of SP1-mediated transcription by VHL has also been proposed as a mechanism for the up-regulation of insulin-like growth factor 1-receptor (IGFR1) in cancer. IGFR1 is frequently over-expressed in cancer, mediating cell proliferation, transformation and protection from apoptosis.(*69*)

1.8. microRNAs

1.8.1. Discovery of miRNAs

microRNAs were first discovered in 1993, in the work Caenorhabidititis elegans. Expression of a 22-nucleotide molecule, lin-4, with antisense complementarity to the 3'untransated region of the lin-14 gene, was found to be necessary for progression of worms from the first to second larval stages.(*70, 71*). Another small RNA molecule, let-7, with critical function in larval development was later discovered. Mutations of this gene were associated with heterochronic developmental defects, due to the dysregulation of the lin-41 gene. Genetic analysis revealed that let-7 was an untranslated RNA, which was complementary to part of the 3'untranslated region of the lin-41 gene. It was proposed lin-4 and let-7 were negatively regulating the lin-4 and lin-41 genes respectively by inhibition of translation mechanism.(*72*)

1.8.2. microRNA structure, processing and function

miRNAs are a family of small, single stranded non-protein-coding RNA sequences of 18-25 nucleotides in length. They are transcribed as long primary transcripts (pri-miRNA) containing a local hairpin structure. They are embedded in either independent non-coding RNAs or in the introns of protein-coding genes. Some miRNAs, such as the miR-17 family, are clustered in polycistronic transcripts to allow coordinated expression(*73*). Since the discovery of lin-4 and let-7, the list of known miRNAs has grown to many hundreds, with more predicted to exist.(*74*)

Transcription of the pri-miRNA is carried out by RNA polymerase II or RNA polymerase III. The generation of a poly-A tail and cap structures in many miRNAs

are hallmarks of polymerase II activity, suggesting that it is the predominant enzyme in their transcription. Treatment with the polymerase II inhibitor α-amanitin reduces their transcription.(*75*) However, other miRNAs, including those within the largest known human cluster, C19MC, are believed to be transcribed by polymerase III.(*76*)

Pri-miRNA is processed in the nucleus by the RNAse III enzyme, Drosha (RNASEN) associated with the DGCR8 (DiGeorge critical region 8, also known as PASHA) protein. (*77*) The average pri-miRNA contains a 33 base-pair hairpin stem, a terminal loop and two singled-stranded flanking regions up- and downstream of the hairpin. The flanking regions and the double stranded stem are critical for binding of the structure to the RNA-binding domains of DGCR8, and subsequent cleavage by Drosha. The loop region appears to be less critical. (*78-80*) Drosha contains two RNAase domains which cleave the pri-miRNA at the 5' and 3' ends, with the DGCR8 providing stability to the complex, and acting as a molecular ruler to ensure the cleavage occurs at precisely the right site. The cleavage occurs 11 base pairs from the single stranded RNA/double stranded RNA junction at the base of the hairpin stem.(*78, 81*)

Cleavage by Drosha results in a pre-miRNA molecule about 70 nucleotides in length, and moves to the cytoplasm assisted by the nuclear export factor Exportin 5/RAN GTP complex. Knockdown of Exportin 5(XPO5) results in a reduced expression of mature miRNAs, but not an accumulation of pre-miRNA in the nucleus. This suggests that it is involved in the stability of the molecule, in addition to its transport to the cytoplasm.(*82, 83*)

Maturation and activity of miRNA is carried out in the cytoplasm by RISC (RNA-induced silencing complex) loading complex (RLC), consisting of Dicer, TRBP (Tar

RNA binding protein), PACT (protein activator of PKR) and Argonaute-2 (Ago2). Following assembly of the complex, the pre-miRNA binds to it and the RNASE III Dicer cleaves off the loop to leave an approximately 22-nucleotoide double-stranded miRNA molecule. Crucially, the double stranded molecule contains a 2-nucleotide overhang at each 3' end, which is essential for further miRNA processing.(*84*) Dicer and the other cofactors TRBP or PACT now dissociate from the complex, leaving only Ago2 and the miRNA duplex. The duplex now needs to be separated so that one strand (the guide strand) remains bound to Ago2, and the other strand (the passenger strand) is removed and degraded. This may be facilitated by helicases, though it is possible that this process is mediated by Ago2 itself. The strand of the duplex that eventually acts as the guide strand is that which has the least stable base pair at its 5' end.(*85*) The mature miRNA/RISC complex is now assembled and ready to bind to complementary RNA sequences and induce translational repression or mRNA degradation. (Fig. 1-4)

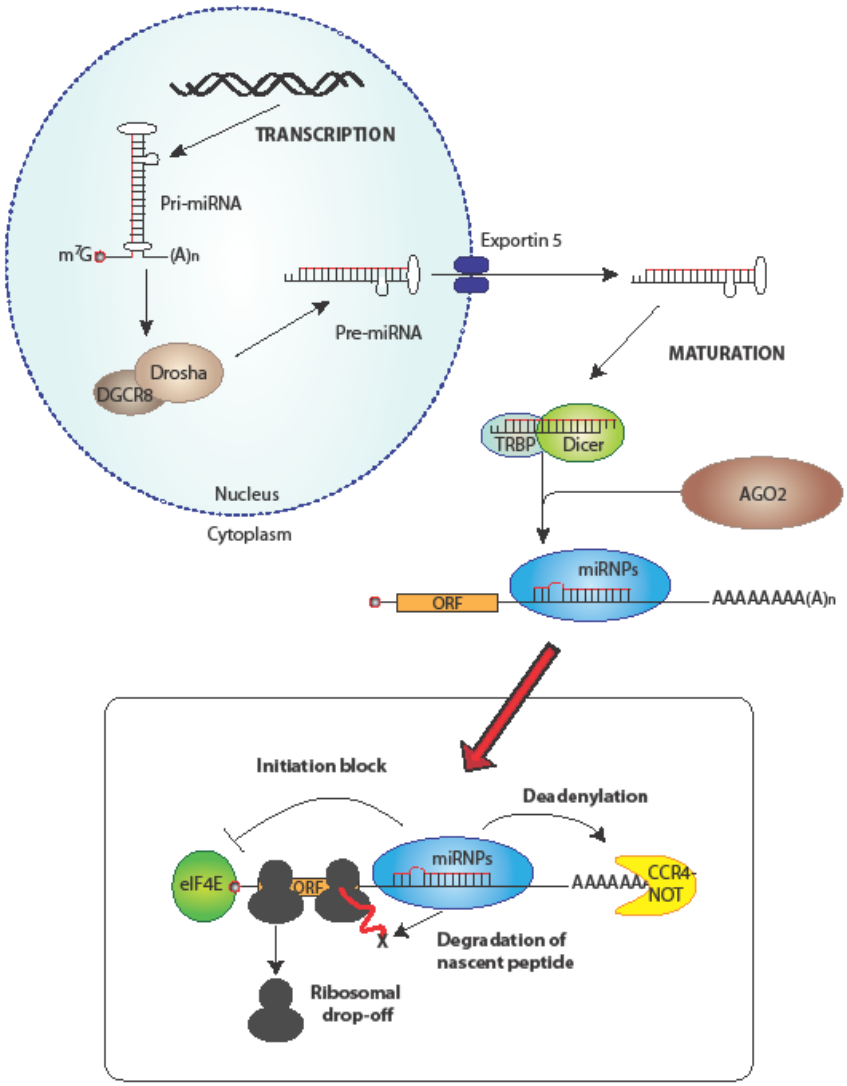


Figure 1-4. The pri-miRNA transcript is processed in the nucleus by the Drosha/DGCR8 complex to a ~70 nucleotide pre-miRNA. It is exported in to the cytoplasm by Exportin 5, where it is further cleaved by Dicer/TRBP. One strand of the double-stranded RNA molecule becomes associated with the Ago2/miRNP complex, acting as a guide strand. Binding of the miRNP to a complementary region on the target mRNA leads to inhibition of translation or degradation of the mRNA molecule.

1.8.2.1. Translational regulation and mRNA degradation

The mature miRNA/RISC complex acts as a regulator of gene translation through binding to complementary sites in the 3'untranslated regions of mRNAs. If the complementarity is perfect, the binding of the miRNA to the mRNA results in cleavage and degradation of the mRNA molecule. This mechanism is thought to be more prevalent in plants, and in animals the degree of complementarity is usually imperfect.

Efficient binding and silencing activity of a miRNA requires exact binding of positions 2-7 of the miRNA, known as the seed region, to the complementary sequence on the target mRNA molecule. Perfectly matched complementary binding of the seed region alone, however, does not accurately predict target repression. Positions 12-17, towards the 3' end of the miRNA, are often highly conserved, and may be important in determining specific target interaction. Additionally, the sequences surrounding the miRNA-responsive element could affect miRNA binding or silencing efficacy (*86-88*). Despite years of refinements to computational target prediction algorithms, it is still an inexact science, and with significant variability in predicted targets between different algorithms. This fact is perhaps reflected in our limited understanding of the mechanism in which miRNAs and their associated protein complex (together known as the microribonucleoprotein complex, or miRNP) lead to gene silencing. Pioneering studies in *c. elegans* demonstrated that lin-4 inhibited lin-14 protein expression, while mRNA levels remained relatively constant, suggesting a post-transcriptional mechanism of repression. They found that the lin-14 3'UTR was necessary and sufficient to enable repression of the lin-14 protein (*70*). Since the first studies of miRNAs, increasing evidence has emerged pointing to the role of these molecules in both translational repression *and* mRNA degradation.

1.8.2.2. Translational inhibition

Theories on translational inhibition can broadly be categorised into those describing blocking of translation *initiation,* and those describing repression of translation *post*-initiation. Before describing these theories, a brief description of the steps of mRNA translation, namely initiation, elongation, and termination, is merited. Initiation occurs with binding of eIF4E, a subunit of the eukaryotic translation initiation factor (eIF) eIF4F, to the 5' mRNA cap structure (m^7GpppN). eIF4G, another component of the eIF4F complex, binds to the poly-A tail binding protein (PABP1), forming a circular mRNA structure. eIF4G simultaneously binds eIF3 to facilitate assembly of the ribosome complex. The participation of at least 10 initiation factors is required to instigate protein translation. Following the assembly of the 40S and 60S ribosomal subunits at an initiation codon (AUG), translation and polypeptide elongation continues until a termination codon is encountered. This results in disassembly of the translational machinery. The circularisation of the mRNA is thought to aid in reassembly of the translational machinery at the 5' end of the molecule, in readiness to begin the synthesis of another polypeptide molecule (*89*).

Investigations demonstrating that miRNA-mediated repression occurs exclusively in mRNAs with a m^7G cap structure, but not internal ribosomal entry sites (IRES), suggested that repression is occurring at the initiation step (*90*). In support of this were studies using polysome gradients. It was shown that miRNA-repressed mRNAs sedimented closer to the top of the gradient, indicating reduced ribosomal binding (*90*). However, another group subsequently demonstrated cap-independent miRNA repression, and suggested that ribosomal drop-off was a more likely mechanistic explanation (*91*). Notrott *et al.* showed repression of protein production on actively translating polysomes by let-7, and concluded that

the miRNA was interfering with the accumulation of growing peptides (*92*). Wakiyama *et al.* showed miRNA-mediated deadenylation of mRNA, and suggested that shortening of the poly-A tail would prevent PABP1 association and binding to the cap structure, thus preventing translation initiation (*93*). Kiriakidou *et al.* reported that the Ago proteins contain a limited cap-recognition motif, and argue that competition with eIF4E for binding of the cap would inhibit translational inhibition (*94*). Against this argument is the fact that Ago would appear to have a lower binding affinity for the cap than eIF4E, and more recent evidence showing that the Ago structure contains amino acids that are incompatible with eIF4E-like mRNA-binding (*95*).

A number of studies have reported co-sedimentation of miRNA with polysomes, and have argued that this supports a post-initiation inhibitory mechanism. However, it has been pointed out that binding of single miRNP to a mRNA will frequently have no significant repressive effect. Co-sedimentation of the miRNPs with polysomes may therefore represent bound miRNAs exerting little or no repressive effect, and therefore cannot be taken as proof of a post-initiation mechanism (*96*).

1.8.2.3. mRNA degradation and P-bodies

Microarray analyses of cells transfected with synthetic miRNA have demonstrated that mRNA expression of many genes is down-regulated as a result, suggesting that degradation or sequestration of the transcripts must be occurring. In addition, analysis of the significantly down-regulated transcripts indicates that their 3'UTRs are enriched with complementary seed-binding regions to the miRNA under investigation (*97-99*).

Processing bodies contain a number of proteins that are involved in mRNA degradation. These include the 5' decapping enzymes DCP1 and DCP2, exoribonulcease 1 (XRN1) which causes 5'-3' decay, and deadenylating enzymes (CCR4-CAF1-NOT complex). Ribosomes and other factors which are required for translation initiation are notably absent, with the exception of eIF4E and eIF4E-transporter, which is implicated in translational repression (*100*). Argonaute, miRNAs and their mRNA targets have all been shown to localise to P-bodies. miRNA-mediated mRNA decay has also been shown to be dependent on the components mentioned above, in addition to the GW182 protein (so-called because it contains glycine and typtophan repeats, and because of its molecular weight) (*90, 101-103*). While this provides compelling evidence that miRNA-mediated mRNA decay requires the presence of P-body components, it is not clear whether the physical environment of P-bodies is required. This is due to the fact that depletion of certain proteins, e.g. LSm1 (part of the decapping co-activator complex) results in diffusion of Ago2 throughout the cytoplasm, but with no impairment of miRNA-mediated mRNA degradation activity. However, depleting cells of RCK/p54 (a DEAD box helicase), results in P-body loss and relief of miRNA-mediated translational repression (*104*). Treatment of cells with cyclohexamide stabilises mRNAs in to polysomes, and leads to loss of P-bodies. Conversely, inhibition of translation initiation by puromycin, for example, leads to accumulation of P-bodies. This supports the hypothesis that P-bodies are the result of non-translating mRNP accumulation (*105*). In other words, P-bodies may well be the consequence of miRNA-mediated mRNA repression, rather than the cause of it.

1.8.2.4. Translational stimulation by miRNAs

AU-rich elements (AREs) appear in the 3'UTR of 12% of mammalian genes. ARE-binding proteins are known to target these transcripts for exonucleolytic decay of the poly-A tail, leading to mRNA degradation. It was discovered, however, that in the state of cell-cycle quiescence, the presence of AREs can lead to translational stimulation. Studies using reporter assays containing the highly conserved 3'UTR ARE of Tumour Necrosis Factor α (TNFα) revealed that in conditions of serum deprivation (leading to quiescence), translation was increased 5-fold. Fragile X mental retardation protein 1 (FXR1) was found to be necessary for translational up-regulation, in addition to Ago2. Further studies revealed that a miRNA, miR-369-3p, was essential for TNFα ARE-directed translational up-regulation. Additionally, it was found that miR-369-3p switched from activation of translation (in G0/G1 arrest – quiescence) to repression during the cell cycle, with optimal repression occurring in late S-phase, close to the G2 boundary (*106-108*). Cell cycle dependence of miRNA activity could prove to be highly relevant in the study of tumour biology. Fluctuating vascular supply leading to hypoxia and serum deprivation will likely lead to areas of cellular quiescence, and thus variable responses to miRNAs.

1.8.3. microRNA in development and differentiation

Since the discovery of the lin-4 miRNA and its role in *c. elegans* progression through larval stages 1 to 2, much work has been done to further elucidate the role of miRNAs in development. Roles have been described in stem cell differentiation, left-right asymmetry, apoptosis, neurogenesis, angiogenesis,

haematopoiesis and viral defence.(*109*) Let-7 has been shown to regulate several transcription factors at the larval to adult transition in *c. elegans.* (*110*)

Homeobox (HOX) clusters are groups of related transcription factor genes which regulate development in a variety of animals. Mammals have four such clusters, which contain a total of 39 genes. Mir-106 has near-perfect complementarity to a 3'UTR region on HOXB8. This complementarity site is well conserved through frog and fish species, despite divergence in the surrounding UTR sequences, indicating its importance. Possibly due to the high complementarity, miR-196 regulates this gene, at least in part, by mRNA cleavage. Due to partially complementary sites, miR-196 likely regulates expression of other HOX genes (HOXC8, HOXD8, HOXA7) (Yekta). The miR-430 family has been shown to be important in zebrafish brain morphogenesis by creating loss-of-function dicer mutants, which leads to severe defects in gastrulation, brain formation, somitigenesis and heart development. Injection of synthetically made miRNA duplexes was then carried out to evaluate changes in phenotype.(*111*) Further zebrafish studies, using microarray in in-situ hybridization technologies, demonstrated that most microRNAs are expressed in a highly tissue-specific manner during segmentation and later stages, and not in early development. This suggests that miRNAs play a key role in cell differentiation and maintenance of tissue identity.(*112*) Certain tissues express particular miRNAs very highly – for instance miR-124 in the brain and miR-1 in heart and skeletal muscle. Transfection of miR-124 miRNAs into HeLa cells and subsequent microarray gene expression analysis demonstrated that many of the down-regulated genes were expressed at low levels in brain tissue. Likewise, miR-1 transfection down-regulated genes that had low expression in muscle tissue, suggesting that these miRNAs contribute to the differentiation of these tissues. (*97*) This work also provided evidence that the mechanism of action of miRNA

gene regulation in animals is not purely that of translation repression, but also includes (perhaps more than originally thought) mRNA degradation.

1.8.4. microRNAs and cancer

If miRNA is involved in the control of gene expression, it is reasonable to assume that abnormal miRNA expression could contribute to cancer pathways. Early evidence of this was demonstrated in the Bantam miRNA, which caused overgrowth of wing and eye tissue in Drosophila through negative regulation of the pro-apoptotic gene hid. Another miRNA, miR-14, was demonstrated to suppress cell death.(*113*) More recently, studies have demonstrated that tumour cells show a general down-regulation of miRNA expression compared with normal tissues.(*114*) It has also been shown that the ratio of precursor miRNA to mature miRNA goes up in cancer, possibly pointing to a defect in processing, contributing to cancer cell phenotypes. An analysis of gene expression in primary tumours point to a failure in processing at the Drosha stage.(*115*)

It has been shown that different solid tumours express different miRNA expression profiles.(*116, 117*) A study, using bead-based flow cytometry, of miRNA expression in multiple human tumours, demonstrated that it had significantly greater diagnostic accuracy than a mRNA classification system. (*114*). In fact, it is possible that miRNA classification could also detect pro-malignant states. The apparent richness of information that can be derived from miRNA expression profiles therefore has obvious diagnostic potential. It remains to be seen how such profiles might be used – for instance, miRNA extracted from urine, could herald a new way of diagnosing transitional cell carcinoma. Of course, miRNA can be extracted from tumour samples and analysed, possibly helping in

situation where microscopy and immunohistochemistry fail to provide an unequivocal diagnosis. Eventually, it may even be possible to reach diagnosis from extraction of miRNA from blood plasma for analysis.

miRNA has been shown to fit in to a more classical model of cancer biogenesis as well. Here follow some examples of miRNA exhibiting tumour suppressor and oncogene-like behaviour:

1.8.4.1. microRNAs as tumour suppressors

Let-7a-1 is located at chromosome 9q22.3, a locus frequently deleted in colon cancer. It was demonstrated that transfection of let-7a-1 precursors in to let-7 low-expressing DLD-1 colon cancer cells caused a reduction in growth rate, in a dose-dependent manner. Western blot analyses showed that expression of RAS and c-myc was reduced in the DLD-1 cells transfected with exogenous let-7, adding further evidence to its function as a tumour suppressor in this cell type (AKAO). Reduced expression of let-7 in lung cancer has been linked to shortened post-operative survival in one study. As with the colon-cancer DLD-1 cells, over-expression of let-7 resulted in inhibition of lung cancer cell growth.(*118*) These results suggest a potential future therapeutic role for miRNA in cancer. A further example is miR-15-a/miR-16-1, which is located on chromosome 13 in a region frequently deleted in B-chronic lymphocytic leukemia (B-CLL). Its target gene is BCL2, which is strongly anti-apoptotic. Deletion of the above miRNAs would thus promote cell proliferation in B-CLL.

1.8.4.2. microRNAs as oncogenes

The miR-17-92 cluster is the most studied group of miRNAs with pro-proliferative and anti-apoptotic properties. It consists of 6 miRNAs, and is located at 13q31, a locus which is amplified in a number of tumours. A study was performed using Eμ-myc transgenic mice (carrying the c-myc oncogene, driven by the immunoglobulin heavy chain enhancer Eμ), which develop B-cell lymphomas by 4-6 months of age. A truncated form of the miR-17 cluster, highly expressing all but one of the five miRNAs, was introduced in to the haematopoeitic cells of these mice. This resulted in a dramatic acceleration of onset of disease, at 51 days on average, and death. When individual animals were reconstituted with only *individual* miRNAs from the miR-17 cluster, there was no acceleration of disease, suggesting that cooperative interaction between the cluster miRNAs is required for its oncogenic effect.(*119*) Other studies have supplied a possible explanation for this activity: c-myc appears to activate transcription of the cluster, and two of the miRNAs within it – miR-17-5p and miR-20 – cause translational repression of the pro-apoptotic transcription factor E2F1. (*113*)

It is likely that the growth in our understanding of miRNA regulator mechanisms and expression profiles in different tumour types will have important implications in the fields of diagnostics, patient prognosis and, ultimately, treatment.

1.9. Hypothesis and aims of this thesis

As miRNA has been shown to have a role in cancer, one can hypothesise that miRNA expression profiles will change, as do mRNA profiles, in a hypoxic microenvironment. Hypoxia-regulated miRNAs could therefore be relevant in

orchestrating gene and protein expression patterns which result in cancer phenotypes.

The aims of this project are to answer the following questions:

1. Which microRNAs are regulated by hypoxia?
2. What are the mRNA and protein targets of hypoxia-regulated miRNAs (HRMs)?
3. What are the effects of HRMs on cancer cell growth *in vitro* and *in vivo*?
4. Are HRMs relevant in clinical practice?

CHAPTER 2
Materials and methods

2.1 Cell culture and procedures

2.1.1 Cell lines

Cell lines were obtained from Clare Hall, the CRUK storage facility. Cells were cultured in 175 cm^2 coated flasks (Corning Incorporated, New York). A variety of culture media were used, depending on cell type. Culture medium was supplemented with 10% foetal bovine serum (PAA Laboratories), and 1% glycine.

Cell cultures were maintained in humidified culture chambers with 5% CO2 and 21% oxygen, unless stated otherwise.

- MCF7 and MDA-MB-231 breast cancer cell lines were cultured in Dulbecco's Modified Eagle Medium, supplemented with 10% foetal calf serum (FCS) and 5mM L-glutamine.
- LNCAP and PC3 prostate cancer cells were cultured in 1%RPMI with 10% foetal calf serum and 5mM L-glutamine. LNCAP cells grow in clumps, and for this reason were passaged at about 60% confluence to prevent cell detachment and death.
- 5637 and RT112 cell lines were cultured in 1%RPMI supplemented with 10% fetal calf serum and 5mM L-glutamine.
- RCC4 and 786-O cell lines were maintained in DMEM with 10%FCS.

2.1.2 Cell passage

The cell growth medium was aspirated, and the cells were washed once in phosphate buffered saline (PBS). This was aspirated, and 1ml trypsin + EDTA solution (trypsin 4mg/ml and 0.2mM EDTA in PBS) was applied to the cells, ensuring all cells were covered. Following a 5 minute incubation at 37°C, the cells were re-suspended in medium, and centrifuged at 1000g for 4 minutes. The supernatant was aspirated, and the cells were re-suspended in medium. Cells were typically passaged at 1:5.

2.1.3 Cell counting

In order to achieve consistent cell densities in experiments, cell concentrations were determined using an automated cell counter (Coulter). 400 µl cell suspension was placed in specialised counter vessels, to which a standard volume of Isoton isotonic fluid was added. The sample was then immediately placed in the counter, which determined the number of cells as cells/ µl. An alternative method for cell counting used was the hemocytometer. A coverslip was placed over the hemocytometer plate, and 8 µl of cell suspension was applied to the slide. A microscope and manual counter was used to determine cell numbers.

2.1.4 Cell freezing and storage

Cells were harvested when in the exponential growth phase. Following pelleting, they were re-suspended FCS with 10% DMSO. They were cooled at a rate of 1 degree per minute in the -80 freezer using an isopropanol-insulated container, and transferred to liquid nitrogen for long-term storage. On recovering cells from liquid nitrogen, the cells were thawed as quickly as possible by warming in gloved hands, before being placed in a culture flask with warm medium and left overnight. The following day, the medium was replaced to remove the remaining DMSO.

2.1.5 Exposure of cells to hypoxic conditions

Specialised hypoxic incubators were used for this purpose. Cells were exposed to 0.1% or 1% oxygen, in 5% CO_2, with the remainder of the gas being composed of nitrogen. The chambers were humidified to reduce dehydration of the cell culture medium, and to ensure accurate reading by the CO_2 and O_2 sensors.

A hypoxia workstation was employed for time-course experiments. The gas composition of the chamber was identical to those above, but the system contained an air-lock allowing samples to be moved in and out of the chamber without re-oxygenation of other samples.

2.2 Cell Transfection

2.2.1 Transient transfection of cells with microRNA mimics and inhibitors

Dharmacon Miridian reagents were used in transient transfections of cells to increase or decrease the expression of mature miRNA. miRIDIAN mimics consist of chemically modified double-stranded RNA molecules which contain the active miRNA strand and an excluded passenger strand. The meridian miRNA inhibitors are chemically modified RNA oligonucleotides complementary to the miRNA hairpin molecules.

800,000 cells were added to 10cm culture dishes, and incubated overnight. For each transfection, 24µl oligofectamine was added to 96µl Optimem (serum-free culture medium) in a 1.5ml sterile tube (A), and incubated at room temperature for 10 minutes. Stock solutions of mimic or inhibitor were made up to 20 µM concentrations. For 20nM transfections, 8µl of 20µM inhibitor or mimic (or

control oligo) was added to 1472µl Optimem in a separate 1.5ml sterile tube (B). Tube A was added to tube B, and mixed gently before incubating for 20 minutes at room temperature to allow complexes to form. Meanwhile, the cells were washed in 10 ml Optimem. 6400µl was then added to each 10cm plate, followed by the complex solution (A+B), and gently mixed by swirling the plate. The plates were incubated for 4 hours at 37°C. 1 ml of growth medium and 1 ml FCS were then added to each plate, and mixed gently. The plates incubated overnight at 37°C, and the following morning the medium was changed to the standard growth medium for the cell being cultured.

2.2.2 Block-It shRNA system

The BLOCK-iT™ Pol II miR RNAi Expression Vector Kits were obtained from Invitrogen. These facilitate the generation of an expression construct which results in over-expression of a pre-miRNA in cells for RNAi analysis of a target gene. The vector (pcDNA ™6.2GW / EmGFP-miR) allows expression of the pre-miRNA, based on miR-155, under the control of the Pol II CMV promoter and Herpes Simplex Virus thymidine kinase polyadenylation signal. The section of the pre-miRNA that forms the mature miRNA can be altered to express a 22 nucleotide molecule of your choice. The Invitrogen BLOCK-iT designer software was used to design RNAi molecules to pre-miR-210. Oligos were designed to target the flanking sequences of the mature miRNA, and the mature sequence itself. In total, five sequences were designed to target different parts of the pre-miR-210 molecule. The software designs two complementary single-stranded DNA oligonucleotides, with one encoding the siRNA sequence of interest.

Following synthesis (by Invitrogen) of the complementary oligos, the two molecules were annealed. The following reagents were combined in a 0.5 ml tube:

Reagent	Amount
Top strand DNA oligo (200 µM)	5 µl
Bottom strand DNA oligo (200 µM)	5 µl
10 x Oligo Annealing Buffer	2 µl
DNAse / RNAse-free water	8 µl
Total	**20 µl**

Table 2-1. Reagents for annealing oligonucleotides in Block-It protocol.

The contents were mixed and incubated at 95°C for 4 minutes. The tube was then allowed to cool over 10 mins, and centrifuged for a few seconds. Two dilutions of the double-stranded oligo were made, to give concentrations of 500 nM and 10 nM.

5 µl of the 500 nM double stranded oligos was run on a 4% Agarose gel with single and double-stranded control LacZ oligos supplied by the manufacturer, to ensure efficient annealing had occurred. A molecular weight standard was included on the gel (10 bp DNA Ladder, Invitrogen).

The double stranded oligos were then cloned in to the pre-linearised vector. The following reagents were combined in a 1.5 ml tube (in the order shown):

Reagent	Sample	Positive control	Negative control
5x ligation buffer	4 µl	4 µl	4 µl
pCDNA™6.2GW/miR, linearised (5ng/ µl)	2 µl	2 µl	2 µl
miR-ds oligo (10nM)	4 µl	--	--
miR-lacZ positive ds control oligo (10nM)	--	4 µl	--
DNAse / RNAse-free water	9 µl	9 µl	13 µl
T4 DNA ligase (1U/ µl)	1 µl	1 µl	1 µl
Total volume	**20 µl**	**20 µl**	**20 µl**

Table 2-2. Ligation reagents for Block-It protocol.

The reaction mixture was mixed by pipetting up and down, and incubated for 5 min at room temperature, then placed on ice. The ligation reaction was used to 'heat-shock' transform *E. coli* as follows:

2 µl of the above ligation reaction was added to one vial of One Shot® TOP10 Chemically Competent *E. coli*, and mixed gently. The cells were 'heat shocked' by immersing the tubes in a water bath at 42°C for exactly 30 seconds, and then transferred immediately to ice. 250 µl S.O.C. medium was added to the tubes, which were shaken horizontally at 200 rpm for 1 hour at 37°C. 50-200 µl of each transformation was then spread on to LB agar plates containing 50 µg/ml spectinomycin, and incubated at 37°C overnight. From each plate, 10 positive colonies were picked and cultured overnight in 10 ml LB medium in a shaking

incubator at 37°C. DNA was extracted and purified using the HiSpeed Plasmid Purification Maxi Kit (Qiagen), as per the manufacturer's protocol. The plasmids were sequenced using the WIMM in-house service using the supplied forward primer, in order to ensure that the cloned sequences were correct and in the proper orientation.

MCF7 and MDA-MB-231 cells were transfected using Fugene6® Reagent (Roche). Before transfection, a kill curve experiment was set up to determine the lowest concentration of Blasticidin required to kill cells at 10-14 days after addition of antibiotic. The cells were plated at 25% confluency, and the antibiotic-containing medium replaced every 4 days. On the day before transfection, cells were plated (in a standard 6-well plate) to achieve 50-80% confluency, in 1 ml of medium. On the day of transfection, Fugene 6 reagent and plasmid DNA were combined in a total volume of 100 µl made up with serum-free medium:

Ratio Fugene:DNA	Serum Free Medium (µl)	FuGENE 6 reagent (µl)	Plasmid DNA (µg)
3:1	97	3	1
3:2	97	3	2
6:1	94	6	1

Table 2-3. Fugene6 protocol reagent ratios for transfection.

The contents were mixed gently and incubated at room temperature for 15 min, and then added to the culture plate. The cells were left to incubate at 37°C overnight. The medium was then replaced by the Blasticidin-containing medium, and left until all the control (non-transfected) cells were dead. Cell cultures were then analysed by qRT-PCR for miR-210 expression.

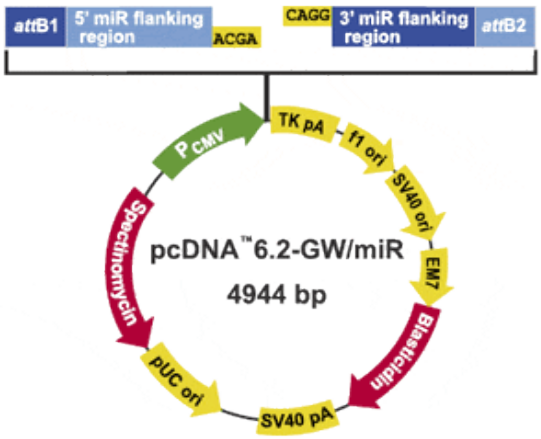


Figure 2-1. Block-It vector diagram.

2.2.3 Stable up-regulation of miR-210 in cancer cells

Dr Mircea Ivan kindly provided pBabe vectors with a cloned pre-miR210 sequence including about 100 bp of flanking sequences, plus an empty vector. 1 µl of each vector was added to a vial of One Shot® TOP10 Chemically Competent *E. coli*, which were transformed by the heat shock procedure as described above. The rest of the protocol, including transfecting the cells (except for the antibiotic resistance genes encoded for in the pBabe vector), is as per the Block-It shRNA protocol. The antibiotic resistance genes were ampicillin (for transformed bacterial selection) and puromycin (for transfected cell selection).

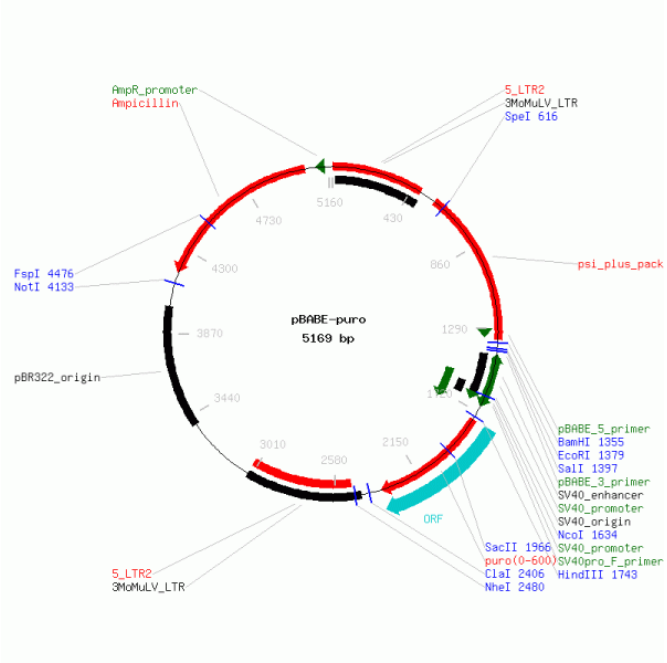


Figure 2-2. pBabe vector diagram.

2.3 RNA extraction

2.3.1 RNA extraction from monolayer cell cultures

The cell medium was aspirated from the culture dish, and 1 ml Trizol (Invitrogen) was added to the dish, ensuring it covered all cells. The dish was incubated at room temperature for 1 minute, and a cell scraper used to dislodge cellular material. The cell lysate was transferred to a 1.5 ml tube, to which 200 ml of chloroform was added. The sample was vigorously mixed using a vortex, and incubated at room temperature for 5 minutes. The sample was centrifuged at 12,000 x g for 15 minutes, and the supernatant transferred to a new tube. 500 µl isopropanol was added to the tube, which was mixed 8 times by inversion, and incubated at room temperature for 10 minutes. The sample was the centrifuged at 12,000 x g for 10 minutes at 4°C. The supernatant was removed, and 1 ml 75% ethanol added. The sample was mixed, and then centrifuged at 7,500 x g. The

supernatant was removed and the pellet air dryed for no longer than 5 minutes, before being re-dissolved in DNAse/RNAse free water. Total RNA quantification was achieved using a Nano-drop ND1000® spectrophotometer. Absorbance at 260nm (n260) was used to calculate RNA yield as follows:

RNA concentration (µg/ml) = n260 x 40 x dilution

2.3.2 Extraction of purified microRNA for microarrays

For examination of miRNA expression using in-house microRNAs, the use of purified miRNA was necessary. The extraction of total RNA is identical to that described above. The purification steps are carried out using RNeasy and minElute column fractionation kits from Qiagen.

To 100 µl total RNA solution in water was added 350 µl RLT buffer, and mixed by inversion. 350 µl 80% ethanol was added and mixed by inversion. An RNeasy Mini kit column was placed over a 2 ml tube, and the sample placed in to the column. This was centrifuged for 15 sec at 8,000 x g. The flow-through contains the miRNA, and the mRNA remains bound to the column. 980 µl 100% ethanol was added to the flow-through in the 2 ml tube, and mixed by inversion. The contents were added to an RNeasy MinElute column 800 µl at a time, and centrifuged for 15 sec at 8,000 x g. The flow through was discarded, and 500 µl of RPE buffer was added, before centrifuging at 8,000 x g. The flow through was discarded, and 800 µl 80% ethanol was added to the column. It was centrifuged for 15 sec at 8,000 x g, followed by a further centrifuge for 1 minute with the caps open. 14 µl of DNAse/RNAse free water at 95°C was added to the column, and left for one minute. Following this, the columns were inverted and placed over 1.5 ml tubes,

and centrifuged for 1 min at 8,000 x g. The resulting elution contains miRNA, and is stored at -80°C.

2.3.3 Extraction of RNA and DNA from tissue samples

2.3.3.1Tissue homogenisation

This was achieved using the fast-prep homogeniser system. Tumour or normal kidney tissue was removed from liquid nitrogen storage and placed on dry ice. Using a scalpel, pieces of tissue were resected, and cut in to pieces not larger than 1 mm in any dimension. This was done on 10 cm plastic dishes on dry ice to ensure the samples remained frozen. The pieces of tissue were then placed in a 2 ml tube containing lysing matrix D (Q-Biogene) containing 1.4mm ceramic beads and Trizol reagent at 4°C. Samples were then immediately placed in the Fast-Prep® homogeniser (Q-biogene) at setting 6.0 for 40 secs. If there was incomplete homogenisation, samples were replaced on ice to cool, and the homogenisation process was repeated.

2.3.3.2 RNA extraction

Following homogenisation, the samples were then centrifuged at 12,000 x g for 5 minutes, and the supernatant transferred to a new tube. RNA extraction then proceeds as described for monolayer cell culture.

2.3.3.3 DNA extraction from tumour samples

The same samples were used for extraction of RNA and DNA. Following addition of chloroform and centrifuging, the sample splits in to three layers – the top (aqueous) layer is removed and used for RNA extraction. The intermediate (white layer) contains DNA and protein. To the remaining sample, 300 µl 100% ethanol was added and mixed by inversion. The samples were incubated for 2 minutes at room temperature, then centrifuged at 2,000 x g for five min at 4°C to sediment

the DNA. The supernatant was removed, and the pellet washed in DNA wash solution (0.1M trisodiumcitrate in 10% ethanol). The sample was then centrifuged at 2000 x g for 5 minutes at 4°C. The supernatant was removed, and 1.5 ml 75% ethanol added. This was incubated for 10 min at room temperature with periodic mixing. This was then centrifuged as above, the supernatant removed, and the pellet dried for 3-5 minutes. It was then re-solubilised in DNAse/RNAse free water, and quantified using the Nano-drop® spectrophotometer.

2.4 Protein extraction, quantification, and expression analysis

2.4.1 Protein extraction from monolayer cultures

Prior to extraction urea lysis buffer was made up, consisting of 5%glycerol, 0.5ml Tris-HCL pH6.8 1M, 250µl 1M dithiothreitol, 5ml 10% sodium dodecyl sulphate, protease inhibitor cocktail (Complete, Roche UK), phosphate inhibitor (PhoSTOP, Roche UK), made up to 50ml with 8M urea. At all stages the culture dishes and reagents were kept on ice to minimise protein degradation. The cell medium was aspirated, and the cells washed twice in ice-cold PBS. 200 µl ice-cold lysis buffer was added to the dish, and a cell scraper was used to remove the cells. The lysate was passed through a 25-guage needle and syringe until it lost its 'gloopy' nature, indicating that DNA was adequately sheared, leaving a homogeneous sample.

Protein quantification

1. **Biorad assay**

   The protein lysate was diluted 1:10 with water. BSA protein standards were made up in water to the following concentrations: 0, 0.125, 0.25, 0.5, 1.0, and 1.5 µg/ml. To a 96 well plate, 5 µl of each sample to be

measured, and 5 µl of each standard were added in triplicate. Reagent A* was made up using 100 µl reagent S and 5 ml reagent A. 25 µl of reagent A* was added to each well using a multichannel pipette. 200 µl reagent B was then added to each well using a multichannel pipette. The plate was then covered, and incubated at room temperature for 30 minutes. An optical plate-reader was then used to measure the colour change, and by plotting a standard curve of the BSA standards, the concentration of protein in the samples was calculated.

2. **Spectrophotometry**

   Samples were measured by placing 1.4 µl of well homogenised samples on the the Nano-drop® spectrophotometer (ThermoScientific, UK), taking care not to have any bubbles in the sample. Absorbance at 260nm (n260) is used to calculate RNA yield:

   RNA conc (µg/ml) = n260 x 40 x dilution

2.4.1 Western blotting (Polyacrylamide gel electrophoresis)

Polyacrylamide gelss were made up using BioRad equipment. Firstly, the glass plates were assembled to leave a gap of 1.5 mm for the gel. Water was placed between the plates first to ensure there were no leaks. The following buffers were mad up in advance:

5 X running buffer

- 125 mM Tris Base (=15.125 g/L)
- 1.25 M Glycine (=93.75 g/L)
- 0.5% SDS (=50 ml 10% SDS/L)

Transfer Buffer

- 25mM Tris (3.025 g/L)
- 192mM glycine (14.4 g/L)
- 15% methanol (150 ml/L)
- Make up to 1 litre with water

TBST

- 1 ml Tween
- 100 ml 10X TBS
- 900 ml water

M-TBST

- Take 500 ml TBST
- Add 25g milk powder

6 X SDS sample buffer (gel loading buffer)

- 1.8 ml 1M Tris (pH6.8)
- 4.95 ml glycerol
- 11.25 ml 10% SDS
- 2.475 ml b-mercaptoethanol
- A pinch of bromophenol blue
- 5 ml distilled water

The resolving gel was made up using the following components, depending on the percentage gel required, and poured between the glass plates. The solution was covered with 100 µl isopropanol to prevent dehydration.

Solution	6% - 2 gels	8% - 2 gels	10% - 2 gels	12% - gels
30% acrylamide	4 ml	5.33	6.66 ml	8 ml
4X Tris-HCL/ SDS pH 8.8	5 ml	5 ml	5 ml	5 ml
Water	10.78	9.45	8.128 ml	6.78 ml
10% APS (1g in 10ml)	200 ul	200 ul	200 ul	200 ul
Temed	12 ul	12 ul	12 ul	12 ul

Table 2-4. PAGE resolving gel reagents.

Once the resolving gel had set, the stacking gel was made up using the following components:

Solution	Enough for 2 gels
30% acrylamide	1.66 ml
4X Tris-HCL/SDS pH 8.8	2.5 ml
Water	5.73 ml
10% APS (1g in 10ml)	100 ul
Temed	10 ul

Table 2-5. PAGE stacking gel reagents.

The isopropanol was poured off the gel surface, and the resolving gel added. A comb was immediately placed on top of the gel to create the loading wells – either a 10 or a 15 well comb was selected. Once the gel had set, the comb was carefully removed, and the wells rinsed in running buffer. The glass plates were then placed in the electrode chamber, which was filled with 1 x running buffer.

Protein samples were prepared to contain 30 µg/ml of protein, made up to 18 µl with the 6 x SDS gel loading buffer and PBS. Samples were heated at 95°C for 5 minutes, and then loaded in to the wells of the gel. 5 µl of a protein ladder (universal rainbow marker) was added to at least one well to enable assessment of the size of protein bands. A voltage was applied across the gels using a power-pack (details), typically 125 volts for 60-90 minutes, depending on the size of protein under investigation and the percentage of the gel.

After the samples were run on the gel, they were transferred to a nitrocellulose membrane, using a semi-dry method. Filter paper was soaked in transfer buffer. A nitrocellulose membrane was cut and soaked in methanol for 60 seconds, before being washed in transfer buffer. For each gel, 3 pieces of buffer-soaked filter paper were placed on the base plate electrode, followed by the nitrocellulose membrane. On top of this were placed the gel, and three further pieces of filter paper. At each stage, excess fluid was removed gently using a roller, ensuring no air bubbles were present. The second electrode was placed over the gels, and a current of 0.13 amps was run across the gels (0.26 amps if two gels present on the same electrode) for one hour.

Following transfer, the nitrocellulose membrane was blocked in M-TBST for 1 hour. The membrane was then placed in a sealed bag with the primary antibody diluted as per the manufacturer's recommendations, in M-TBST. This was incubated overnight on a shaker at 4°C. The membrane underwent 3 five-minute washes in M-TBST, and was then incubated for an hour with the appropriate horseradish-peroxidase (HRP)-conjugated secondary antibody for 1 hour at room temperature, on a shaker. The membrane then underwent three 10 minute washes in TBST.

Developing the blot was achieved using ECL reagent (GE Healthcare, UK). ECL reagents A and B were combined in equal proportions as per the manufacturer's instructions. About 1 ml of the combined reagents was applied to the membrane, and incubated at room temperature for one minute. The excess fluid was removed, and the membrane was placed in a developing cassette between layers of clear plastic film. Photgraphic film was exposed to the membrane in a dark room, and developed.

Quantification of western blots was achieved by digital scanning of the film, and determination of band intensity using Image-J® software. The band intensity of the protein of interest was normalised to the loading control band intensity.

2.4.2 Immunohistochemistry on paraffin-embedded tissues

This was performed by Dr Helen Turley and Dr Adrian Jubb. The protocols are as per the publication by Biswas et al. (*120*) Briefly, 5 micron sections were prepared for immunohistochemistry by application of 0.3% hydrogen peroxide, before washing with PBS and immersion in 2.5% horse serum for 30 minutes at room temperature. Following antigen retrieval, sections were incubated with one of the following primary antibodies:

Antibody	**Source**
HIF-1α	Clone 54, BD Biosciences
HIF-2α	EP190B, ABCAM
CA9	M75, University of Oxford(*121*)
VHL	Clone IG32, BD Biosciences
ISCU	Abnova

Table 2-6. IHC primary antibodies.

Unless stated otherwise, scoring was performed using the percentage-intensity (PIS) method, whereby the intensity of staining is multiplied by the percentage of the specimen stained.

2.5 RNA expression analysis

2.5.1 Quantitative Real-Time PCR for *microRNA*

Total RNA was extracted as described above. Applied Biosystems reagents were used to create cDNA and perform qRT-PCR.

2.5.1.1 cDNA synthesis

The Applied Biosystems primers contain hairpins in order to specifically bind to mature microRNAs, and not the precursor molecules. Due to the chemistry involved, each miRNA under investigation requires incubation with a specific primer. During cDNA synthesis it is possible to incubate the RNA sample with a single primer, or to use pooled primers to create cDNA for a number of miRNAs. I will describe the methods separately.

Use of single primers – For each reaction, the following reagents were combined as a mastermix:

Reagent	Volume (µl)
100 mM dNTPs (with dTTP)	0.15
MultiScribe™ Reverse Transcriptase, 50 U/µl	1.00
10 X Reverse Transcription Buffer	1.50
RNAse Inhibitor, 20U/µl	0.19
Nuclease-Free Water	4.16
Primer	3.00

Table 2-7. cDNA synthesis for miRNA qRT-PCR

For each reaction 5 ul total RNA at a concentration of 1-100ng/µl was added to a 0.2 ml polypropylene reaction tube, along with 10 µl of the above mastermix. The tubes were mixed gently and centrifuged. The tubes were placed in a thermal cycler, and run using the following parameters:

Step	Time (mins)	Temperature (°C)
1	30	16
2	30	42
3	5	85
4	∞	4

Table 2-8. Run setting for miRNA CDNA synthesis.

2.5.1.2 Synthesis of cDNA using pooled primers

The Applied Biosystems Megaplex primer kit was used for this purpose. A mastermix containing the following reagents was prepared (scaled up for the total number of samples required):

RT Reaction Mix Component	Volume (µl)
Megaplex RT primers (10X)	0.80
dNTPs withdTTP (100mM)	0.20
Multiscribe Reverse Transcriptase (50U/µl)	1.50
10X RT Buffer	0.80
$MgCl_2$ (25 mM)	0.90
RNase Inhibitor (20U/µl)	0.10
Nuclease-free Water	0.20
Total	4.50

Table 2-9. Pooled primer cDNA synthesis reagents for miRNA qRT-PCR

To 0.2 ml polypropylene reaction tubes was added 350-1000 ng total RNA in 3 µl DNAse/RNAse free water. 4.5 µl of mastermix was added to each tube, which were then mixed, centrifuged and placed in a thermal cycler with the following parameters:

Step	Time	Temperature (°C)
Cycle (40 cycles)	2 min	16
	1 min	42
	1 sec	50
Hold	5 min	85
Hold	∞	4

Table 2-10. Run settings for pooled primer miRNA cDNA synthesis.

Following cDNA synthesis, 6 µl of the reaction was diluted in 444 µl RNAs/DNAse free water prior to amplification by qRT-PCR.

2.5.1.3 qRT-PCR

Reactions were all performed in triplicate using a Corbett Robotics Real-Time capillary based system. For each reaction, the following was prepared:

RT Reaction Mix Component	Volume (µl)
cDNA	1.70
TaqMan Universal PCR Mastermix (No Amperase® UNG)	10.00
Nuclease Free Water	7.30
PCR Real-Time assay (primers + probe)	1.00
Total	20.00

Table 2-11. qRT-PCR mastermix reagents for miRNA analysis.

The samples were transferred to PCR capillary tubes, placed in the real-time machine, and run using the following parameters:

Step	**Enzyme Activation**	**PCR**	
	HOLD	Cycles (50 cycles)	
		Denature	Extend/Anneal
Time	10 min	60 sec	15 sec
Temp (°C)	95	95	60

Table 2-12. Run settings for miRNA qRT-PCR

Relative miRNA expression was calculated using the ΔΔCT method, using the following formula:

Relative expression = 2^ (CT control miRNA) - (CT miRNA of interest)

2.5.2 Quantitative Real-Time PCR for *messengerRNA*

2.5.2.1 cDNA synthesis

The Applied Biosystems High Capacity cDNA Reverse Transcription Kit was used.

For each cDNA synthesis reaction, the following reagents were combined:

Component	Volume/Reaction (µl)
10x RT Buffer	2.0
25x dNTP mix	0.8
10x RT Random Primers	2.0
Multiscribe™ Reverse Transcriptase	1.0
Nuclease-free Water	4.2
RNA (up to 2 µg)	10.0
Total	**20.0**

Table 2-13. cDNA synthesis for mRNA qRT-PCR

The combined reagents were then mixed, centrifuged, and placed in a thermal cycle with the following settings:

	Step 1	Step 2	Step 3	Step 4
Temp (°C)	25	37	85	4
Time	10 min	120 min	5 sec	∞

Table 2-14. Run settings for cDNA synthesis for mRNA qRT-PCR

The cDNA samples were then diluted 1:5, and stored at -80 °C.

2.5.2.2 qRT-PCR

Prior to the PCR reaction, forward and reverse gene-specific primers were designed using the Roche Universal Probe Library Assay Design Center online, and manufactured on request.

Each PCR reaction was performed in triplicate, and for each reaction, the following reagents were used:

Reagent	**Volume (µl)**
2xqPCR Matermix*	12.5
Forward primer (10µM stock)	1
Reverse primer (10µM stock)	1
Probe, undiluted	0.25
cDNA (1-5 ng/µl)	5
Nuclease-free water	5.25
Total	25

Table 2-15. Mastermix for mRNA qRT-PCR.

* This contains heat-activated Taq polymerase, dNTPs, $MgCl_2$, and reaction buffer.

The samples were placed in to the reaction capillary tubes, and then transferred to the qRT-PCR machine. The following run settings were used:

Step	Enzyme Activation	PCR	
	HOLD	Cycles (50 cycles)	
		Denature	Extend/Anneal
Time	15 min	60 sec	15 sec
Temp (°C)	95	95	60

Table 2-16. Run settings for mRNA qRT-PCR.

Gene expression was calculated from the CT values of the gene of interest and control gene as described previously.

2.5.3 Microarray expression profiling

2.5.3.1 Hybridization, and labelling

In-house manufactured microarrays with sense probes to x miRNAs were used to screen for expression profiling. The Array 900miRNA RT kit from Genisphere (MIRT180) and the Superscript II Reverse Transcriptase reaction kit (Invitrogen) were used. 50-500ng of purified miRNA was used per labelling reaction, diluted in to 13.5 µl RNAse free water. An A-hyb automated hybridisation system was used for all hybridisation processes.

Pre-hybridisation wash. The first step is a pre-hybridisation wash, requiring a specific buffer. The following reagents were added to a 50 ml conical tube: 8.75ml 20 x SSC (Ambion), 5 ml BSA solution (100mg/ml), 500 µl 10% SDS solution (Ambion), all topped up to 50ml with milli-Q water and filter-sterilised. The microarray slides were placed in the A-Hyb machine, which cycles the buffer over them for about 15 minutes.

Creation of labelled cDNA. The ATP solution (vial 4) was diluted according to the starting miRNA in 1mM Tris pH 8.0 using the formula 5000/x ng. For example, for 100 ng starting RNA: 5000/100 = 50, therefore 1 µl ATP was diluted in 49 µl of

Tris. To a 1.5 ml tube was added the following: 1 µl RNAse-inhibitor (vial 12), 1 µl spike-in control, 5 µl 5x miRNA reaction buffer (vial 2), 2.5 µl $MnCl_2$ (vial 3), 1 µl diluted ATP (as above), and 1 µl PAP enzyme (vial 5). The reaction was mixed gently by flicking and brief microfuge. The reaction was incubated at 37°C in a heat block for 15 mins, briefly centrifuged, and placed on ice. 2 µl of Cy3 or Cy5 RT primer (vial 9) was added to the reaction tube, and mixed gently. The tube was incubated at 65°C for 10 minutes, and placed on ice for at least 2 minutes. To the reaction tube was added the following: 10 µl 5x first strand buffer, 5 µl 0.1M DTT, 2.5 µl dNTP mix (vial 8), 1 µl Superscript II reverse transcriptase, and 4.5 µl RNAse-free water. The reaction tube was mixed gently and incubated at 42°C for 1 hour. 8.75 µl of 0.5M NaOH/50mM EDTA was added, mixed gently, and incubated for 15 mins at 65°C. The enhanced hybridization buffer (vial 7) was thawed at 70°C for at least 10 minutes. 12.5 µl 1M Tris pH 8.0 was then added to the reaction tube. Paired Cy3 and Cy5 samples were then combined to give a total volume of about 150 µl. To this was added 150 µl of enhanced hybridisation buffer (which had been thawed at 70°C for at least 10 minutes and left to cool), mixed, and incubated at 80 °C for 10 minutes. On completion of the pre-hybridisation step as described above, the labelled cDNA samples were loaded in to the A-hyb machine, which cycles the solution over the microarray slides overnight.

On day 2, two 50 ml tubes were made up with 0.2xSSC and two 50 ml tubes were made up with 2xSSC/0.2%SDS, and topped up to 50 ml with milliQ water. These were then filter-sterilised. The buffers were added to the A-hyb machine. Before proceeding to the next step, the 3DNA capture reagents were allowed to thaw in the dark for 20 minutes, and the incubation buffer (vial 6) was incubated at 70°C

for 10 mins, then centrifuged. The 3DNA capture reagents were then incubated at 55°C for 10 mins.

For each array, the following was made up in a 1.5 ml tube: 2.5 µl of cy3 3DNA capture reagents, 2.5 µl of cy5 capture reagent, 75 µl RNAse-free water, 100 µl hybridisation buffer (vial 6, prepared as above), and 20 µl 25% dextran sulphate. This was then mixed, incubated at 80°C for 10 min, and maintained at 62°C until loading. A 50 ml tube containing pure isopropanol was added to the A-hyb machine, and the capture reagent mix loaded in to the machine. Following a 1 hour hybridisation and cleaning step, the slides were removed and scanned using a dedicated microarray laser scanner, producing a TIF (non-compressed) image file. The images were analysed using Bluefuse array quantification software, and normalized using Global Lowess.

2.6 Polysomal Fractionation

The purpose of this procedure was to fix cells with chlorhexidine, in order to bind ribosomes to mRNA, and then fractionate the RNA according to weight. mRNA undergoing more active translation, i.e. with more bound ribosomes, would thus fractionate at a greater weight.

2.6.1 Preparation of sucrose gradients

Firstly, the fractionation buffer was made up in DEPC water, consisting of 0.3 M NaCl, 15 mM $MgCl_2$, 15 mM Tris-HCl (pH7.4), 0.1 mg/ml Cyclohexamide, and 0.1 mg/ml Heparin. Solutions of 50%, 40%, 30%, 25% and 20% sucrose in fractionation buffer were made up and kept on ice at 4°C. Note, the cyclokexamide and heparin must be added to the buffer when cold, prior to

adding the sucrose. Beckman 15 ml ultracentrifuge tubes were used for the gradients. First, 3 ml 50% sucrose was placed in the tube, and frozen at -80°C. Once frozen, 2 ml of 40% sucrose buffer was added, and frozen at -20°C, ensuring that the 50% sucrose layer did not thaw. This process was repeated with 1 ml 30% sucrose, 2ml 25% sucrose and finally, 2 ml 20% sucrose. The gradients were kept at -20°C until the night before use, when they are left in a cold room at 4°C to thaw slowly overnight.

2.6.2 Preparation of cell extract

The cells were incubated with 0.1mg/ml cyclohexamide for 3 mins at 37°C, then washed twice with PBS containing cyclohexamide at 0.1mg/ml. They were then scraped in lysis buffer (1%Triton X-100, 0.3M NaCl, 15mM MgCl2, 15mM Tris (pH 7.4), 0.1mg/ml cyclohexamide, 100 unitse RNAse-In (Ambion)). 200µg/ml heparin was added to the cytoplasmic lysate. The sample was centrifuged to remove debris.

2.6.3 Size Fractionation of RNA

500 µl cell extract was placed on top of each sucrose gradient. The gradients were then placed in a SW-41Ti rotor, and centrifuged for 90 min at 39,000 rpm at 4°C. Meanwhile, the fractionator was prepared by cleaning all equipment and tubing in ethanol and then water containing RNAse Zap. The pump speed was set to 0.25 ml/min, and the time per aliquot 45 sec. The UV readings were set to record absorbance at 254 nm. Once the apparatus was ready, the gradients were mounted on the machine, and the inferior part of the tubes perforated with a hollow needle attached to the pump. Ensuring no bubbles are introduced, the gradients were forced out (with 80% sucrose buffer solution) through the UV spectrometer and in to approximately 30 aliquots. As the sucrose gradient passed

through the spectrometer, it produced an absorbance plot similar to the following.

2.7 Xenograft experiments

In each experiment, ten BALB/c SCID mice received subcutaneous injections, in to the flank, of 10^7 cells in matrigel. Five mice received the pBabe EV-containing cells, and five received cells with the pBabe+miR-210. The MCF7 cells are an oestrogen-dependent breast cancer cell line, and thus the mice used for this experiment required oestrogen supplementation to ensure adequate tumour growth. This was achieved using a slow-release oestradiol pellet placed subcutaneously two days prior to injection of the tumour cells. Three-dimensional tumour size was measured every 3 days. Following sacrifice, tumours were collected – 50% of the tumour was snap frozen in liquid nitrogen, and 50% was fixed in formalin overnight. The organs were examined for metastases. The serum was collected from the mice and stored at -80°C.

CHAPTER 3 – Results

Identifying hypoxia-regulated miRNAs and their targets in human cancer cell lines

3.1 Introduction

The initial aim of this part of the project was to determine which miRNAs were regulated by hypoxia. Due to the fact that hundreds of microRNAs are known to exist, any approach to answering this question must use a high throughput screening tool to enable expression profiling of cells in normoxia and hypoxia.

3.1.1 Microarrays as screening tools

DNA Microarray technology is based on hybridization between complementary sequences of DNA. Microarrays typically consist of hundreds of short DNA probes (DNA sequences complementary to particular genes) to different genes, fixed on a solid surface such as a glass slide or a piece of silicon. Microscopic beads can also be used to mount DNA probes. The principle is that a fluorescent-labelled cDNA solution is applied to the microarray to allow hybridization. The amount of a given gene or miRNA present in the solution will be proportional to the intensity of fluorescence at the site of the DNA probe for that gene. This technology allows the expression profiling of many genes for just one sample of cDNA. It is, therefore, faster and more cost-effective that using qRT-PCR for individual genes, and considerably cheaper as a screening tool than deep sequencing technology (e.g. Solexa). Microarray analysis was was therefore selected as a starting point for screening for hypoxia-regulated miRNAs.

3.1.2 miRNA target prediction

In order to investigate the function of miRNAs, one needs to determine their mRNA target genes. Computational analyses of the genome have been used to predict and identify the microRNAs known to exist. A number of bioinformatic tools have also been developed to predict the target mRNAs of miRNAs. The various computational algorithms do vary in both structure and data output, but they share a number of features in common. Most importantly, a valid target must have complementary matching (usually in the 3'UTR) to the 5' seed region (nucleotide positions 2-8) of the miRNA. Less commonly, complementary regions can be found in the coding sequence of a target mRNA. Secondly, the resulting miRNA:mRNA duplex must have a higher negative folding energy. Thirdly, miRNAs and their target sites must be conserved across species.(*122*) Figure 3-1 illustrates the principle by which prediction algorithms work.

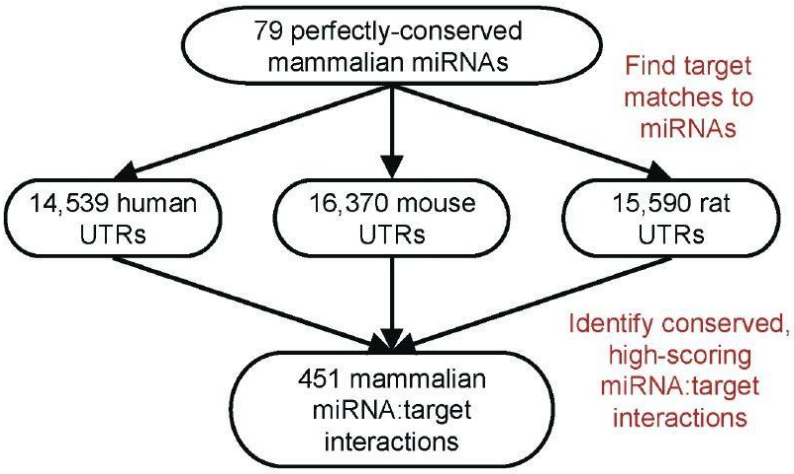


Figure 3-1. The TargetScan algorithm finds complementary sequences in the UTRs to a miRNA, and scores the target based on conservation across species and the negative free energy of duplex binding.(123)

Machine-based learning approaches are used in some algorithms. For example, PicTar scans the 3'UTR for alignments to a miRNA, and filters them according to thermodynamic stability. In addition, extra weighting is given to targets with multiple binding sites for a given miRNA.(*124*) The prediction tools selected for use in this project were the TargetScan and Pictar algorithms. Two studies using proteomic approaches to measure large-scale expression changes in response to miRNA over- or under-expression were undertaken in 2008. Reassuringly, Pictar and TargetScan, along with Diana MicroT, were the algorithms found to predict most accurately the experimental target findings in these studies.(*125, 126*)

3.2 In vitro studies of miR-210

3.2.1 Identifying hypoxia-regulated miRNA

Initial studies using an in-house miRNA platform had large variances, and the quality of the output data was insufficient to reach statistical significance. Our group and its collaborators had been working on a project to identify HRMs in breast cancer, using higher quality commercially available microarray platforms. miR-210 had emerged as the most strongly up-regulated miRNA in breast cancer cell lines, and its up-regulation was confirmed with qRT-PCR. In addition, it had been confirmed as a HIF-1, but not HIF-2, transcriptional target using siRNA to produce selective HIF-1 or -2 knockdown in hypoxia.(*127*) It had been shown that miR-210 expression in breast cancer samples correlated significantly with a hypoxia signature based on the expression of 96 known hypoxia-regulated genes. It was decided, therefore, that this project would concentrate on the study of miR-210 from this point onwards.

3.2.2 miR-210 is up-regulated in hypoxia in MCF7 and MDA-MB-231 cell lines

Two breast cancer cell lines – MCF7 (oestrogen receptor positive) and MDA-MB-231 (oestrogen receptor negative) were chosen for further study of miRNAs due to the fact that our group has collected a significant amount of experimental data from other projects using these cell lines.

Before continuing with further experiments to determine the targets and function of miR-210, its induction after 24 hours in 0.1% O_2 was confirmed by qRT-PCR. miR-210 was up-regulated 4.5-fold in MCF7 cells, and 3-fold in MDA-MB-231 cells. (Fig. 3-2)

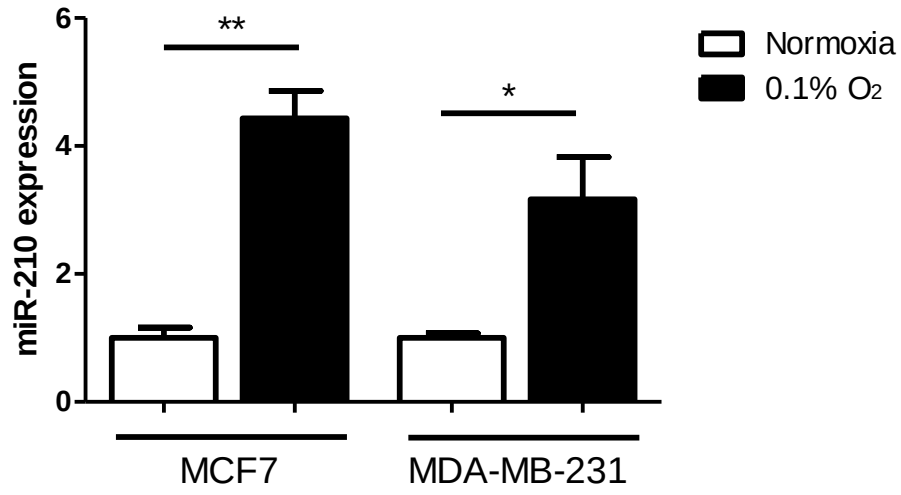


*Figure 3-2. Effect of hypoxia on miR-210 expression in MCF7 and MDA-MB-231 cells. Cell lines were incubated in normoxia or 0.1% O_2 for 24 hours. miR-210 in MCF7 cells was up-regulated 4.5 fold; miR-210 in MDA-MB-231 cells was up-regulated 3-fold. Plotted = mean + SEM, N=3. * $p < 0.05$, ** $p < 0.01$, T-test.*

3.2.3 Computational prediction of miR-210 targets

3.2.3.1 *In silico* search

The use of algorithms to predict miRNA targets is commonplace. The three most commonly used algorithms – TargetScan, PicTar and Miranda, were used to compile a miR-210 target list. The algorithms differ considerably in both the targets they predict, and the total number of targets. TargetScan and Pictar have greater overlap in their predictions, and produce a much more manageable number of targets. These two algorithms were therefore primarily used to select targets for investigation. Tables 3-1 and 3-2 show the highest ranked target predictions for miR-210 using Pictar and TargetScan.

Pictar Rank	Gene symbol	Gene name
1	MGC20255	Hypothetical protein MGC20255
2	MDGA1	MAM domain containing glycosylphosphatilyinositol anchor 1
3	EGR3	Early growth response 3
4	NPTX1	Neuronal Pentraxin 1
5	SEH1L	SEH1-like
6	GLT2	Glutaminase 2
7	CHAD	Chondroadherin
8	HYPB	Huntingdin interacting protein B
9	MEIS1	Myeloid ectopic viral integration site 1
10	GPD1L	Glycerol-3-phosphate dehydrogenase 1-like
11	FLJ34969	Hypothetical protein
12	KCMF1	Potassium channel modulatory factor 1
13	HYPB	Hungtingtin interacting protein B transcript variant 2
14	HOXA3	Homeobox A3 transcript variant 1
15	HOXA3	Homeobox A3 transcript variant 2
16	HOXA3	Homeobox A3 transcript variant 3
17	EFNA3	Ephrin A3
18	E2F3	E2F transcription factor 3

Table 3-1. The mRNA targets for miR-210 predicted by the Pictar algorithm.

TargetScan Rank	Gene symbol	Gene name
1	ISCU	Iron-sulphur cluster scaffold homolog
2	GIT2	G-protein16 -coupled receptor kinase interactor 2
3	ZNF462	Zinc finger protein 462
4	DIMT1L	DIM1 dimethyladenosine transferase 1-like
5	FAM116A	Family with sequence similarity 1, member A
6	ARMC1	Armadillo repeat containing 1
7	B4GALT5	UDP-Gal:betaGlcNAc beta 1,4-galactosyltransferase, polypeptide 5
8	MLL2	Myeloid/lymphoid or mixed-lineage leukaemia 2
9	KCMF1	Potassium channel modulatory factor 1
10	FAM73B	Family with sequence similarity 73, member 3
11	EFNA3	Ephrin-A3
12	SYNGAP1	Synaptic Ras GTPase activating protein 1 homolog (rat)
13	BDNF	Brain-derived neurotrophic factor
14	NDUFA4	NADH dehydrogenase (ubiquinone) 1 alpha sybcomplex, 4, 9kDa
15	MID1IP1	MID1 interacting protein 1 (gastrulation specific G12 homolog (zebrafish))
16	ELFN2	Extracellular leucine-rich repeat and fibronectin type III domain containing 2
17	NEUROD2	Neurogenic differentiation 2
18	SCRT1	Scratch homolog 1, zinc finger protein (Drosophila)

Table 3-2. The mRNA targets for miR-210 predicted by the TargetScan algorithm. (Note: The results shown reflect a more recent build of the algorithm than would have been used at the beginning of the project. For instance, ISCU would not have appeared in earlier versions).

Potential miR-210 targets which were common to both search algorithms were considered for further investigation. Of these, potential targets that were more likely to be of relevance to cancer, and were more relevant to pathways in our field of study, were chosen.

3.3 Investigating potential miR-210 targets using miRNA knockdown

The strategy selected for identifying miR-210 targets was to perform loss-of-function experiments through knock-down of miR-210 using miRNA hairpin inhibitors ('miRIDIAN' inhibitors, Dharmacon). Suppression of native miRNA is achieved through specific and irreversible binding to the endogenous miRNA under investigation. The hairpin inhibitors contain chemical modifications that increase the stability and longevity of their binding.

3.3.1 Validation of antimiR-210

Initial experiments were designed to test the efficacy of the miRIDIAN miR-210 inhibitors (referred to henceforth as 'anti-210'). An experiment was carried out to determine the efficacy of anti-210. MCF7 cells were cultured with different concentrations of anti-miR to determine the optimum dose for knockdown in hypoxia. It was established that a 20nM concentration of anti-210 provided optimum knockdown of miR-210 in normoxia, and was sufficient to prevent the hypoxic induction of miR-210 in hypoxia in both MCF7 and MDA-231 cell lines. (Fig. 3-3)

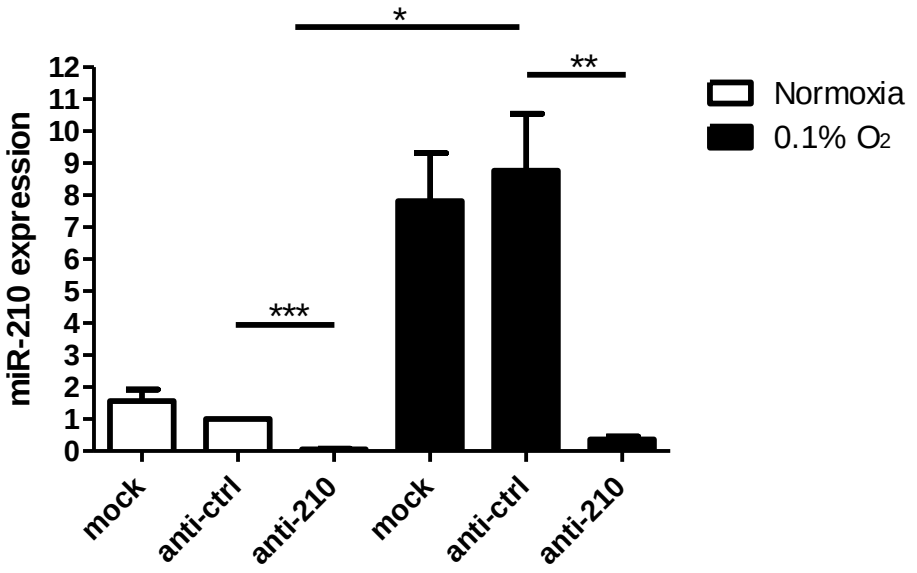


*Figure 3-3. Effect of anti-210 on miR-210 expression in MCF7 cells. MCF7 cells were incubated in normoxia or 0.1% O_2 for 24 hours. They were transfected with either a hairpin control molecule (anti-ctrl - 20nM), anti-210 (20nM), or the oligofectamine carrier molecule alone (mock). The ant-ctrl molecule had no effect on miR-210 expression in normoxia or hypoxia. Anti-210 efficiently knocked-down miR-210 in normoxia, and was sufficient to block the hypoxic induction of miR-210. Plotted = mean + SEM, N=3. *p < 0.05, **p < 0.01, ***p < 0.001, T-test.*

3.3.2 miR-210 inhibitors specifically knocked down miR-210

The effect of the anti-210 on another miRNA, miR-21 was evaluated as a control, to ensure the specificity of the knockdown. Expression of miR-21 did not change significantly in hypoxia, nor was it affected by the anti-miR-210 transfection. (Fig. 3-4)

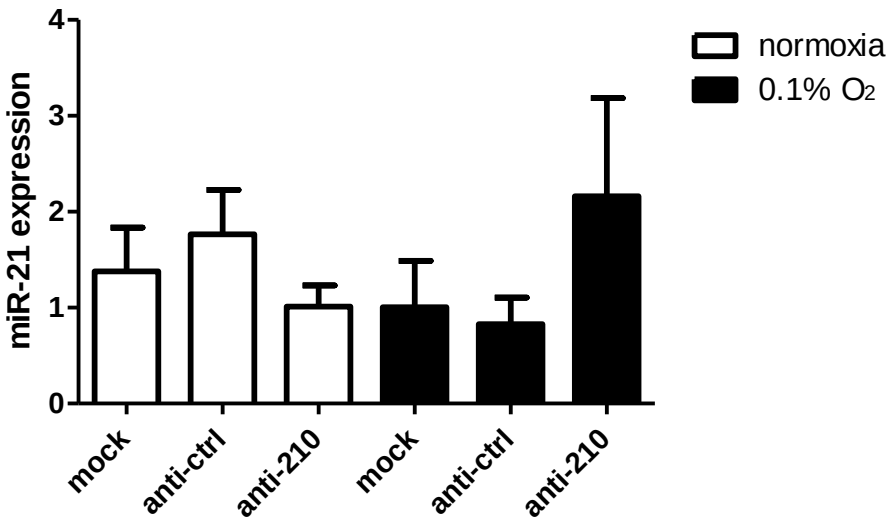
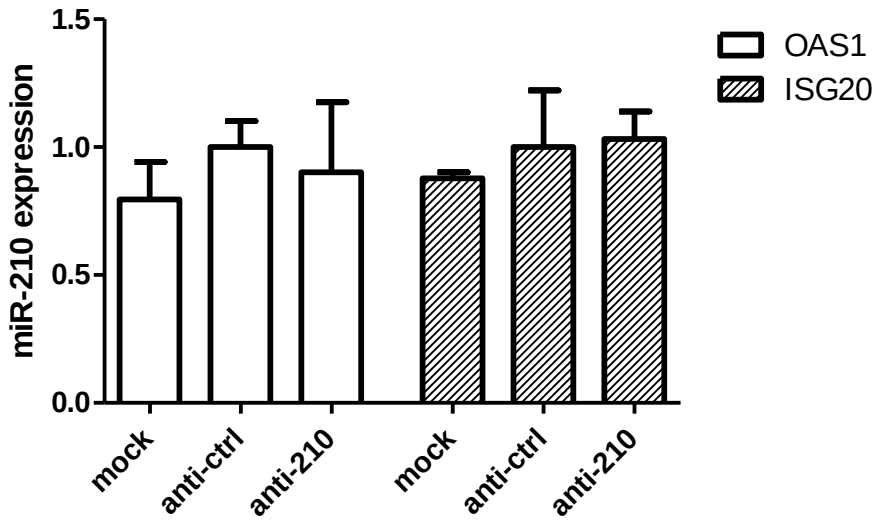


Figure 3-4. The effect of anti-210 on miR-21. MCF7 cells were incubated in normoxia or 0.1% O_2 for 24 hours. They were transfected with either a hairpin control molecule (anti-ctrl - 20nM), anti-210 (20nM), or the lipofectamine carrier molecule alone (mock). miR-21 expression was not significantly affected by anti-210, or hypoxia. Plotted = mean + SEM, N=3.

3.3.3 Anti-210 does not induce an interferon response

Small RNA molecules can stimulate a response in cells, which mimics exposure to viral particles. This response is mediated by interferon, and results in the up-regulation of several genes which are involved in the defence against viral particles. Stimulation of this response following RNAi transfections can invalidate any observed results or phenotypes, and it is therefore important to ensure this is not occurring. The expression of Interferon-stimulated exonuclease gene (ISG20) and 2',5'-oligoadenylate synthetase 1 (OAS1) were measured by qRT-PCR. There was no up-regulation of OAS1 or ISG20 induced by transfection of anti-miR reagents. (Fig. 3-5)



Fig

Figure 3-5. Effect of anti-210 on interferon-responsive genes in normoxia. MCF7 cells were transfected with ant-ctrl or anti-210 molecules. After 24 hours, the expression of interferon-responsive genes OAS1 and ISG20 was measured. There was no induction of expression of these genes following transfection of these molecules. Plotted=mean+SEM, N=3.

3.4 Searching for predicted targets using anti-miR-210

In principle, knock-down of a miRNA should result in de-repression of its target mRNA transcripts, resulting in increased protein expression. Western blotting was chosen as the method to investigate the effect of anti-miR-210 on potential targets' protein expression in both normoxia and hypoxia.

3.4.1 Anti-210 does not directly affect hypoxic HIF induction

Although the HIFs were not computationally predicted targets of miR-210, it was decided to investigate the effect of anti-210 on HIF and some of its targets to ensure that no reciprocal inhibition of HIF by miR-210 was occurring in hypoxia. The expression of HIF-1α, HIF-2α, and HIF-1 targets carbonic anhydrase 9 (CA9), and pyruvate dehydrogenase kinase 1 (PDK1) were measured in normoxia and

hypoxia, with or without anti-210. Hypoxic induction of the HIFs and their targets occurred as normal, and were unaffected by anti-210 transfection. (Fig. 3-6)

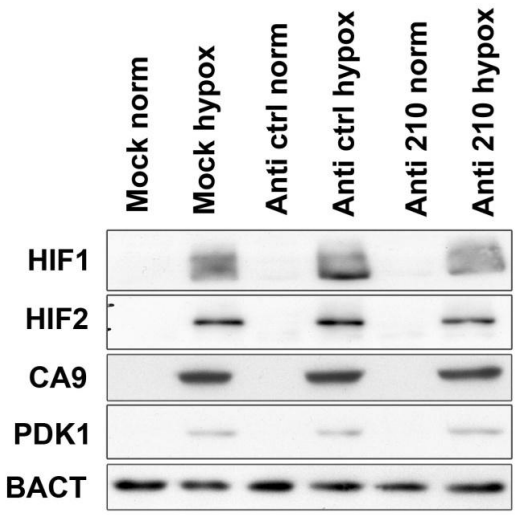


Figure 3-6. The effect of anti-210 on HIF, CA9, and PDK1 expression. MCF7 cells were transfected with anti-ctrl or anti-210, and incubated in normoxia or 0.1% O_2 for 24 hours. Protein induction of the HIFs, and their targets CA9 and PDK1 was normal and unaffected by anti-miR transfection.

Lactate dehydrogenase A (LDHA, which is known to be induced by HIF) and LDHB are enzymes known to catalyze the conversion of lactate to pyruvate in the final step of the anaerobic glycolysis pathway. The effect of hypoxia and anti-210 on these molecules was evaluated as in the experiment above. LDHA exhibited up-regulation in hypoxia, as expected, but neither subtype was affected by transfection with anti-210. (Fig. 3-7)

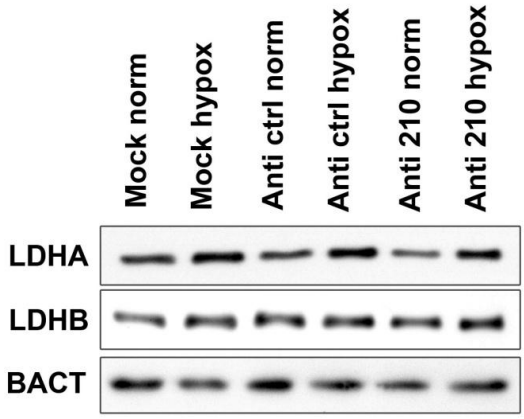


Figure 3-7. Effect of anti-210 on LDHA and B. MCF7 cells were incubated in normoxia or 0.1% O_2 for 24 hours with mock, anti-ctrl or anti-210 transfection. LDHA expression increased in hypoxia. Anti-210 did not affect expression.

3.4.2 Neuronal Pentraxin 1

Neuronal Pentraxin 1 (NPTX1) is part of a family of long-pentraxins which are homologous to the c-reactive and acute-phase proteins of the immune system. NPTX1 was found to be induced in rat brain following hypoxic injury. Blockade of NPTX1 in central nervous system hypoxia models in rat brain appeared to confer a protective effect.(*128*) NPTX1 was predicted as a target by the Pictar algorithm, and it was therefore decided to investigate the effect of anti-210 on its expression. Initial experiments with MCF7 and MDA-MB-231 cells were inconclusive as the protein was expressed at very low levels, if at all, in the breast cancer samples. (Fig. 3-8)

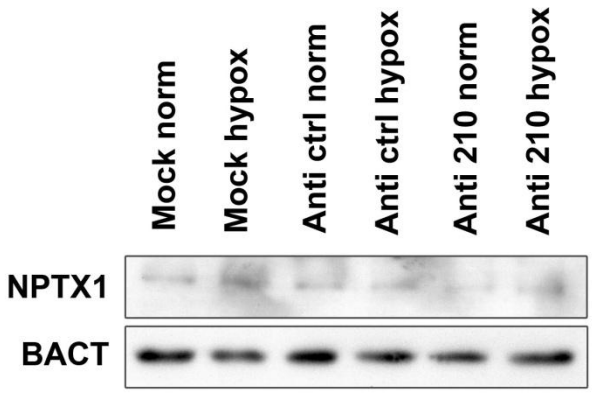


Figure 3-8. NPTX1 was poorly expressed, if at all, in MCF7 cells. There was no apparent effect of anti-210 on protein expression.

In view of the above, and that NPTX1 is known to be expressed primarily in the central nervous system, glioblastoma cell lines were obtained and cultured. They were incubated in normoxia and hypoxia for 24 hours, and NPTX1 expression was measured by Western blotting. This time, it was possible to detect a protein band clearly. However, there was no effect of hypoxia on the expression of NPTX1, and therefore the molecule was not investigated further as a target. (Fig. 3-9)

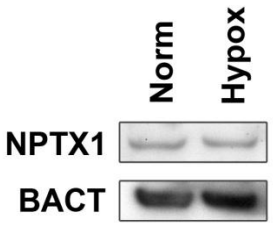


Figure 3-9. The effect of hypoxia on NPTX1 expression. 24 hours of incubation in 0.1% O_2 had no effect on NPTX1 expression in glioblastoma cancer cell lines.

3.4.3 Activin Receptor Type-1B

Activins are known to have roles in embryogenesis, stem cell differentiation, glucose metabolism, and in the immune response. Activin receptor type-1B (ACVR1B) acts as a transducer for activin and other similar ligands, and its regulation in hypoxia could therefore have significant effects on the cell.(*129*) However, ACVR1B was not demonstrated to be regulated in hypoxia, nor was it sensitive to anti-210 transfection. (Fig. 3-10)

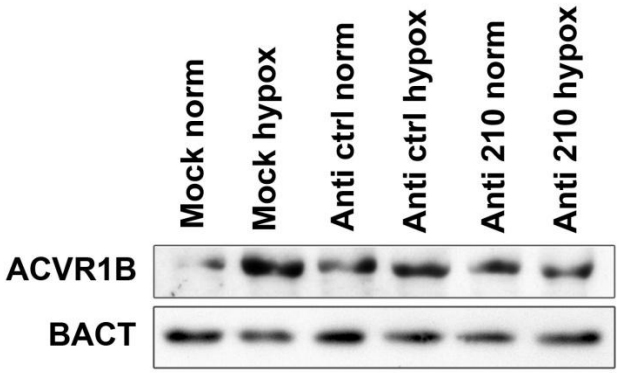


Figure 3-10. The response of ACVR1B to hypoxia and miR-210 knockdown. ACVR1B was not regulated by hypoxia or miR-210 loss-of-function.

3.4.4 NDUFA4 and other investigated targets

NDUFA4 (NADH dehydrogenase 1 alpha subcomplex 4) is a component of complex I of the mitochondrial electron transfer chain. Although an antibody to this protein was not available at the time, a collaborator kindly provided an antibody to complex I. Although the complex I antibody worked well, there appeared to be no effect of hypoxia or anti-210 on the expression of complex I.

Antibodies for Ephrin A3 (EFNA3) and the E2F3 transcription factor were obtained but in both cases the assay worked poorly and no effect of hypoxia or miR-210 loss-of-function was demonstrated.

3.5 Use of anti-210 to look for miR-210 targets with microarrays

The search for targets using target prediction algorithms alone was proving unsuccessful. Therefore, it was decided to employ the use of microarray technology to look for targets. This was carried out using the principle that miR-210 would likely have an effect on mRNA expression as well as protein expression, as discussed in chapter 1.

MCF7 cells were cultured in normoxia or hypoxia (0.1% O_2 for 48 hours), and incubated with either anti-210, or a control molecule. The experiment was performed in biological triplicate, and gene expression was measured using Illumina human genome arrays. Table 3-3 shows the results of this experiment. The interaction score is the difference between the fold change (Log2) in gene expression caused by hypoxia, between the anti-ctrl experiment and the anti-210 experiment. The interaction score thus represents the genes whose down-regulation in hypoxia is most rescued by miR-210 knockdown, in an attempt to increase specificity for target identification. Only genes which are down-regulated in hypoxia (in the control group) by greater than 0.1 (log2) were included in the analysis. The adjusted p-value was calculated using the Benjamini-Hochberg method. Note that the genes in the table are ranked by interaction score, and not p-value, though all reach statistical significance.

Gene	Log2 Fold Change in Hypoxia		Interaction	adj.P.Val
	anti-ctrl	anti-210		
ISCU	-0.482	-0.129	0.353	0.017
AMDHD2	-0.761	-0.487	0.274	0.032
DIMT1L	-0.335	-0.115	0.220	0.014
CITED4	-1.045	-0.889	0.156	0.027
CA12	-0.845	-0.691	0.155	0.018
PAOX	-0.500	-0.349	0.151	0.016
GCAT	-0.554	-0.404	0.150	0.040
L1CAM	-0.168	-0.019	0.149	0.038
RARA	-0.247	-0.119	0.127	0.041
C14ORF129	-0.430	-0.312	0.119	0.049
C1ORF31	-0.243	-0.126	0.117	0.030
RAB30	-0.400	-0.282	0.117	0.014
YARS2	-0.246	-0.130	0.116	0.050
RICS	-0.246	-0.135	0.112	0.043
ERGIC1	-0.380	-0.269	0.111	0.027
KIAA0391	-0.420	-0.312	0.108	0.030
FAIM3	-0.250	-0.147	0.103	0.047

Table 3-3. Genes down-regulated in hypoxia ranked by the degree of rescue in expression by miR-210 knockdown (anti-210).

The genes were then analysed for the presence of putative miR-210 binding sites, using prediction algorithms previously described, and BLAST analysis of the miR-210 seed region. It was found that ISCU, AMDHD2 and DIMT1L contained potential miR-210 binding sites.

3.7 Discussion

The initial aim of this project was to identify miRNAs up-regulated in hypoxia. The first approach to this was to use in-house manufactured microarrays. The infancy of the application of this technology to miRNA expression profiling was demonstrated in the technical problems that ensued. One of the principal difficulties in determining the expression of miRNAs is the very short length of the mature molecules – about 21 nucleotides. This cans result in reduced specificity of binding of cDNA to the probes, with increased variability of results. Non-specific binding of the cyanine reporter dyes caused multiple false positive results in the in-house manufactured arrays, which also suffered from poor image quality manifesting as high signal to noise ratios.

Commercially available arrays from companies such as Illumina and Agilent were used by other members of the research group to look at the effect of hypoxia on RCC4 renal cancer cells. These platforms had a much better signal to noise ratio, were much more reproducible between experiments, and produced statistically significant results. miR-210 emerged as the most up-regulated miRNA in hypoxia, and this was confirmed by qRT-PCR. miR-210 correlated positively to a hypoxia metagene score in breast cancer samples, and its high expression in tumours correlated to a poor prognosis in the breast cancer patients.(*127*) It was therefore decided that the project would focus on miR-210, with a view to determining its targets and performing functional studies of this miRNA.

A number of potential targets as predicted by the *in silico* algorithms previously described were highlighted for further investigation. It should be remembered that, during the course of this project, these algorithms were frequently refined and updated. Thus, the targets predicted for a given miRNA were prone to

change as the algorithms were developed. Nevertheless, a group of targets including ACR1B, NPTX1, EFNA3 and E2F3 were selected for further investigation. The experimental design looked at the effect of loss-of-function of miR-210 in both normoxia and hypoxia. Of these initial targets selected, none were proven to be affected by either hypoxia or the use of anti-210 transfection. In some cases, the protein was expressed too poorly to draw any firm conclusions.

The lack of success with finding targets at this stage could be down to a number of reasons. Firstly, the effect of the miRNA could be very subtle, and significant translational regulation could rely on the cooperative binding of a number of different miRNAs to the UTR. The expression of miR-210 may be too low within the cell (even in hypoxia) to cause a significant effect. The expression of miRNAs in different cell types varies greatly, and the effects of miRNAs on their targets could also vary significantly, which could be due to redundancy in the control over certain targets. One could speculate that certain tumour cell lines harbour mutations in the UTRs of certain genes, which would prevent the binding of miRNAs which would originally have targeted the gene.

Of course it is possible that some, or indeed all of the targets, were predicted in error by the algorithms. On comparison of the miR-210 target predictions between algorithms, it is immediately obvious that there is considerable variation in the targets predicted, indicating that the positive prediction value of the algorithms is probably far from ideal. There are also issues in that the cell line under investigation will not always express a particular target protein. Some protein targets that were of interest, for example KCMF1 or GPD1L, could not be

investigated due to the lack of a commercially available antibody to enable immunoblotting.

NDUFA4, as a target of complex I of the mitochondrial electron transfer chain, was an intriguing prospect for a miRNA target. NDUFA4 is only one of 45 subunits that make up this large structure, but it is found in a central region which bridges two larger parts of the molecule. It was therefore speculated that down-regulation of this protein by miR-210 could result in impaired assembly or degradation of complex I as a whole. Due to the lack of an antibody specific for NDUFA4, the only option was to look at an antibody raised against complex I as a whole. The experiment demonstrated that there was no change in complex I expression in hypoxia, nor was it affected by miR-210 knockout. However, the experiment does raise some important points on interpretation of miRNA experiments. Firstly, one might expect the half life of a large structure to be quite long, and even if there was failure of assembly of the complex I due to NDUFA4 down-regulation, this may not become apparent for a time period much greater than 24-48 hours. This principle, of course, would be applicable to any other protein target under investigation. Additionally, the lack of change in overall complex I expression is not proof that its function is not impaired. Proof of this would require further functional assays specific to complex I function.

At this stage, attempts to validate a predicted target using loss-of-function of miR-210 experiments in hypoxia had proved unsuccessful. However, the use of anti-210 in the microarray study uncovered three genes rescued in hypoxia with potential miR-210 binding sites. Recent updates to one of the target prediction algorithms, TargetScan, resulted in a new set of genes appearing as potential miR-210 targets. The Iron Sulphur Cluster Homolog (ISCU) was now the highest

predicted target of the latest build of the TargetScan algorithm. It was decided to investigate this target with the methods previously described, but this time also incorporating *gain*-of-function assays. The investigation and validation of ISCU as a target is the subject of the following chapter.

CHAPTER 4 - Results
ISCU target validation

4.1 Introduction

4.1.1 Iron Sulphur Clusters

Clusters of non-heme iron and inorganic sulphide (Fe-S clusters) form an essential family of prosthetic groups in nature. They have great structural and functional diversity due to the versatility of both iron and sulphur chemistry (Figure 4-1). The ability of iron-sulphur clusters to delocalize electron density over the iron and sulphur atoms enables them to act as electron transporters, and they have a role as essential co-factors for many enzyme activities.(*130*)

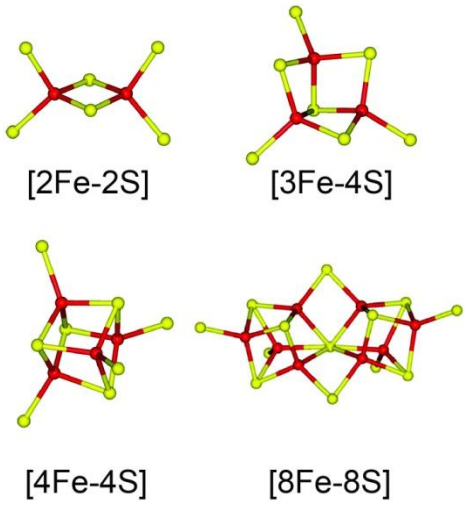


Figure 4-1. Structure of iron-sulphur clusters. The chemical versatility of iron and sulphur enables a diverse collection of iron-sulphur clusters. Red=Iron, Yellow= Sulphur(130)

4.1.2 Biological functions of iron-sulphur clusters

One of the principal functions of Fe-S clusters is to act as an electron donor or acceptor in redox reactions of the cell. This makes them vital components of the respiratory electron transfer chain, forming integral parts of complexes I, II and III within the mitochondria. Furthermore, they are important in components of the tricarboxylic acid (TCA) cycle, acting as components of aconitase and succinate dehydrogenase.(*131*) The Fanconi anaemia group J protein (FancJ) and the *Xeroderma pigmentosum* group D protein (XPD) are components of the DNA damage recognition and repair pathways, and these enzymes require Fe-S clusters to facilitate their activity. (*132*) Cellular iron regulation is another example of Fe-S cluster importance. The enzyme aconitase exists in the cell in two forms. Mitochondrial aconitase acts as part of the TCA cycle. Cytosolic aconitase is bi-functional. In the absence of an Fe-S cluster, its function shifts from that of an aconitase to a translational regulator, known as iron-regulatory protein 1 (IRP1). This protein binds to iron-responsive elements (IREs), resulting in translational repression of the iron-storage protein ferritin, and increased translation of the transferrin receptor.(*133*)

4.1.3 ISCU and the biogenesis of iron-sulphur clusters

Construction of a Fe-S cluster first requires the extraction of a sulphur atom from the amino acid cysteine, which is achieved by a desulferase such as ISCS (cysteine desulferase), and then its transfer to a scaffold protein. The iron-sulphur cluster homolog (ISCU) protein is an example of such a scaffold protein that is able to assemble [2Fe-2S] or [4Fe-4S] clusters, and donate these to other proteins requiring them. Other proteins are involved in the assembly – for example Frataxin (FXN) likely facilitates iron delivery to the scaffold (*134*), while assembly

of the clusters on the scaffold is facilitated by redox proteins such as ferredoxin 1 (FDX1) and ferredoxin reductase (FDXR).(*135*) Numerous other proteins are involved in conformational change and maturation of Fe-S cluster proteins.(*131*)

4.1.4 Iron sulphur clusters in human disease

The importance of Fe-S clusters is reinforced by the presence of a number of diseases caused by their dysregulation. The frataxin gene is mutated in 1-2 per 50,000 live births, and results in the syndrome known as Friedrich ataxia. The resulting deficiency of aconitase and complex I-III, in addition to increased mitochondrial iron in the heart, leads to progressive limb and gait ataxia, hypertrophic cardiomyopathy, and early death.(*136, 137*) Sideroblastic anaemia is caused by mutation in glutaredotoxin (GNRX5), which acts as an intermediate Fe-S cluster carrier protein. The erythroblasts and macrophages of sufferers display increased iron staining, and there is reduced aconitase activity in their peripheral blood mononuclear cells.(*138*)

Homozygous intronic mutation in ISCU results in a splicing defect leading to reduced mRNA production. This results in a myopathy that is associated with severe exercise intolerance(*139*), lactic acidosis(*140*), muscle swelling and pain, and myoglobinuria. Examination of muscle biopsies in these patients reveals deficiency in succinate dehydrogenase and aconitase, as well as significantly increased mitochondrial iron. (*140*)

4.1.5 Rationale for selection of ISCU as a potential miR-210 target

We know that continued hypoxia leads to the generation of reactive oxygen species (ROS) by complexes, I, II and III of the mitochondria.(*141, 142*) Generation

of ROS by the mitochondrial complexes has been the subject of controversy, but it is now widely accepted to be the case.(*143*) miR-210 is predicted by the TargetScan algorithm to target ISCU. In the context of hypoxia, this could represent an important regulatory mechanism for mitochondrial respiratory electron chain activity, as well as lactate and iron metabolism. In light of the findings of experiments in the previous chapter with anti-210, the principal aim of this chapter was, therefore, to validate ISCU as a target of miR-210.

4.2 ISCU is down-regulated by hypoxia and miR-210

Because miR-210 expression in hypoxia is greater at 48 hours than 24 hours, and in order to allow greater time for an effect of increased miR-210 levels on protein expression to occur, the following experiments were carried out for 48 hours post transfection and incubation of cells. MCF7 cells were transfected with anti-miR-210, or control molecule (anti-ctrl), in normoxia or hypoxia, and miR-210 mimic (mim-210) or control molecule (mim-ctrl) in normoxia. The mimic molecules are chemically modified double-stranded RNAs designed to replicate a gain-of-function effect of endogenous mature miRNAs. Following protein extraction, the samples were immunoblotted for ISCU and β-actin as a loading control. HIF-1α and HIF-2α were also immunoblotted to ensure the expected hypoxic response was occurring in the cells. As shown in figure 4-2, the expression of ISCU in the cells decreases markedly in hypoxia after 48 hours. Transfection of anti-210 partially rescues the effect of ISCU down-regulation in hypoxia, whereas transfection of mim-210 dramatically reduces expression of ISCU in normoxia. The reciprocal effects of miR-210 knock-down and gain-of-function assays provide strong evidence that ISCU is a genuine target of this miRNA.

HIF-1α was induced in hypoxia, acting as evidence for true hypoxia in the incubators, and the normal activation of the HIF response to hypoxia despite the presence of transfected agents in the cell. HIF-1 was not detectable in normoxia.

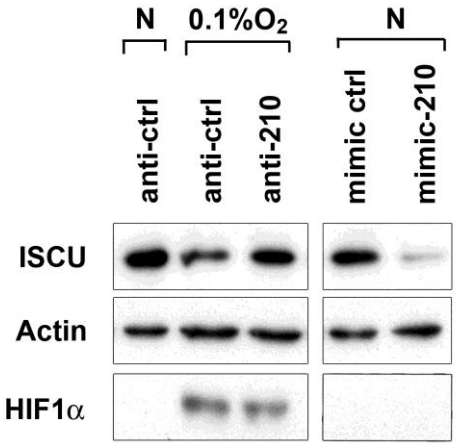


Figure 4-2. MCF7 cells were transfected with anti-ctrl, anti-210 or mimic-210, and cultured in normoxia or hypoxia for 48 hours. ISCU was down-regulated in hypoxia, and this effect was partially reversed by anti-210.Transfection of mim-210 down-regulated ISCU in normoxia.

4.2.1 miR-210 targets both cytosolic and mitochondrial ISCU

A previous study has shown that two forms of ISCU exist, both deriving from the same pre-mRNA, but differing in size due to alternative splicing. ISCU1 encodes a 142 amino acid protein, and has a predicted molecular mass of 15.4 kDa, and is located primarily in the cytosol and nucleus of the cell. ISCU2 encodes a 168 amino acid protein, and has a predicted molecular mass of 17.9 kDa.(*144*) As can be seen from figure 4.2.1, ISCU immunoblots as a single band, and it is difficult to determine whether it represents ISCU1, ISCU2, or a merged band of both subtypes. Examination of the 3'UTR sequences harbouring the potential miR-210

binding sites revealed that they were identical in both ISCU 1 and 2. In theory, therefore, miR-210 should target them both equally well.

In order to demonstrate this, MCF7 cells were transfected with mimic-ctrl, mimic-210, a scramble siRNA or a siRNA to ISCU (siISCU). The siISCU had been designed using the Roche Universal Probe Library siRNA designer software, and validated on other samples (data not shown). Following transfection and incubation in normoxia for 48 hours, the cellular extract was purified in to both cytosolic and mitochondrial fractions. These were immunoblotted for ISCU, βactin (as a cytosolic-specific loading control) and Tom 20 (as a mitochondrial-specific loading control (mitochondrial import receptor subunit)). The mitochondrial fraction expressed only the Tom20 control, whereas the cytosolic fraction expressed only the β-actin contol, indicating that the purification of each fraction was successful. Both fractions immunoblotted positively for ISCU, demonstrating that the antibody can successful detect both ISCU1 and ISCU2. Importantly, mimic-210 and siISCU both down-regulated ISCU in the mitochondrial and cytosolic fractions when compared to their respective controls. (Fig. 4-3)

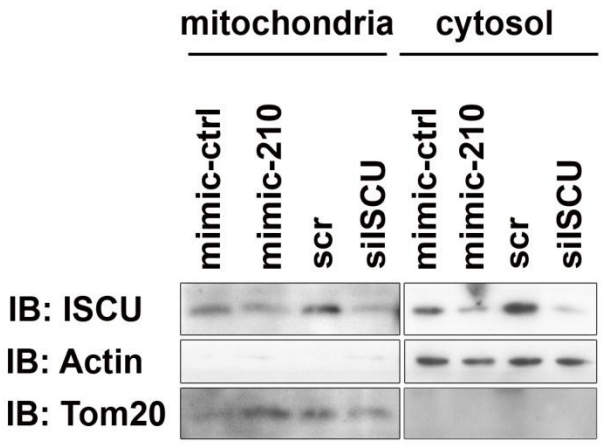


Figure 4-3. Mitochondrial and cytosolic fractions of MCF7 cells, following incubation with mimic-210 or siISCU and their respective control molecules, were immunoblotted for ISCU, Tom20 and β-actin. miR-210 and siISCU down-regulated both cytosolic and mitochondrial ISCU.

4.2.2 Knockdown of ISCU by miR-210 is dose-dependent

MCF7 cells were incubated with either a 20nM or 100pM concentration of mimic-210. The 100pM concentration resulted in an approximately two-fold down-regulation of ISCU, whereas the 20nM concentration reduced its expression to a much greater extent. (Fig. 4-4 A&B)

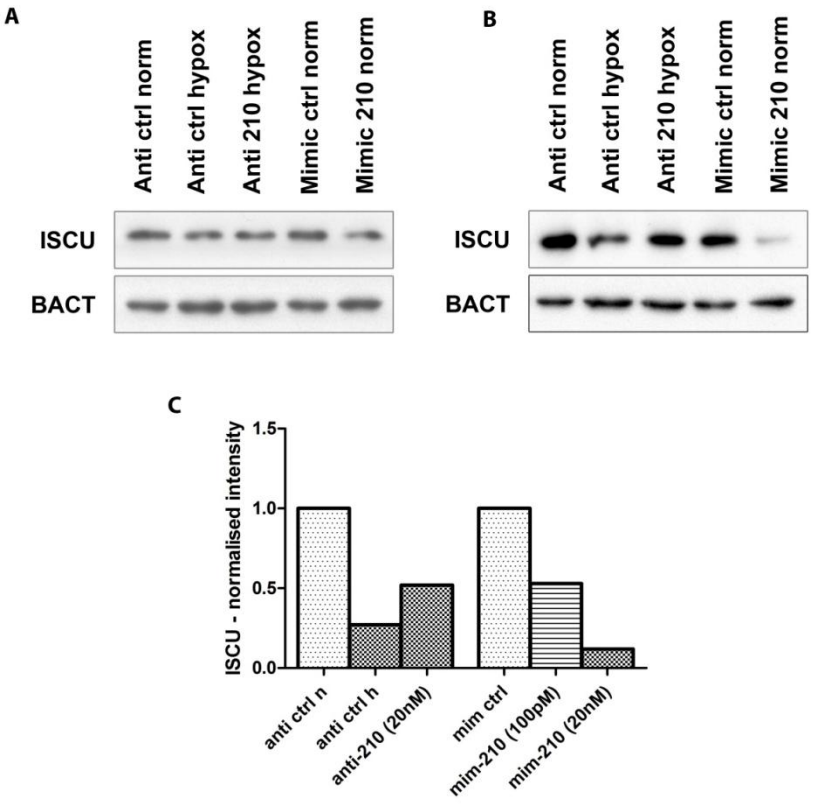


Figure 4-4. The effect of concentration of transfection reagents on ISCU expression – pilot experiment. A. Effect of anti-210 and mimic-210 at 100pM concentrations. B. Effect of ant-210 and mimic-210 at 20nM concentrations. C. Quantification of ISCU expression as normalised band intensity. N=1

The effect of anti-210 in a rescuing ISCU expression in hypoxia could only be observed with the higher concentration of 20nM. The immunoblots were analysed for band intensity using ImageJ software (Broken Symmetry Software). Figure 4.4.1 C shows ISCU expression as immunoblot intensity normalised to β-actin control. A rescue of approximately 25% of normoxic ISCU expression is seen in hypoxia with anti-210 at a 20nM concentration.

While the effect of mimic-210 is clear, the effect of anti-210 is much more subtle. The experiment was therefore completed in quadruplicate and ImageJ

quantification undertaken to determine if the rescue was statistically significant. As shown in figure 4-5, the rescue is reproducible and statistically significant.

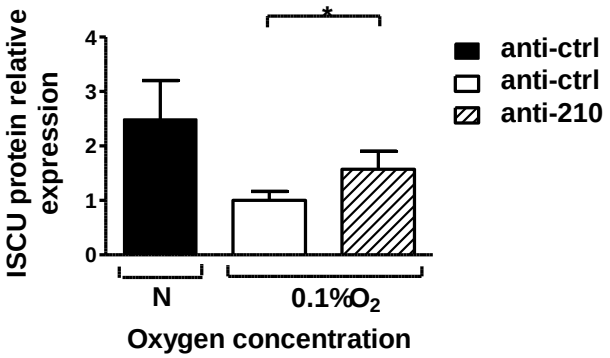


*Figure 4-5. Rescue of ISCU expression in hypoxia with anti-210. MCF7 cells were incubated normoxia or 0.1% O_2 for 48 hours with anti-ctrl or anti-210. Anti-210 provided a statistically significant rescue in hypoxia. Plotted = ISCU band intensity normalised to actin control intensity. N=4, * p <0.05, unpaired T-test.*

4.5 miR-210 down-regulates ISCU in multiple cell lines

Following confirmation of ISCU as a target in MCF7 cells, it was decided to test the effect of miR-210 over-expression and knock-down in other cell lines, Those chosen were PC3 (prostate cancer), SCC25 (squamous cell carcinoma) and PEO1 (ovarian cancer).

4.5.1 anti-210 and mimic-210 in PC3 cell lines

As with MCF 7 cells, hypoxia induced a reduction in ISCU expression, which was reproduced by incubation of the cells with mimic 210. The level of ISCU repression was again dose dependent, with 20nM concentrations providing a much greater knockdown of ISCU. Unlike MCF7, however, a rescue with anti-210 in hypoxia was not observed. (Fig. 4-6)

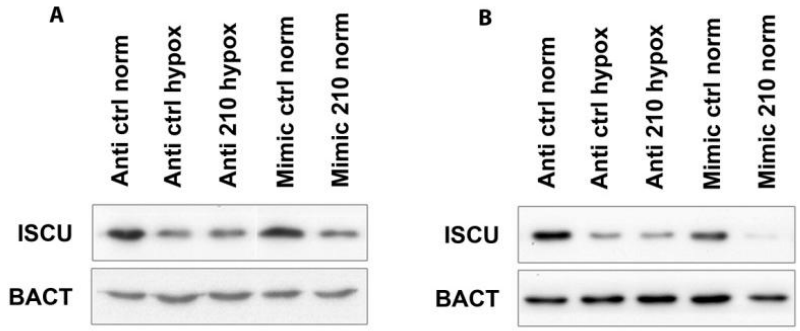


Figure 4-6. The effect of miR-210 on ISCU in PC3 cells. A. Effect of anti-210 and mimic-210 at 100pM concentrations. B. Effect of anti-210 and mimic-210 at 20nM concentrations.

4.5.2 anti-210 and mimic-210 in SCC25 cell lines

The experiment in section 4.5.1 was repeated in SCC25 ovarian cancer cell lines. As with PC3 cells, the mimic-210 transfection reduced ISCU expression in a dose-dependent fashion. Hypoxia alone was sufficient to reduce ISCU expression in these cells. Again, transfection with anti-210 did not produce a rescue in this cell line.

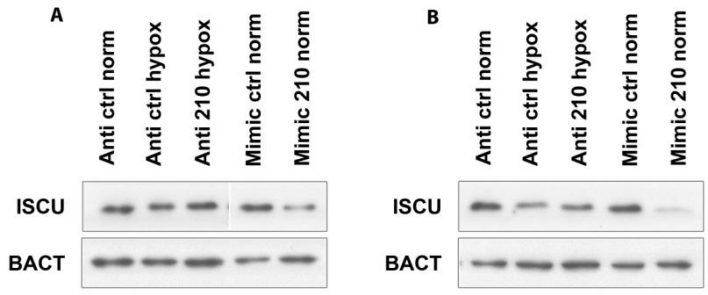


Figure 4-7. The effect of miR-210 on ISCU in SCC25 cells. A. Effect of anti-210 and mimic-210 at 100pM concentrations. B. Effect of anti-210 and mimic-210 at 20nM concentrations.

The knock-down of ISCU in hypoxia is 2-fold, which is less than that in the MCF7 and PC3 cells (about 4-fold knockdown in hypoxia).

4.5.3 miR-210 knocks down ISCU in PEO1 cell lines

PEO1 ovarian cancer cell lines were chosen for investigation because they harbour a homozygous deletion for the miR-210 gene.(*145*) Experiments by a colleague used qRT-PCR to determine the miR-210 expression in these cells. It was found that, although miR-210 was detectable, it was expressed at a much lower level than in the other cells under investigation here.

PEO1 cells cultured in hypoxia showed a reduction in ISCU expression, despite the low expression of miR-210, suggesting that another mechanism for ISCU down-regulation must be present. Transfection with mimic-210 at 20nM concentrations resulted in a reduction in ISCU expression, though not as marked as in MCF7, PC3 or SCC25 cells. Mimic-210 at 100pM concentration had little effect (Fig. 4-8).

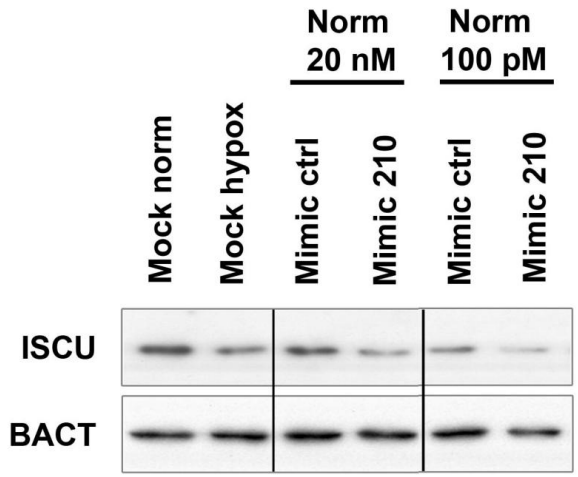


Figure 4-8. Effect of hypoxia and miR-210 on PEO1 cells. PEO1 cells were incubated in normoxia or hypoxia, with of mimic-ctrl or mimic-210. Hypoxia and mimic-210 both reduced ISCU expression.

4.6 miR-210 inhibits ISCU mRNA expression

miRNAs are known to act by both translational repression and mRNA degradation. In order to determine if mRNA degradation was a significant mechanism with ISCU repression, MCF7 and HCCT116 cells were incubated in normoxia or hypoxia, with or without mimic-210 or anti-210. This experiment, performed by a colleague, demonstrated that ISCU mRNA expression was reduced by 40-50% in normoxia, and partially rescued by anti-210. Incubation of the cells with mimic-210 resulted in a 50-70% knockdown of ISCU mRNA expression in normoxia. (*146*)

In order to prove that miR-210 was regulating ISCU through direct binding to the UTR, luciferase reporter constructs containing the 3'UTR of the ISCU gene were made. MCF7 cells transfected with the vectors demonstrated strong suppression of luciferase activity in hypoxia, which was almost completely rescued with anti-210. Transfection with mimic-210 led to a 60% knockdown in luciferase activity in normoxia. (*146*)

4.7 miR-210 over-expression reduces aconitase activity, but not protein expression

As cytoplasmic (Aco1) and mitochondrial aconitase (Aco2) rely on iron sulphur clusters to catalyse the reaction of citrate to isocitrate, it was hypothesized that down-regulation of ISCU by miR-210 over-expression would reduce aconitase activity. The first experiment was designed to look at the effect of mimic-210 and anti-210 on the expression of the aconitase protein expression. Transfection of

MCF7 cells with mimic-210 did not decrease expression of aconitase protein. Additionally, transfection of anti-210 did not reduce aconitase protein expression. (Fig. 4-9)

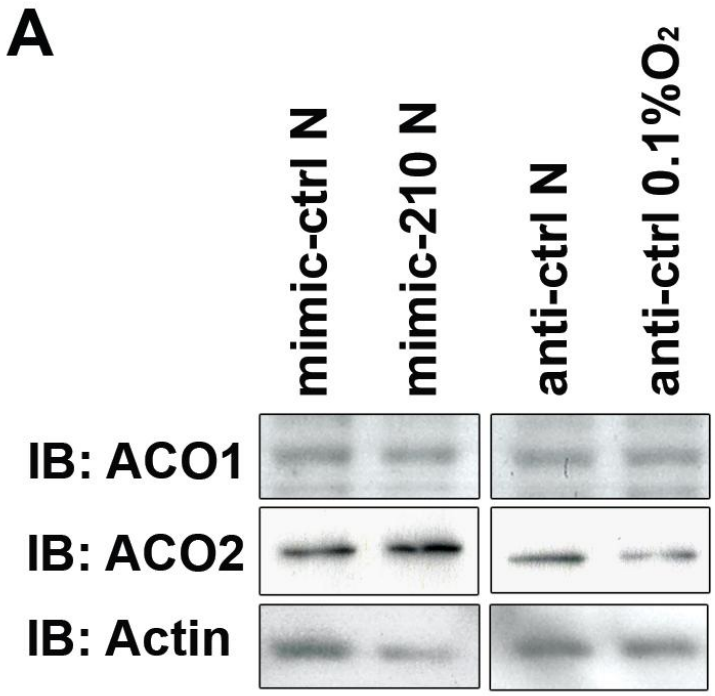


Figure 4-9. Effect of miR-210 on aconitase expression. MCF7 cells were transfected with mimic-210 or mimic-ctrl in normoxia. MCF7s were also transfected with anti-ctrl in normoxia and hypoxia. There was no effect on aconitase protein expression levels.

An experiment, performed by a colleague and presented in our joint paper, was performed to look at the effect of miR-210 and siRNA to ISCU (siISCU) on aconitase activity, using a commercially available assay (Bioxytech Aconitase-340, Oxis International Inc). Incubation of MCF7 cells in hypoxia (0.1% O_2) for 48 hours led to an approximately 50% in decrease in aconitase activity compared to

normoxic controls. Incubation of MCF7 cells in normoxia for 48 hours following transfection with siISCU also led to a 50% decrease in aconitase activity compared to the scramble control transfected cells. Transfection with mimic-210 led to a reduction in aconitase activity of 35-40%, which was statistically significant ($p<0.001$, data not shown). Conversely, transfection with anti-210 in hypoxia led to a rescue of aconitase activity ($p<0.05$, data not shown). Similar experiments looking at mitochondrial complex I activity demonstrated that siISCU and mimi-210 reduced activity in an almost identical fashion to aconitase activity ($p<0.001$, data not shown).

4.8 Iron studies

In theory, down-regulation of ISCU by miR-210 should result in reduced availability of iron-sulphur clusters. As mentioned previously, cytoplasmic aconitase functions as IRP1 in the absence of Fe-S clusters, resulting in up-regulation of the transferrin receptors and increased cellular iron accumulation.(*133*) We therefore hypothesized that over-expression of miR-210 would lead to increased intracellular iron levels.

HCCT116 cells were transfected with siISCU, mimic-210 or their respective controls in normoxia. Following 48 hours incubation, the cells were fixed, stained and mounted. As shown in figure 4-10, depletion of ISCU by siRNA or mimic-210 leads to an increase in intracellular iron staining, consistent with reduced Aco1 activity and increased IRP1 activity.

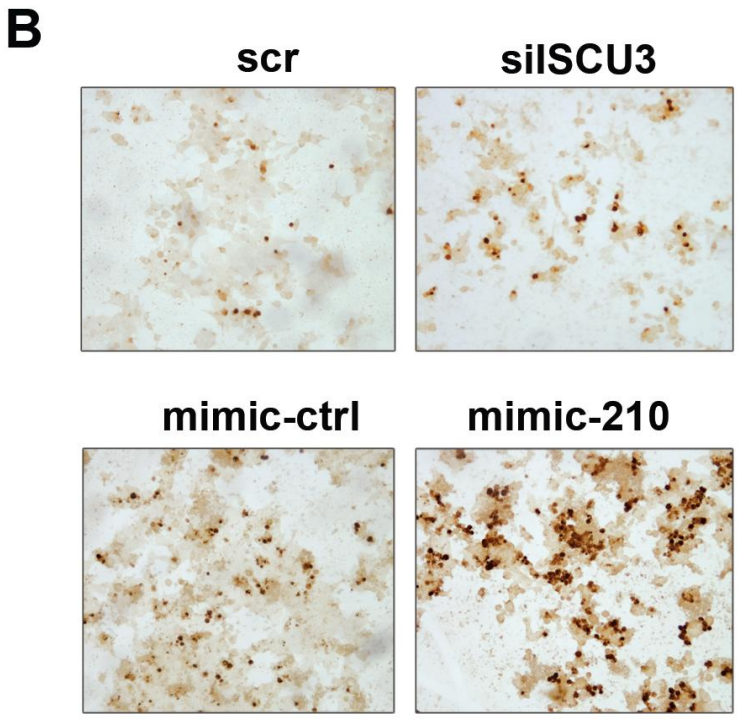


Figure 4-10. Intracellular iron staining of HCCT116 cells transfected with with siISCU or mimic-210 in normoxia. Depletion of ISCU with siISCU or miR-210 resulted in increased intracellular iron staining.

4.9 miR-210 increases free radical and lactate production in normoxia and hypoxia

Experiments by other member of the research group looked at the effect of miR-210 on reactive oxygen species (ROS) in normoxia and hypoxia, using the MitoSox Red kit (Molecular Probes, Eugene, OR, USA). Transfection of MCF7 and HCCT116 cells with miR-210 in normoxia resulted in a 4-fold increase in superoxide concentration. A marked increase in superoxide concentration was also observed

in these cells in hypoxia, and this was almost completely reversed by the addition of anti-210, or by over-expression ISCU through vector transfection ($p<0.001$, data not shown). Lactate production in MCF7 cells in normoxia was observed to increase by 40-50% with mimic-210 transfection, with a corresponding 50% reduction in pyruvate production. Increased lactate production in hypoxia was reversed with transfection of anti-210.

4.10 Discussion

It was decided that a prerequisite for investigating a potential target of miR-210 was that it should be down-regulated in hypoxia if it is to represent a physiologically relevant aspect of miR-210 gene regulation. ISCU was established as being down-regulated in hypoxia at the protein level, and confirmation of the cellular hypoxic response being intact was provided with immunoblots for HIF1 and HIF2, which were both up-regulated in the expected fashion. In MCF7 cells, miR-210 over-expression resulted in a significant decrease in ISCU protein expression, and this was partially reversed by addition of anti-210 in hypoxia. The fact that the reversal is only partial indicates that miR-210 is not likely to be the only mechanism by which ISCU is down-regulated in hypoxia. Indeed, it is well established that hypoxia results in a general reduction in mRNA translation. Hypoxic inhibition of the mTORC1 complex leads to reduced phosphorylation of 4E-BP1. This leads to its increased binding to EIF4E, and resulting in the inhibition of cap-dependent translation.(*147*) Under conditions of endoplasmic reticulum (ER) stress, a process called the unfolded protein response (UPR) is initiated due to the reduced ability of the ER to enable protein maturation, leading to the accumulation of misfolded protein. The UPR will reduce the accumulation of such misfolded proteins by reducing overall translation, and increasing the expression

of molecular chaperones involved in protein folding. Hypoxia is a known activator of the UPR, and this may contribute to some of the hypoxic down-regulation of ISCU.

ISCU was found to be down-regulated in PC3 and SCC25 cell lines, providing evidence that the miR-210 pathway is relevant across multiple cell lines. However, a rescue of ISCU expression with anti-210 was not observed in these cell lines, perhaps indicating a stronger hypoxic suppression of ISCU by one of the mechanisms described above. It is worth noting that our group has confirmed the presence of a rescue effect in HCT116 cell lines, and others have shown a rescue effect in human pulmonary arterial endothelial cells (HPAECs). The down-regulation of ISCU in HPAECs indicates that miR-210 regulation is relevant in primary cell lines as well as tumour cell lines.

PEO1 cell lines, which have a homozygous deletion for the miR-210 gene, were investigated for the effects of miR-210 on ISCU expression. It was found that ISCU expression was reduced in hypoxia despite the low levels of miR-210, indicating another mechanism of control. Nevertheless, ISCU expression did decrease by 2-fold with the addition of mimic, indicating that the mechanism for response to the miRNA is still intact.

ISCU is known to exist in two isoforms, as cytosolic ISCU1 and mitochondrial ISCU2, which have slightly different molecular weights. They did not resolve in to separate bands using SDS-PAGE, so it was important to determine whether both isoforms were present in the cell and if so, whether siISCU and miR-210 had similar effects on both isoforms. Experiments confirmed that both isoforms of ISCU were present, and that both were knocked down using siISCU and mimic-210. Both isoforms would be predicted to be equally affected as they both have

identical 3'UTRs. Establishing the effect of miR-210 on both isoforms is important in interpreting the results of further functional studies of miR-210 and its effect on ISCU expression.

4.10.1 miR-210 and mitochondrial function

The role of HIF1 in altering cell metabolism in hypoxia is well described, causing increased glucose uptake, and a shift towards glycolytic anaerobic metabolism with increased production of pyruvate. It was hypothesized that, due to its effect of knocking down ISCU, miR-210 may aid the cell in hypoxia by depriving key enzymes in the TCA cycle and electron transfer chain of Fe-S clusters, and so reduce oxidative phosphorylation. It was shown that aconitase activity was reduced by miR-210 as well as by hypoxia. Importantly, anti-210 rescued the hypoxic impairment of aconitase, highlighting the physiological relevance of miR-210 in this process. In parallel, an increase in lactate levels, and a decrease in pyruvate was also observed, providing a link by which HIF-1 can control the switch to glycolysis through miR-210 induction and consequent ISCU repression.

Complexes I, II and III of the mitochondrial electron transfer chain contain Fe-S clusters,(*142, 148*) and would thus all be predicted to have reduced function in the presence of reduced ISCU levels. It was decided to measure complex I function and, as expected, this was reduced in the presence of both hypoxia and miR-210 gain-of-function experiments.

Reactive oxygen species (ROS) are oxygen molecules containing an unpaired electron in their outer shell, making them highly reactive. The mitochondria are an important source of ROS, and overproduction of this can lead to mitochondrial damage. (*141*) Mitochondrial dysfunction, manifested as the loss of succinate dehydrogenase (SDH) or fumarate hydratase (FH) activity, has been linked to

tumorigenesis. Paragangliomas with mutations of the SDH D or B subunits have been shown to be particularly vascular and have an activated HIF-angiogenesis pathway.(*149*) FH-deficient tumours have also been shown to have increased HIF activity, along with increased glycolytic enzyme activity.(*150*) A well-described paradox is that of increased ROS production in hypoxia, which has been linked to HIF-1 activity. Excess production of ROS is thought to stabilise HIF further by decreasing PHD activity, thus forming a potential feedback loop in hypoxia. It has also been demonstrated that an intact respiratory chain is required for this to occur, and loss of cytochrome c, or the Rieske Fe-S cluster of Complex III, impairs this 'ROS' signal.(*141*)

The central role of ISCU in Fe-S clusters and its identification as a miR-210 target presented the intriguing possibility that miR-210 could be involved in ROS production through impairment of the respiratory chain. Interestingly, rather than reducing ROS production as a protective mechanism in hypoxia, in our experiments it was found that miR-210 over-expression was responsible for *increasing* the production of ROS in MCF7 and HCT116 cells in normoxia. In hypoxia, the cells exhibited increased ROS production which was almost completely reversible with transfection of anti-210, thus showing an important role of miR-210 in the physiology of this process. Another group studying miR-210 found no increase in ROS upon exposure to hypoxia. However, a reason for this may be that they were investigating normal endothelial cells, in contrast to the cancer cells under investigation in our studies.(*151*)

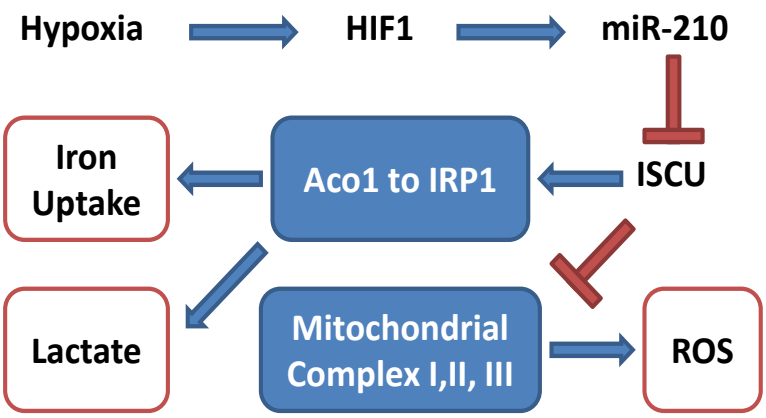


Figure 4-11. The relationship of hypoxia and miR-210 with ISCU, and the physiological consequences to the cell.

In conclusion, ISCU has been proven as a miR-210 target, and via regulation of Fe-S clusters in key enzymes, has a role in regulating important aspects of cell metabolism in hypoxia, via the HIF-1α transcription factor. Increased iron uptake and shift of metabolism away from oxidative phosphorylation are well known traits of cancer, and thus miR-210 represents a potential therapeutic target. Alternatively, miR-210 expression in tumours may reflect the metabolic state of tumours, and help to guide therapy.

CHAPTER 5 – Results
Experiments using constitutive miR-210 over-expression

5.1 Introduction

In this chapter, cells constitutively over-expressing miR-210 were used to assess the effect of the miRNA on cell lines *in vitro* and *in vivo.* In addition, these cells were used in an attempt to investigate miR-210 targets using an RNA fractionation technique, the principles of which will now be described.

5.1.1 Polysomal Fractionation

The principle for the polysomal fractionation experiment is based on the assumption that miRNAs inhibit translation of their target genes.(*90, 91*) Cells which have been treated with cyclohexamide in order to block protein translation were lysed and treated with serial centrifugation to extract the cytoplasmic component of the cell. The lysates were size-fractionated by placing them on sucrose gradients, followed by ultracentrifugation. This results in the heaviest particles travelling the furthest through the gradient, with the lightest remaining near the top. Passing the sucrose gradient through a UV absorbance spectrometer, which serves to detect RNA concentration, results in a graph similar to the following:

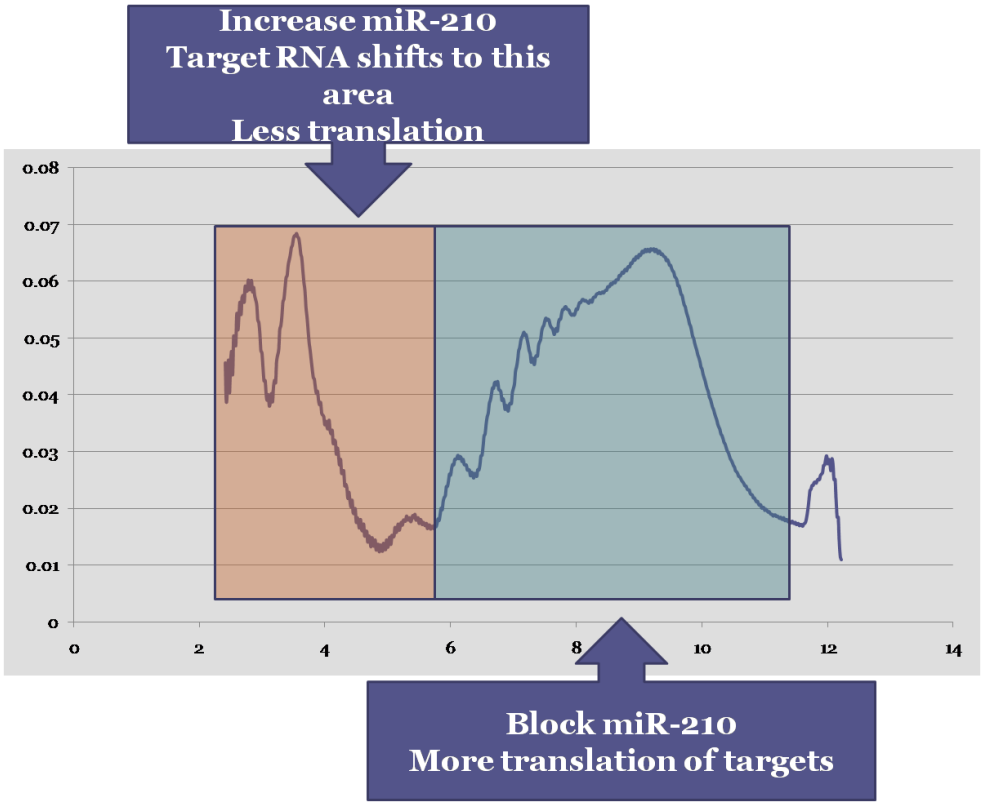


Figure 5-1. RNA absorbance in fractionated RNA. The x-axis corresponds to time, and the y-axis to UV absorbance. The orange section contains monosomal RNA, whereas the blue section contains polysomal RNA.

Figure 5-1 represents RNA concentration on the vertical axis (based on UV absorbance) and molecular weight (represented as time – the top of the gradient is pushed through the spectrometer first, and thus as you travel along the x axis, increasing time corresponds to the heavier molecules in the bottom of the gradient). The orange box in Figure 5-1 represents the part of the gradient containing RNA with one ribosome (monosomes), or no ribosomes attached. The first two peaks represent absorbance spikes from the free ribosomal subunits. The subsequent small peak at the right hand edge represents monosomal mRNA. In the blue region of the graph, further peaks at increasing mass can be seen, each representing the addition of a further ribosome to the mRNA molecules.

This region thus corresponds to polysomal RNA. Due to the higher number of ribosomes bound to the polysomal group, it can be inferred that these mRNAs are being translated with high efficiency. Conversely, those with one or fewer ribosomes bound are undergoing little or no translation.(*152*)

In principle, cells containing a vector causing over-expression of miR-210 should have increased binding of the miRNA to mRNA targets with complementary binding sites in their UTR's or coding regions. One would therefore expect the concentration mRNAs targeted by miR-210 to shift towards the monosomal end of the gradient in the presence of increased miR-210, and vice versa. Microarrays can be used to expression profile the monosomal and polysomal fractions in the cells with miR-210 over-expression or empty vectors, to look for miRNA targets.

5.2 Generation of constitutively over-expressing miR-210 cells

MCF7 and MDA-MB-231 breast cancer cells were transfected, using a method previously described, with pBabe empty vector ($MCF7^{EV}$) or pBabe with a pre-miR-210 insert including ~200 bp flanking sequences ($MCF7^{210}$). The vector was a gift from Dr Mircea Ivan, and was verified by sequencing to ensure the correct nucleotide sequence was present. Confirmation of miR-210 over-expression was made by qRT-PCR for mature miR-210.

miR-210 was up-regulated 5-fold in $MCF7^{210}$ cells, and 17-fold in MDA-MB-231^{210} cells, when compared to their respective cell lines containing an empty vector (Fig. 5-2).

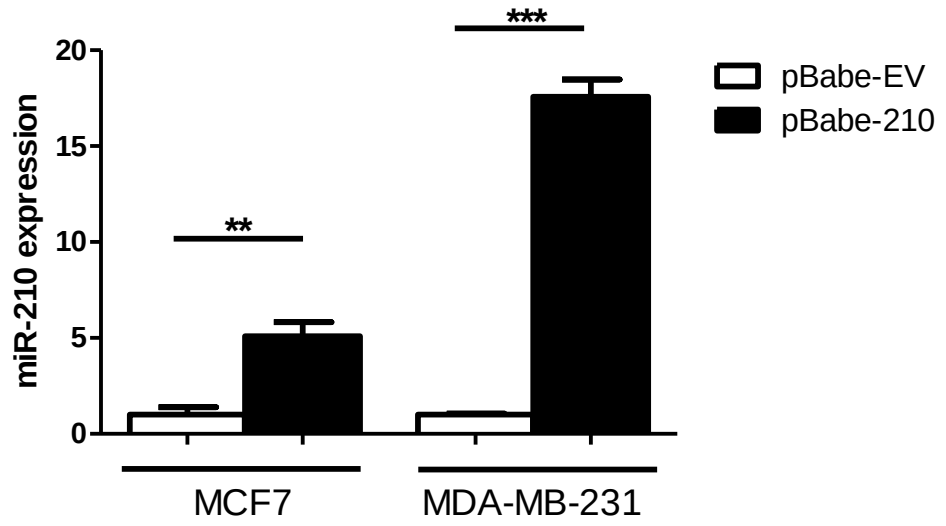


*Figure 5-2. Constitutive over-expression of miR-210 in MCF7 and MDA-MB-231 cell lines using pBabe vectors. MCF7 cells showed a 5-fold up-regulation, and MDA-MB-231 cells showed a 17-fold up-regulation.**p<0.01, ***p<0.001, T-test.*

5.3 The effect of miR-210 over-expression on proliferation in vitro

It was decided to perform cell count experiments with the MCF7 and MDA-231 cells harbouring the pBabe constructs to determine if miR-210 over-expression had an effect on proliferation in either normoxia or hypoxia.

MDA-231 wild type (MDA-231^{WT}), MDA-231^{EV} and MDA231^{210} cells were cultured in normoxia and hypoxia (0.1% O_2) for a period of 5 days. All cells failed to proliferate much under hypoxic conditions. However, there was no difference in proliferation rate between the MDA-231^{WT}, MDA-231^{EV} and MDA231^{210} cells in either normoxia or hypoxia (Fig. 5-3).

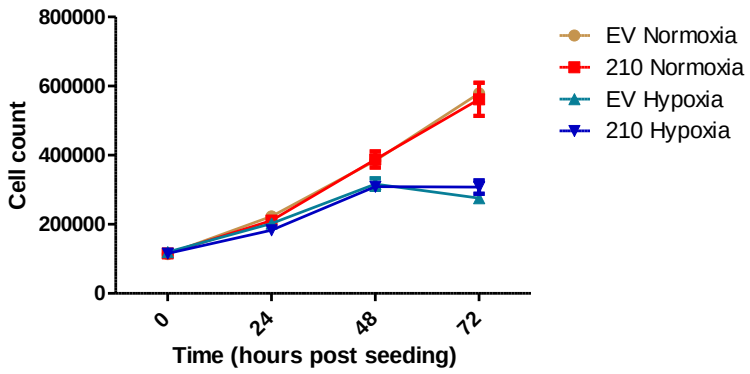


Figure 5-3. Effect of miR-210 over-expression on cell proliferation. Cells were cultured in normoxia or 0.1% O_2. miR-210 over-expression had no effect on growth in normoxia or hypoxia in normal medium. N=3

The experiment was repeated with MDA-231^{EV} and MDA-231^{210} cells in serum-free medium, to determine whether this additional stress was necessary to elicit a phenotype. However as before, no difference in proliferation was seen with increased miR-210 expression (Fig. 5-4).

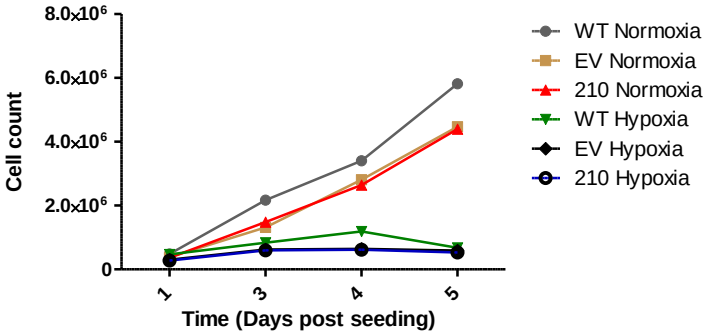


Figure 5-4. Effect of miR-210 in MDA-231 cells in serum-free medium. Cells were cultured in normoxia or 0.1% O_2. No effect of miR-210 over-expression was seen on proliferation rates. N=2.

The above experiment was repeated with $MCF7^{EV}$ and $MCF7^{210}$ cells, which over-express miR-210 to a lesser extent than the $MDA\text{-}231^{210}$ cell line. The results in the MCF7s were consistent with the MDA-231s, demonstrating no difference with miR-210 over-expression in serum-free medium (Fig. 5-5).

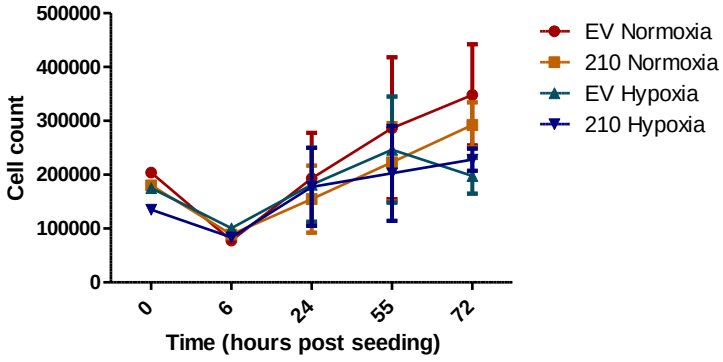


Figure 5-5. Effect of miR-210 over-expression on MCF7 cells in serum-free medium. Cells were cultured in normoxia or 0.1% O_2. No effect of miR-210 over-expression was observed on proliferation rates. N=3

5.4 MCF7 and MDA-231 Xenograft Work

With the in-vitro work not having uncovered any effect of miR-210 over-expression on proliferation, it was decided to investigate its effect in an *in vivo* model. The hypothesis was that a more realistic 3 dimensional model might uncover a phenotype.

5.4.1 Experimental design

Three xenograft experiments were carried out, one involving the MDA-MB-231 cell line, and two involving the MCF7 cell line. In each experiment, ten BALB/c SCID mice received subcutaneous injections, in to the flank, of 10^7 cells in matrigel. Five mice received the pBabe EV-containing cells, and five received cells with the pBabe+miR-210. The MCF7 cells are an oestrogen-dependent breast cancer cell line, and thus the mice used for this experiment required oestrogen supplementation to ensure adequate tumour growth. This was achieved using a slow-release oestradiol pellet placed subcutaneously two days prior to injection of the tumour cells. Three-dimensional tumour size was measured every 3 days. At the end-point, mice were injected with the hydroxyporbe Pimonidazole prior to sacrifice. Following sacrifice, tumours were collected – 50% of the tumour was snap frozen in liquid nitrogen, and 50% was fixed in formalin overnight. The organs were examined for metastases. The serum was collected from the mice and stored at -80°C.

5.4.2 Tumour proliferation

The first experiment with the MCF7 cells showed a significantly reduced growth rate in the miR-210 over-expressing cells. At day 27, the EV tumours were approximately twice the volume of the miR-210 tumours, $p<0.001$. (Fig. 5-6 A) At the later timepoints, it was noted that some of the mice appeared to have bladder stones, which was thought to be a complication of the oestrogen-supplementation. The experiment was repeated with MCF7 cells. This time, however, there was no significant difference between the $MCF7^{EV}$ and $MCF7^{210}$ group. The trend seemed to show the opposite effect, with the EV cells this time proliferating more slowly. (Fig. 5-6 B) The mice in this experiment, however, were noted to be more sick than those in the first, and most of them suffered with bladder stones.

The experiment was also performed with the MDA-MB-231 cell lines. As these are not an oestrogen-dependent cell line, there was no need for oestrogen pellet supplementation. There was no significant difference in growth rate between the MDA^{EV} and MDA^{210} tumours. The trend favoured a slightly faster rate of growth in the MDA^{210} group, but the variation between individual tumours was too great to draw any firm conclusions. (Fig. 5-6 C).

In summary, the xenograft experiments failed to show any consistent effect of miR-210 over-expression on tumour proliferation.

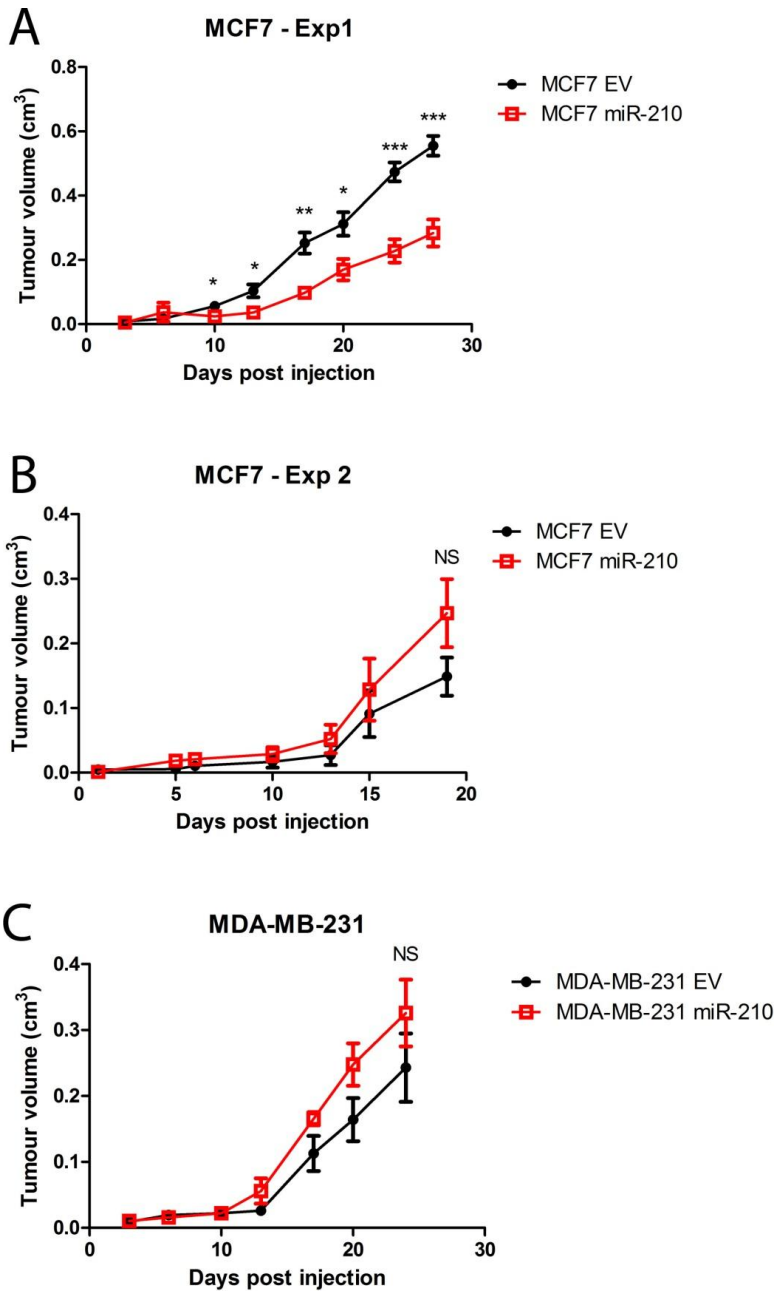


*Figure 5-6. Xenograft experiments with MCF7 and MDA-231 cells. BALB/c SCID mice received 10^7 MCF7 or MDA-231 cells in matrigel in to their flanks, which had been transfected with either pBabe EV or miR-210. A. $MCF7^{EV}$ cell tumours grew faster than $MCF7^{210}$ cells. *p<0.05, **p<0.01, ***p<0.001, T-test. B. Repeat of experiment A showing the opposite finding, with $MCF7^{210}$ tumours growing faster, with no statistically significant difference. C. MDA-231 cells – no significant difference in proliferation rate with miR-210 over-expression was observed. N=5 in each group for all experiments.*

5.4.3 Validation of miR-210 expression

Following sacrifice of the mice, RNA was extracted from the snap-frozen tumours. miR-210 expression was then measured in the EV and miR-210 over-expressing cell lines by qRT-PCR. It was thus shown that the cells continued to over-express miR-210 for the duration of the xenograft experiment. (Fig 5-7)

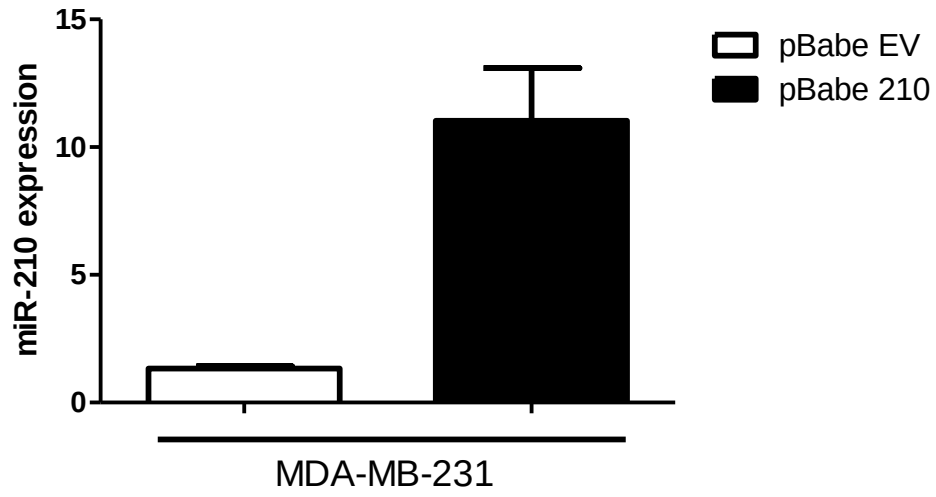


Figure 5-7. Expression of miR-210 in xenografts post sacrifice. MDA-231 xenografts retained over-expression of miR-210 after the experiment, though at a slightly lower level (11- fold over-expression vs 17-fold at the beginning of the experiment). MCF7 cells also continued to over-express miR-210 (data not shown). N=5 in each group.

5.4.4 Immunohistochemistry on formalin-fixed tumours

The formalin-fixed tumours were mounted in paraffin blocks and stained by immunohistochemistry for the following proteins: MIB1 an antibody to Ki-67, a marker of cellular proliferation), HIF-1α and HIF-2α; and CA9, a HIF1 target. A percentage intensity score system was used, in which the area of the tumour with

a given intensity of staining (e.g. 0, 1, 2, 3 or 4) was multiplied by the percentage of tumour staining at that intensity. Therefore, if a tumour stained 20% at zero intensity, 30% at intensity 1 and 50% at intensity 2, its overall percentage intensity score would be (0*20)+(1*30)+(2*50) = 130.

MIB1 was expressed at, or near, maximal intensity in all tumours. This is a common finding in xenografted tumours, the cell lines for which are generally chosen for their ability to proliferate quickly. There was no significant difference in MIB1 expression between the EV and miR-210 groups in either cell line. (Fig. 5-8 A). The $MCF7^{210}$ cells showed reduced expression of HIF-1α compared to the $MCF7^{EV}$ $p<0.05$. (Fig. 5-8 C) They also showed reduced expression of the HIF-1 target, CA9, although this was not statistically significant. (Fig. 5-8 B) There was no difference in HIF-1α or CA9 expression in the MDA-MB-231 cells. There was no significant difference in HIF-2α staining in either the MCF7 or MDA-231 xenografts. (Fig. 5-8 D)

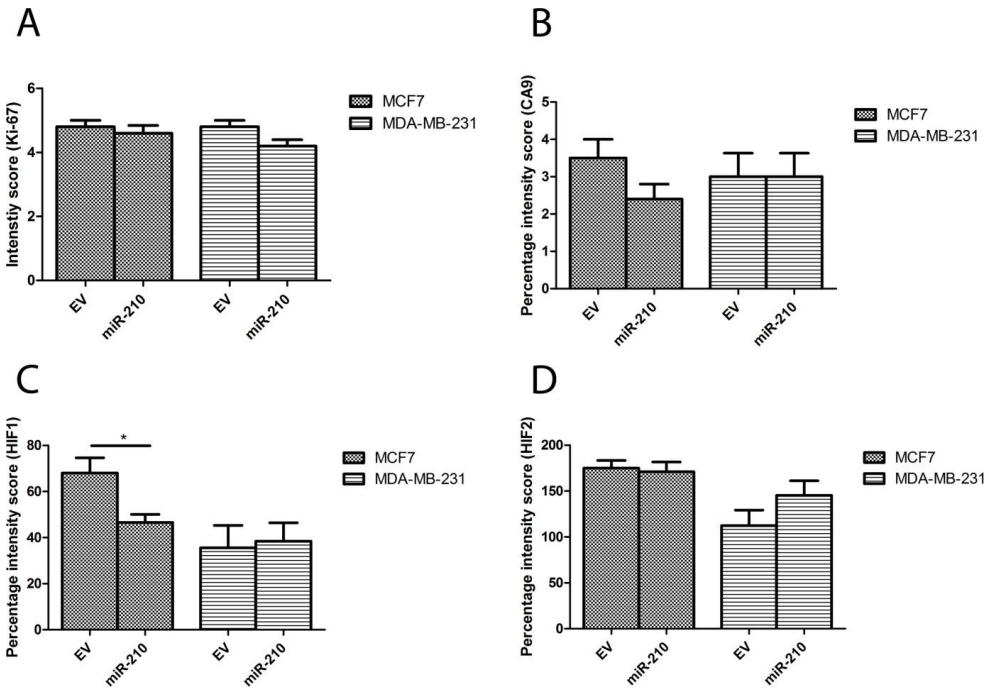


*Figure 5-8. Immunohistochemistry for paraffin-embedded sections of xenograft tumours. A. Ki-67 – there was no difference in intensity score in either cell line. B. CA9 – this had reduced expression in MCF7^{210} which was not statistically significant. There was no difference in the MDA-231 xenografts. C. HIF-1α – There was a significant reduction in HIF-1α intensity score in the MCF7^{210} xenografts, (*p<0.05, T-test) but no difference in the MDA-231 xenografts. D. HIF-2α – there was no significant difference between intensity score in either cell line. N=5 for each group.*

5.4.5 miR-210 in serum

The serum of the mice was processed for extraction of total RNA. miR-210 expression was measured by qRT-PCR. Expression of miR-210 (normalised to the control gene, RNU6B) between the EV and miR-210 over-expressing cell lines was compared. Figure 5-9 demonstrates that the serum of the mice with the miR-210 over-expressing tumours contained 3.7 fold more miR-210 than those with the EV tumours. There was a high degree of variation among samples, and the

difference was not statistically significant. However, this does provide evidence for miRNAs being released from cells in to the circulation, and suggests that miRNAs may be of use as a tumour marker, or other marker of disease.

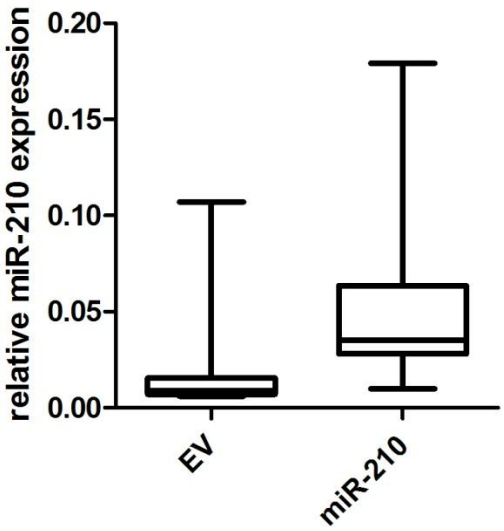


Figure 5-9. miR-210 in serum of xenograft mice. Mice with xenografts containing MCF^{EV} or $MCF7^{210}$ cells had their serum extracted at sacrifice, which was analysed for miR-210 expression. This is the pooled data from 2 the xenograft experiments. There is a trend towards higher miR-210 expression in the mice with the miR-210 over-expressing tumours, though it is not statistically significant. Box and whiskers plot with lines indicating median, interquartile range and total range. N=10 in each group.

5.5 Polysomal fractionation

$MCF7^{EV}$ and $MCF7^{210}$ cell lysates, extracted as previously described, were size-fractionated using sucrose gradients and ultracentrifugation. The experiment was performed in duplicate – referred to as experiment A and B. Figure 5-10 summarizes the fractionation process involved.

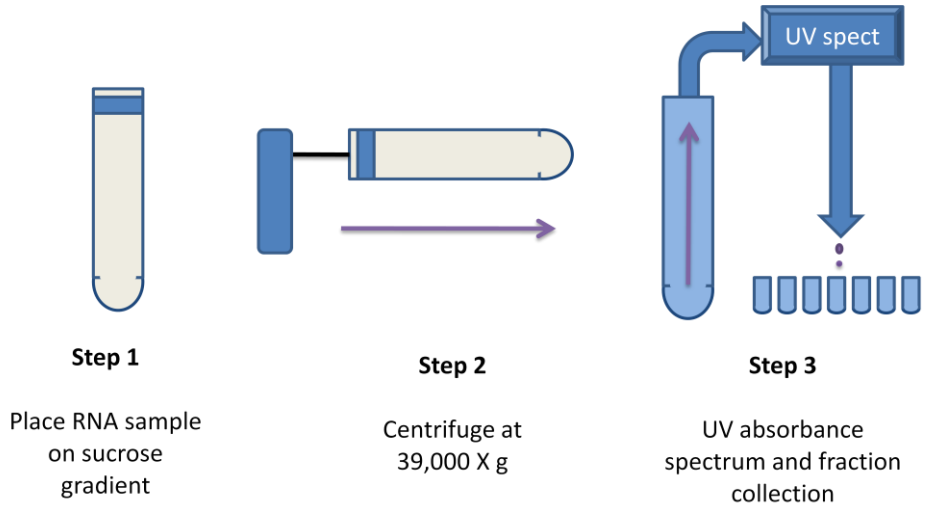


Figure 5-10. Polysomal fractionation workflow.

5.5.1 Validation experiments

Following purification to extract the cytoplasmic portion of the cell lysates, some of the input sample for the sucrose gradient was kept aside before fractionation. This was used to measure miR-210 expression by qRT-PCR, to ensure that the extraction method used here did not interfere with miRNA detection. As demonstrated in figure 5-11, the input samples from the MCF7^{210} cell lysates demonstrated the expected miR-210 over-expression.

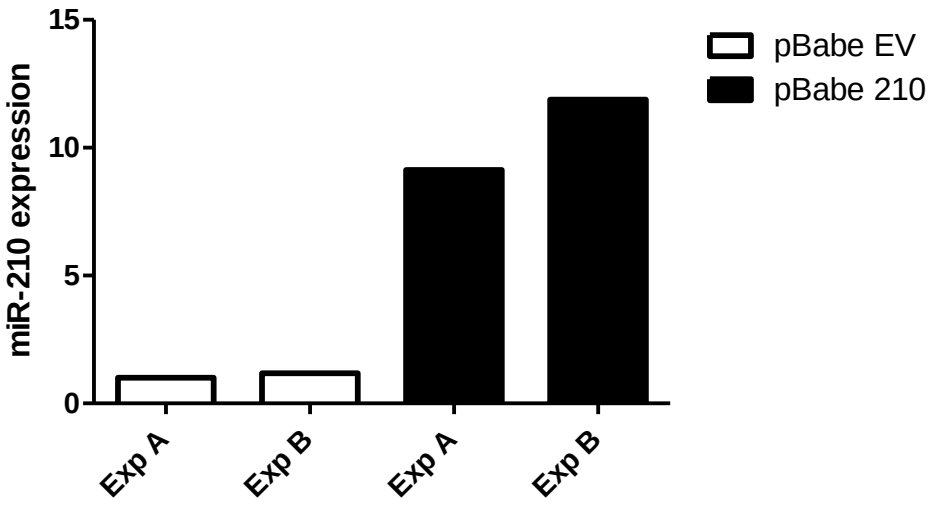


Figure 5-11. miR-210 expression in input samples for fractionation. Following cycloheximide treatments, cell lysis and RNA extraction, miR-210 over-expression was still present in the MCF7^{210} samples (normalised to RNU44 expression).

Following ultracentrifugation, the sucrose gradients were passed through a UV spectrometer measuring UV absorbance at 260nM, to measure relative RNA concentration. The absorbance spectrum confirmed that the size fractionation had been successful, clearly demonstrating peaks corresponding to free ribosomal subunits, and peaks corresponding to mRNAs with increasing numbers of bound ribosomes. (Fig. 5-12)

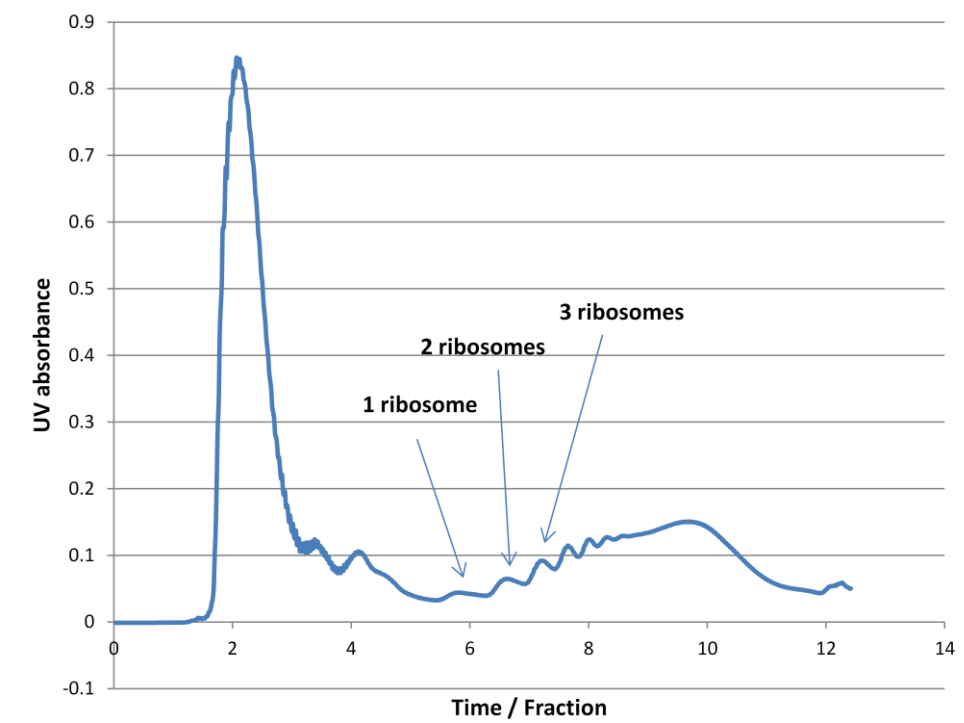


Figure 5-12. The UV absorbance graph for the sucrose gradients following ultracentrifugation. The large first peak is non-specific. The following two smaller peaks correspond to free ribosomal subunits. The subsequent peaks, which eventually merge, represent mRNA with increasing numbers of bound ribosomes (polysomes).

Following fractionation of each gradient in to about 25 tubes, each tube was spiked with 5ng of renilla luciferase spike-in control, prior to RNA extraction. The purpose of this was to control for variation in extraction efficiency between samples. Prior to further experimentation with array analysis, it was decided to measure the expression of beta-actin in both the $MCF7^{EV}$ and $MCF7^{210}$ fractions, to ensure that the distribution of the gene across the fractions was similar in each case. As shown in figure 5-13, the pattern of β-actin expression in the $MCF7^{EV}$ and $MCF7^{210}$ fractions is similar, with peak expression occurring at point 9, corresponding to the region with the most ribosomes bound in figure 5-12.

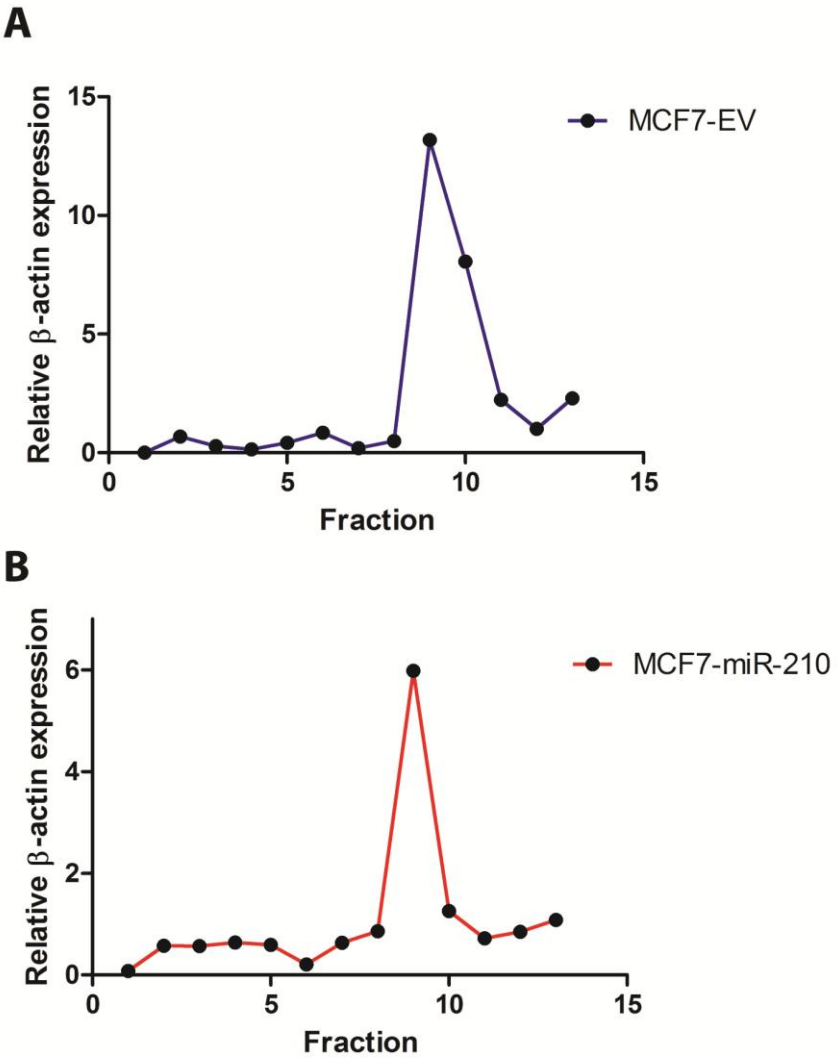


Figure 5-13. β-actin expression in the polysomal fractions. MCF7^{EV} (A) and MCF7^{210} (B) fractions show similar distribution of β-actin. Overall expression appears to be lower in MCF^{210} fractions, although the peak expression occurs at the same point.

5.5.2 Microarray results

An attempt was made to look at enrichment of mRNAs in the monosomal fraction with miR-210 over-expression. However, the variability in the data was very large,

and with only two replicates it was not possible to draw any conclusions from the fractionated samples. The input samples were analysed separately. Again, the data was noisy and the fold-changes observed very low. However, given the previous success with anti-210 in identifying targets, ISCU was used as a reference for trying to normalise this data. A data table containing genes that were down-regulated more than ISCU was generated (supplemental table x). However, this did not match any of the potential targets identified in the anti-210 experiment described in Chapter 3. There was a great deal of variation between both replicates, and proper statistical analysis was not possible due to the lack of a third replicate.

5.6 Discussion

The initial experiments with the cells over-expressing miR-210 were designed to show an effect of the miRNA on proliferation. No such effect was seen, despite the additional stress of serum deprivation which was introduced. The reason for this could be simply that miR-210 does not affect cell proliferation. However, another reason could be that constitutive up-regulation of miR-210 in the cells could allow other pathways to take over in time, thus masking the effect. It may be that an inducible system would be required to observe an effect on proliferation, or the use of transient transfection with miR-210 mimics. It may also be that a different type of stress is required to reveal a phenotype.

In view of the lack of phenotype displayed, an *in vivo* model was set up to investigate whether a 3-dimensional model would reveal differences between the empty vector and miR-210 constructs. Although the first experiment with the MCF7 cells demonstrated slower growth in the $MCF7^{210}$ group, a repeat of the

experiment showed the opposite trend. The mice appeared to be suffering from toxicity due to the oestradiol supplementation that was necessary to allow a reasonable growth rate in the MCF7 oestrogen-dependent cells. This manifested as bladder stones in the mice, and this toxicity may have affected the experiment to such a degree as to render its results unreliable. If the experiment were to be repeated, it should be with a significantly lower oestradiol dose. The MDA-231 experiment did not require any oestradiol supplementation, and the mice did not get any problems with bladder stones. The trend, although not statistically significant, was for the MDA-231^{210} xenografts to proliferate faster.

The results of these experiments, therefore, were inconclusive. Loss of miR-210 over-expression was not a cause of the lack of consistent phenotype found, as the tumours were analysed for miR-210 expression at the end of the experiment. The tumours were found to still be over-expressing miR-210 after sacrifice. A possible explanation for the lack of difference between the EV and miR-210 groups is the intrinsically hypoxic nature of xenograft tumours themselves. This hypoxia is demonstrated on pimonidazole staining of paraffin sections, and there was considerable heterogeneity within and between the xenografts. One would expect miR-210 to be up-regulated in the EV cells due to the hypoxic environment, and this could mask any difference between this group and the miR-210 constitutively over-expressing group. Alternatively, the variability of tumour hypoxia may point to the need for an experiment with greater numbers in order to demonstrate a statistically significant effect of miR-210.

Paraffin sections of the xenograft tumours were stained for Ki-67, Ca9, HIF-1α and HIF-2α. As might be expected, all xenografts displayed high levels of Ki-67, a marker for proliferation. Due to the fact that nearly all xenografts in both groups

displayed maximal intensity for Ki-67 staining, no further conclusions can be drawn on the effect of miR-210 on proliferation in this experiment. Interestingly, HIF-1α was found to be significantly decreased in the $MCF7^{210}$ group compared to the $MCF7^{EV}$ xenografts. There was also a corresponding decrease in CA9 in these xenografts, though it was not significant. This was not, however, observed in the MDA-231 xenografts. This may be a reflection of the result being artefactual due to the low numbers of xenografts within the experiment. Alternatively, it may represent differences in how the cell types respond to the increased miR-210 levels, and there may be a feedback mechanism on HIF due to stabilisation of HIF protein by ROS, as discussed in the previous chapter.

The serum of the mice used for the xenograft experiments was used to examine miR-210 expression levels, with the hypothesis being that the $MCF7^{210}$ or $MDA\text{-}231^{210}$ xenograft mice would have more miR-210 in the serum than the mice with the empty vector xenografts. miRNAs have the potential to be good biomarkers because they are known to be dysregulated in cancer(*153, 154*), and are tissue-specific in some cases.(*114*) Studies looking at miRNA expression in formalin-fixed tissues found a strong correlation with expression in matched fresh frozen tissue, indicating a high degree of stability.(*155, 156*) A study showed that miRNAs also have high stability in serum and plasma, despite incubation at room temperature for 24 hours, or up to eight repeated freeze-thaw cycles.(*157*) They found that miR-16, 15b and 24 remained expressed at similar levels between mice with xenografts, and control mice injected with matrigel alone. Additionally, in human serum samples, they found no significant difference in the expression of these miRNAs between patients with prostate cancer, and their healthy counterparts.(*157*) It is for this reason that miR-16 was selected as a control gene for quantifying miR-210 in the serum of the xenografted mice in our experiments.

miR-210 expression was found to be higher in the mice with miR-210 over-expression xenografts when compared to the empty vector xenograft mice. There was considerable variation between samples, and the difference was not statistically significant. However, further experiments with greater numbers may confirm that miR-210 xenografts do indeed secrete more miR-210 in to the serum than the empty vector controls. Micthell et al did address the possibility that the cells not pelleted in the serum or plasma samples could release miRNAs, thus causing artefactual results. They used filtration to ensure removal of all cells or large cellular fragments, and found the filtrate (and not the cellular debris held on the filter) contained almost all the tumour-derived miRNAs. (*114*)

In conclusion, it was not possible to demonstrate a phenotype in cells harbouring over-expression of miR-210 using the pBabe constructs, either *in vitro* or *in vivo*. The polysomal fractionation experiment failed to provide convincing evidence of any new targets. This was in part due to the lack of replicates, and the noise of the data. However, the mechanism of translational repression by miRNAs is not fully understood, and it is conceivable that they could block translation even on polysomes, without detachment of the ribosomes from the mRNA strand. Another contributing factor could be failure of the pBabe vector to produce *functional* miR-210, despite the fact that it is readily detectable by qRT-PCR.

CHAPTER 6 - Results
miRNA studies in clinical samples

6.1 Introduction

Clear cell renal cell carcinoma is characterised by its frequent mutations in the VHL gene. As VHL is responsible for HIF-degradation in normoxia, the consequences of inactivating mutations are likely to be largely the result of over-expression of the HIF-α subunits. The loss of the HIF-independent functions of HIF may also play a role in renal tumour carcinogenesis.(*50*)

Renal cancer, in particular the clear cell type, therefore represents a good model for cancer incorporating over-activity of the HIF-mediated hypoxia pathway. This chapter looks at HRMs in the context of renal cancer, using clinical material. Use is made of frozen tumours and matched normal renal cortex controls, archival paraffin tissue, and serum from patients with renal cancer. The principal aims of this section are based on the hypothesis that tumour hypoxia and VHL inactivation should up-regulate miR-210 and other HRMs, resulting in down-regulation of their respective targets. The aims were to:

1. Look for differential expression of miR-210 and other HRMs between renal cortex and matched renal tumours
2. Investigate the relationship of miR-210 expression to VHL mutation status in renal tumours
3. Characterize renal tumours by expression of proteins related to HIF expression, and miRNA targets, through the use of tissue microarrays (TMAs).

4. Examine the use of miR-210 as a tumour marker in the serum of patients with renal cancer.

6.2 VHL regulation of miR-210 in renal cancer cell lines

6.2.1 miR-210 is up-regulated in RCC4 cell lines

RCC4 renal cancer cell lines have inactivating VHL mutations. RCC4 cells with either an empty vector transfection (VHL-) or functional VHL transfection (VHL+) were cultured in normoxia or hypoxia (0.1% O_2) for 24 hours, with subsequent protein and RNA extraction.

The samples were immunoblotted for HIF-1α and HIF-2α. The VHL+ cells demonstrated up-regulation of both HIF-1 and-2α in hypoxia, with none detectable in normoxia. The VHL- cell lines demonstrated constitutive expression of both HIFs in normoxia and hypoxia. (Fig. 6-1)

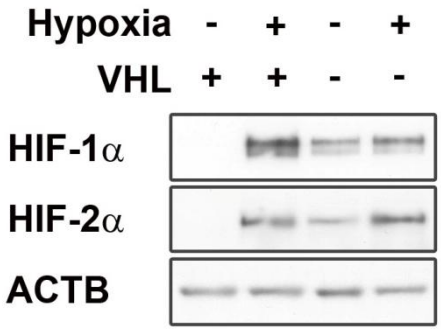


Figure 6-1. HIF expression in VHL- and VHL+ RCC4 cells cultured in normoxia or hypoxia (0.1% O_2) for 24 hours. VHL+ cells showed induction of HIF-1 and -2α in hypoxia, whereas the VHL- cells showed constitutive expression of both in normoxia.

Expression of miR-210 was measured by qRT-PCR. As expected, hypoxia resulted in over-expression of miR-210 in the VHL+ cells. The VHL- cells displayed constitutive over-expression of miR-210 in both normoxia and hypoxia. (Fig. 6-2)

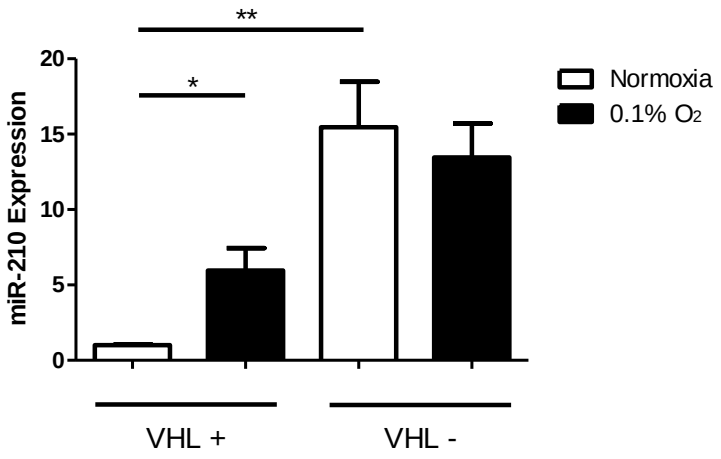


*Figure 6-2. miR-210 expression in RCC4 cells in normoxia or 0.1% O_2 for 24 hours. VHL+ cells demonstrated 6-fold induction of miR-210 in hypoxia. VHL- cells had constitutive 15-fold over-expression of miR-210 compared to the VHL+ cells in normoxia. Plotted = mean + SEM. *p<0.05, **p<0.01, unpaired t-test.*

6.2.2 miR-210 is up-regulated in 786-O cells lacking HIF-1α

786-O renal cancer cells have an inactivating mutation of VHL, and are known to contain no HIF-1α. 786-O cells transfected with either an empty vector (VHL-) or functional VHL (VHL+) were cultured in normoxia or hypoxia as for the RCC4 cells. The purpose of this was to determine whether a cell lacking HIF-1α would up-regulate miR-210.

VHL+ 786-O cells up-regulated HIF-2α in hypoxia, and showed no expression in normoxia. The VHL- cells demonstrated constitutive expression of HIF-2α (Fig. 6-4). HIF-1α was not detected (data not shown). Analysis of miR-210 expression by qRT-PCR showed that miR-210 is up-regulated in hypoxia in the VHL+ cells approximately 2.5-fold, and that the VHL- cells demonstrate constitutive up-

regulation of miR-210. Interestingly, hypoxia appears to further increase the expression of miR-210 in the VHL- cells. (Fig. 6-3)

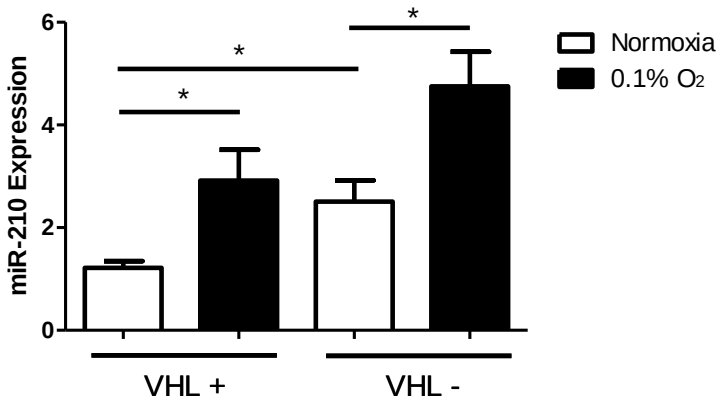


*Figure 6-3. miR-210 expression in VHL+ and VHL- 786-O cells cultured in normoxia or 0.1% O_2 for 24 hours. There is a 2.4 fold induction of miR-210 in hypoxia in VHL+ cells. The VHL- cells showed constitutive induction of miR-210, and this increased further under hypoxia. Plotted = mean + SEM. *p<0.05, unpaired t-test.*

6.2.3 HIF-2 regulates miR-210 in 786-O cells

In order to determine whether HIF-2α was responsible for up-regulating miR-210 in the absence of HIF-1α, the above experiment was carried out following transfection of the cells with either siRNA to HIF-2α, or a scramble siRNA control.

Immunoblotting for HIF-2α confirmed the constitutive expression of HIF-2α in the VHL-ve cells, and demonstrated effective knock-down of the protein with siRNA. (Fig. 6-4)

Expression of miR-210 was measured by qRT-PCR. Up-regulation of miR-210 by hypoxia or VHL deficiency was almost completely reversed by HIF-2α knockdown.

The exception to this was the VHL- cell line in hypoxia, which showed a smaller, non-significant effect. (Fig. 6-5)

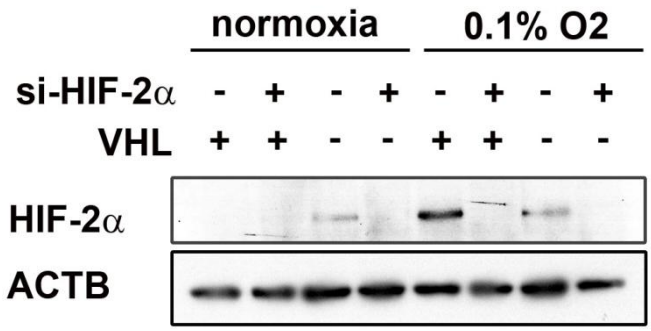


Figure 6-4. Expression of HIF-2α in VHL+ and VHL- 786-O cells with scramble or siHIF-2α transfections, cultured in normoxia or 0.1% O_2 for 24 hours. VHL+ cells showed induction of HIF-2α in normoxia, whereas VHL- cells showed constitutive HIF-2α expression. Si-HIF-2α quenched expression effectively in all groups.

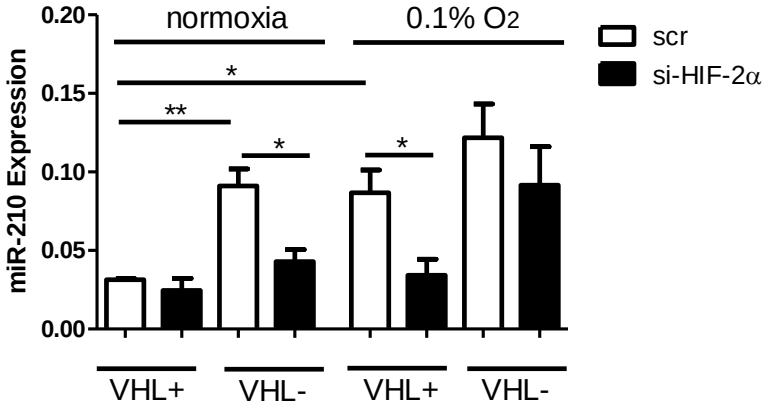


Figure 6-5. Effect of si-HIF-2α on miR-210 expression. si-HIF-2α reduced miR-210 over-expression to baseline in all groups except for the VHL- cells in hypoxia, which showed a small, but non-significant reduction in miR-210 expression.

Further evidence of HIF-2α regulating miR-210 in 786-O cells was sought by examining a database of HIF-2α promoter-binding sites in this cell line. This had

been compiled by Dr. David Mole, who performed an immunoprecipitation with a HIF-2α antibody, and sequenced the associated DNA to look for associated DNA sequences that would indicate HIF-2-binding promotor sites. The experiment revealed that the miR-210 locus in 786-O cells contains a binding site for HIF-2α. HIF-1β is also present at this locus, as would be expected. (Fig. 6-6)

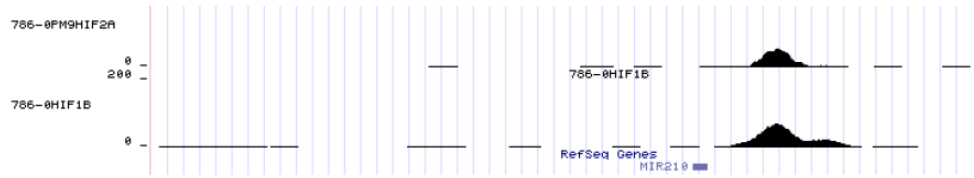


Figure 6-6. Chip-sequencing data for 786-O cells . Binding sites for HIF-2α and HIF-1β were found at the miR-210 gene locus.

6.3 VHL mutations in renal tumour samples

Collection of renal tumour samples and paired renal cortex is routinely performed, with appropriate consent, in association with the urology department. The details of these tumours are located within an in-house secure database. Using this resource, 58 fresh frozen tumour samples and paired normal renal cortex tissue (total N=116) were identified. The samples were processed for DNA and RNA extraction as previously described.

74% were clear-cell carcinomas (CCRCCs), with the remaining 26% consisting of papillary, chromophobe, oncocytoma and sarcoma tumours. (Table 6-1 and figure 6-7)

Histology	Total Number	% with VHL mutation
Clear Cell RCC	**43**	**72**
Papillary	**9**	**0**
Chromophobe	**1**	**0**
Oncocytoma	**4**	**0**
Sarcoma	**1**	**0**

Table 6-1. The distribution of histological subtypes and VHL mutations in 58 renal tumour samples

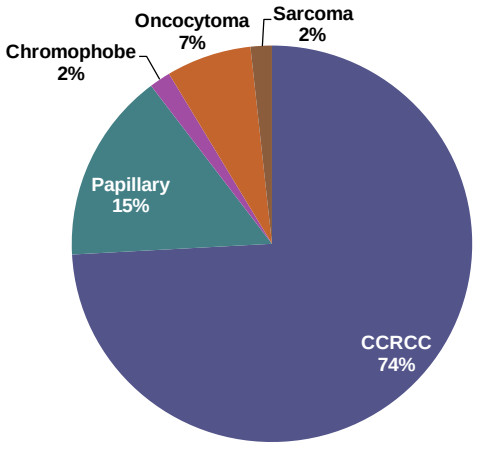


Fig 6-7. The distribution of histological subtypes in 58 renal tumour samples

6.3.1 Sequencing of renal tumours for VHL mutations

DNA from the renal tumours was sent for sequencing (performed by the team of Dr. Roz Banks, Leeds) in order to identify mutations in the VHL gene. The three

exons of the VHL gene were amplified separately and sequenced in order to look for mutations. It was found that, in this group of samples, VHL mutations occurred exclusively in the CCRCCs. Overall, 72% of samples had an identified mutation, with 39% occurring in exon 1, 14% in exon 2, and 19% in exon 3. (Fig. 6-8)

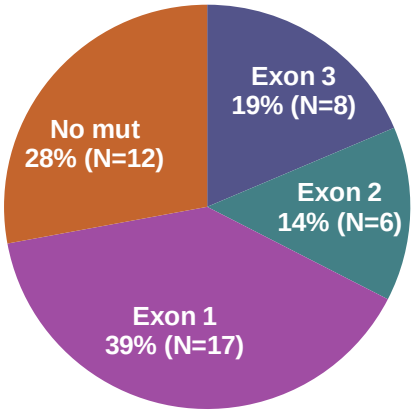


Fig 6-8. The distribution of VHL mutations in the 43 CCRCC tumours

The following table describes the distribution of mutation types in the CCRCC tumours (total number of CCRCC tumours = 42).

Mutation Type	Number	Percentage
Deletion	1	2
Frameshift	10	24
Insertion	1	2
Missense	10	24
Nonsense	7	17
No exon 2	1	2
No mutation	12	28

Table 6-2. The frequency of different types of VHL mutation in the CCRCC tumours

Figure 6-9 demonstrates that the majority of the mutations lie in the α and β domains of the VHL protein, with only 2 mutations lying outside this region. No mutations lie in the pentameric repeat motif (GXXEX).

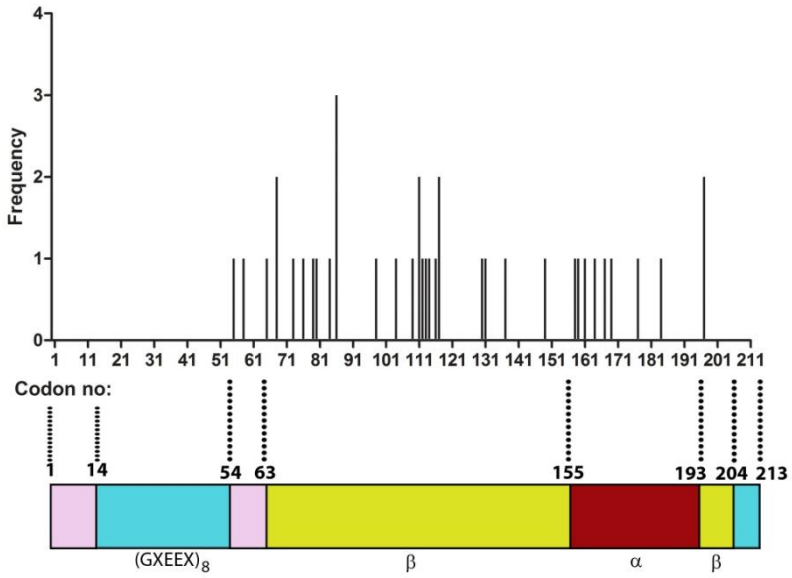


Figure 6-9. Frequency and location of VHL gene mutations. All of the mutations, with the exception of two were found in the α and β domains.

6.4 miR-210 expression in renal tumours

6.4.1 miR-210 is up-regulated in renal tumours

Expression of the mature miR-210 sequence in the tumours and normal cortex was measured by qRT-PCR. This was normalised to three controls (RNU44, RNU48, RNU6B) using GeNorm software. miR-210 was expressed at substantially higher levels in tumour tissue compared to the normal renal cortex. The overall fold change was 9-fold. The level of miR-210 expression in the tumours was dependent on the histology and VHL-mutation status. CCRCCs demonstrated higher levels of miR-210 than papillary tumours, while the benign oncocytomas had no more miR-210 expression than the normal controls. (Fig 4.3) However, it

should be noted that there were far fewer papillary tumour (N=7) than CCRCC (N=42), and only 3 oncocytomas. There were too few oncocytoma samples to draw any firm conclusions about miR-210 expression in this histological type.

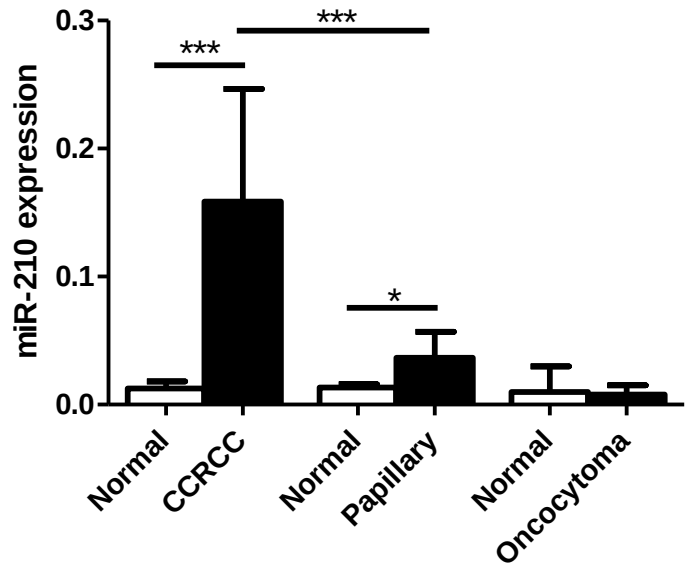


*Figure 6-10 – Graph showing expression of miR-210 in normal tissue and different renal tumour histological subtypes. miR-210 was up-regulated much more in CCRCCs (9-fold, N=43)) than other tumour types (papillary, 2.7-fold (N=9); benign oncocytomas – no up-regulation (N=4)). Plotted = median + interquartile range. *p<0.05, ***p<0.001, Mann-Whitney test*

6.4.2 Degree of miR-210 expression is associated with VHL mutation status

Within the CCRCCs, non-VHL mutant (mut –ve) tumours showed an 8-fold change over normal tissue, whereas the VHL-mutant (mut +ve) tumours showed a 15-fold change – almost twice that of the mut -ve group. (Figure 6-11) It is worth noting that miR-210 expression in the mut -ve tumours appears to be split in to two groups – those with low expression (approximately that of the normal

controls) and high expression. A possible explanation for the mut -ve tumours with high miR-210 expression is inactivation of the VHL gene through an epigenetic mechanism. The methylation status of the tumours has not yet been characterized. Another explanation could be that normal kidney tissue within the tumour sample was examined by mistake.

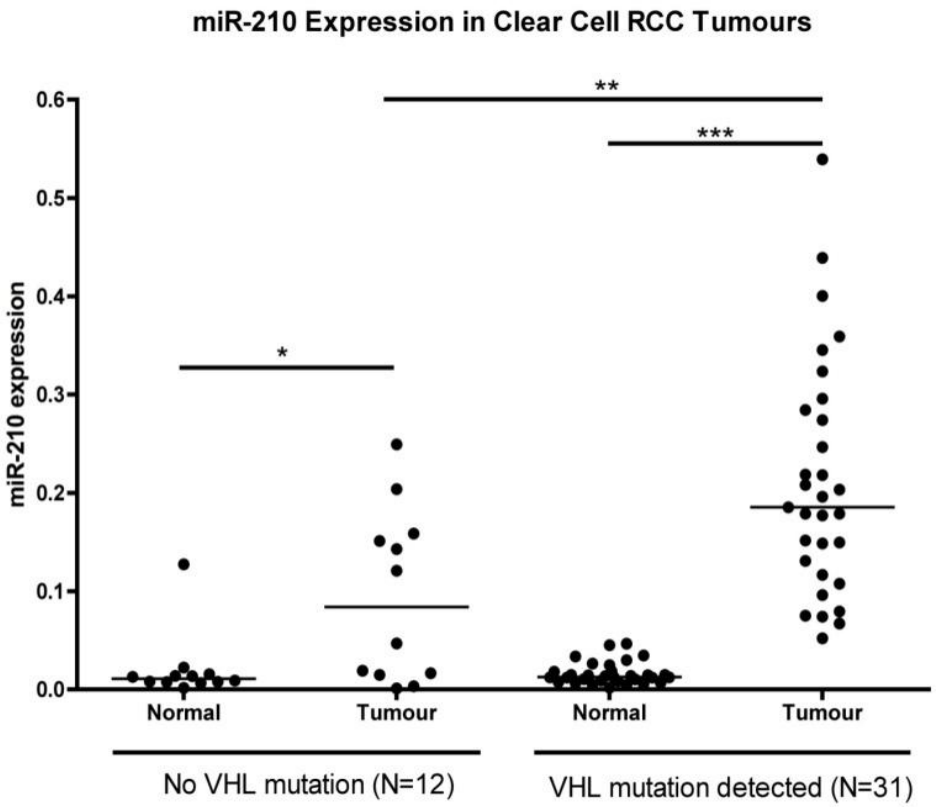


*Figure 6-11. Expression of miR-210 in normal tissue and CCRCCs. In mut-ve tumours there is an 8-fold median up-regulation, compared to 15-fold in the mut+ve tumours. Note that in the mut-ve group, there appear to be two clusters – one around the level of normal tissue, and one with much higher expression – this may represent tumours with VHL inactivation by methylation. Lines = median expression. *p<0.05, **p<0.01, ***p<0.001, Mann Whitney test.*

The tumours were analysed for expression of VHL mRNA by qRT-PCR. It was found that there was a significant negative relationship of VHL expression to miR-210 expression. (Fig. 6-12)

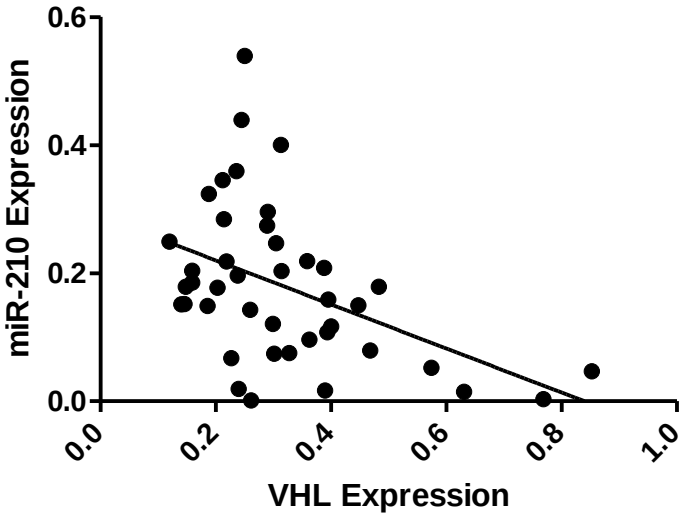


Figure 6-12. Correlation of VHL and miR-210 RNA expression. A significantly non-zero negative correlation was demonstrated. R^2=0.2, p<0.01 (F-test)

RNA from a further 30 CCRCC tumours (with known VHL status) was obtained from collaborators (Dr Roz Banks in Leeds). qRT-PCR was performed for miR-210 and the same three control genes as the above experiments. The data were combined and re-analysed. The increased numbers confirmed the over-expression of miR-210 in both tumours with, and without VHL mutations (p<0.0001 in both groups). However, the difference in miR-210 expression between the tumours with, and without VHL mutations is less clear, and no longer statistically significant. (Fig. 6-13)

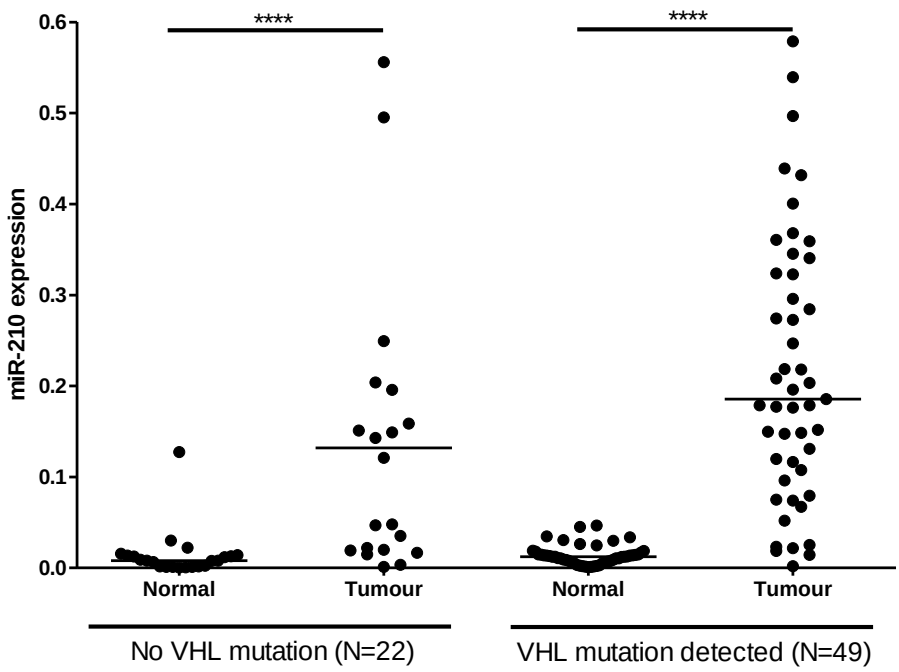


*Figure 6-13. Combined data of CCRCCs from figure 6-12, and 30 additional tumours. miR-210 expression was increased in tumours, compared to normal renal cortex, in tumours with, and without VHL mutations. The difference in expression between tumours with VHL mutations, and those without, is no longer statistically significant. ****p<0.0001, Mann-Whitney test.*

It is worth noting that the extra 30 tumours from the collaborators were also analysed for VHL methylation and loss of heterozygosity (LOH). It was found that all but one of the 30 tumours had inactivation by methylation, LOH or mutation.

6.4.3 CA9 expression correlates with VHL mutation status and miR-210 expression in CCRCCs

In order to correlate miR-210 expression with HIF-1α expression, expression of CA9 (a HIF-1α target) was measured in the CCRCCs by qRT_PCR. CA9 expression

was twice as high in the mut +ve tumours as the mu t-ve tumours, supporting the hypothesis that miR-210 expression in the tumours is regulated by HIF-1α. (Fig. 6-14) There was a correlation of miR-210 expression and CA9 expression, R^2=0.16. (Fig. 6-15)

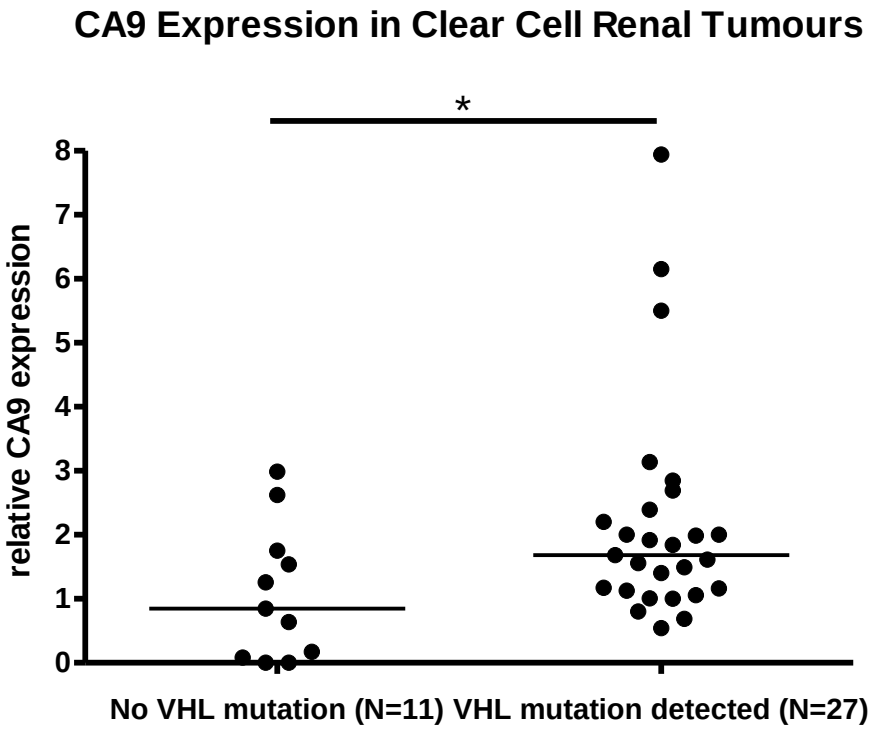


*Figure 6-14. CA9 expression in VHL mut-ve tumours vs mut+ve tumours. CA9 expression is nearly double in VHL mut+ve tumours. Lines = median expression. *p<0.05, Mann Whitney test.*

There was no correlation of the type of mutation (i.e. missense, nonsense, frameshift) or the exonic location of the mutation (Exon 1,2 or 3) with miR-210 expression.

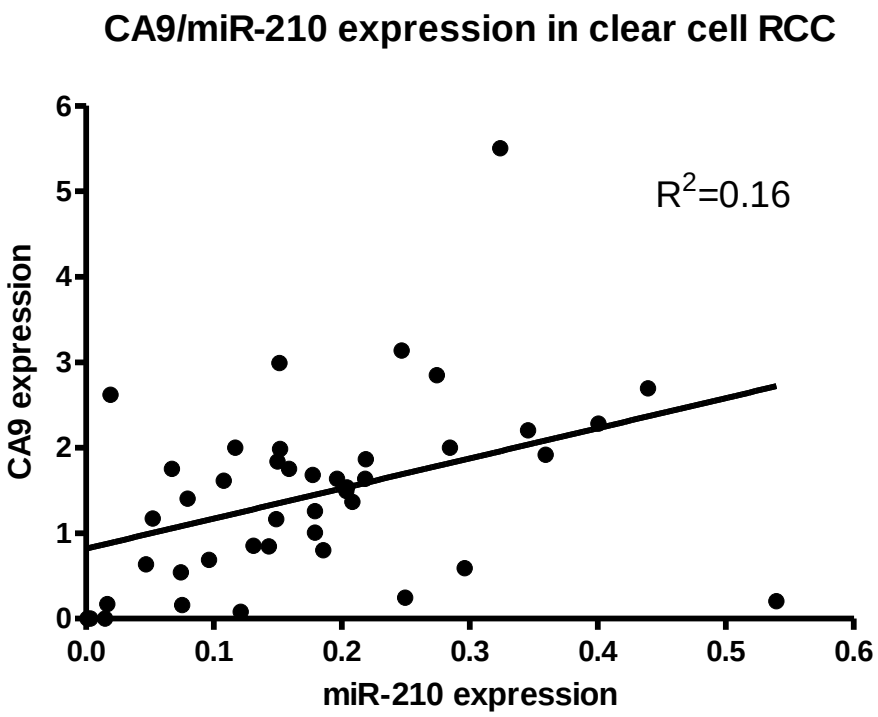


Figure 6-15. CA9 expression vs miR-210 expression. There is a correlation with R^2=0.16. p<0.05, F-test. N=43.

6.4.4 miR-210 correlation with tumour grade and stage

miR-210 expression was slightly lower in high grade tumours (Fuhrman 3-4) than in low grade (Fuhrman 1-2), with high-grade tumours expressing about 55% that of low-grade tumours ($p<0.01$) (Fig. 6-16) High-stage tumours (grade 3+) expressed only 74% of miR-210 expression when compared to low stage (stage 1-2), tumours (Fig. 6-17).

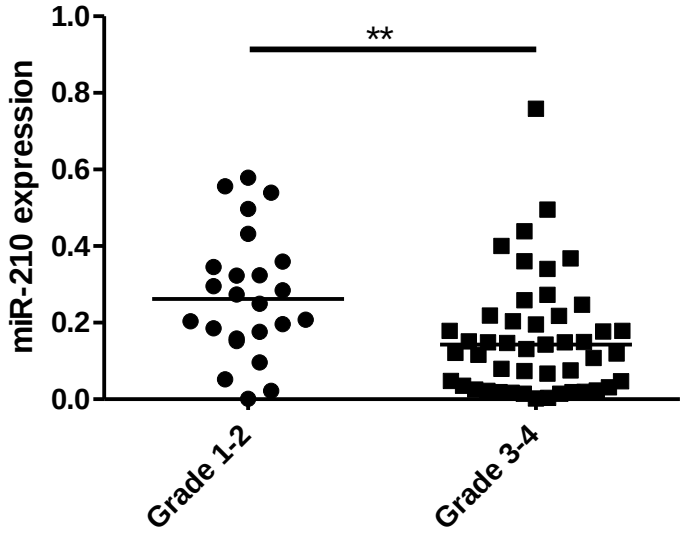


*Figure 6-16. miR-210 expression in low grade (1-2, N=24) and high grade (3-4, N=49) CCRCCs. High grade tumours express approx 55% miR-210 compared to low grade. Lines=median. **p<0.01, Mann-Whitney test.*

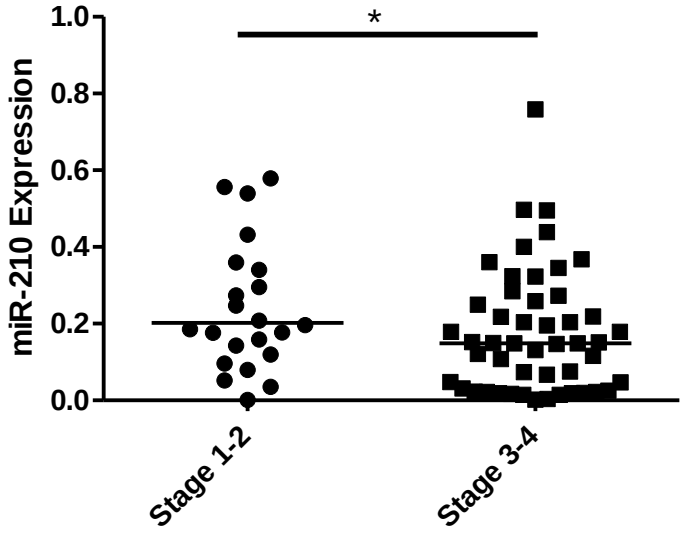


*Figure 6-17. miR-210 expression in early stage (1-2, N=24) RCCs and late stage (3+, N=49). Lines=median. High stage tumours have 74% of the miR-210 expression levels of lower stage tumours. Plotted = median. *p<0.05, Mann-Whitney test.*

6.4.5 miR-210 and survival

In order to assess correlation of miR-210 expression with survival in patients with renal cancer, patients were split in to three groups depending expression levels in their tumours. Each group contained 23 patients, and survival was plotted using the Kaplan Meier method. As shown in figure 6-18, the patients with CCRCCs expressing higher miR-210 had better survival than the other two groups, with 80% still alive at 2000 days compared to approximately 40% in patients with medium/low miR-210 expression. This trend was just short of statistical significance (p=0.054, Chi square test).

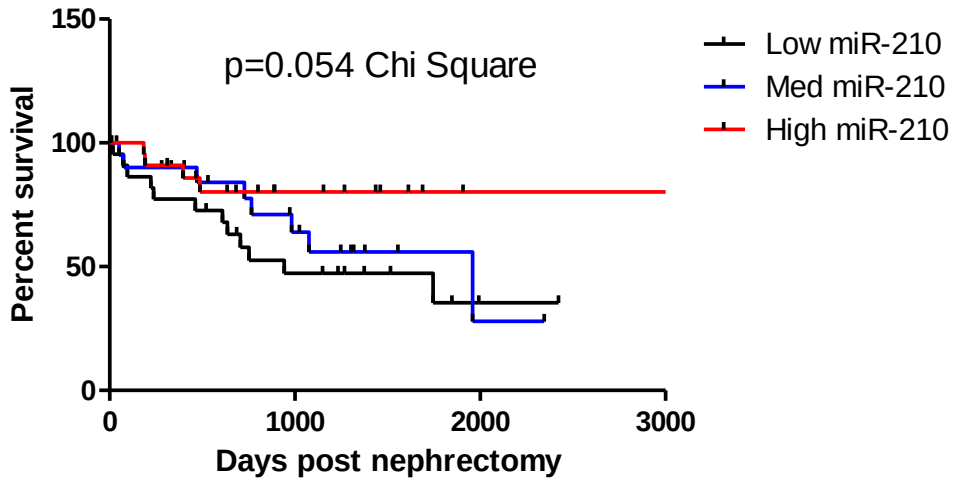


Figure 6-18. miR-210 expression in CCRCCs and patient survival. High miR-210 expression was associated with improved survival. P=0.054, Chi square test for data trend.

6.4.6 miR-210 expression correlates negatively with Ki-67 expression

A tissue microarray containing 40 CCRCC tumours was stained for Ki-67 antigen, a marker of proliferation, using the MIB1 antibody. The tumours were divided in to two groups (low Ki67 (N=20) and high Ki67 (N=20)) based on their expression of Ki67 expression by percentage intensity score (PIS). (Fig. 6-19) The expression of miR-210 in each group was plotted, showing that tumours with high Ki67 expression have only 60% the miR-210 expression of those that have low Ki67. (Fig. 6-20)

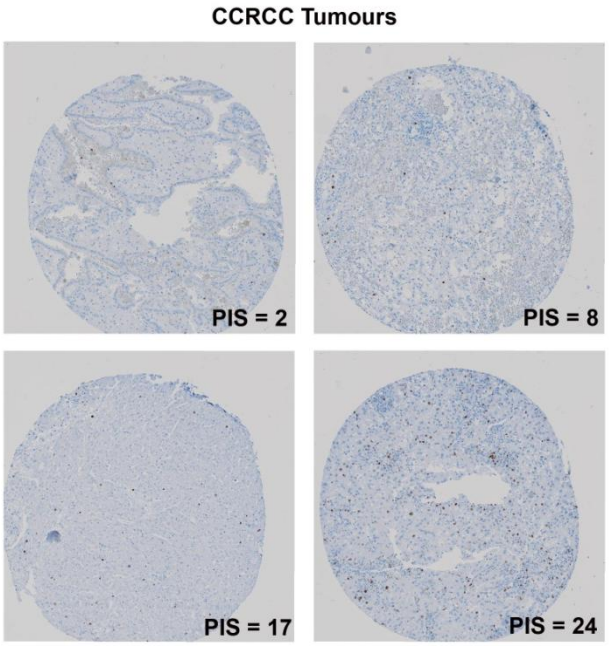


Figure 6-19. Typical appearances of IHC staining for Ki67 on the CCRCC TMAs, showing PIS scores ranging from 2 to 24.

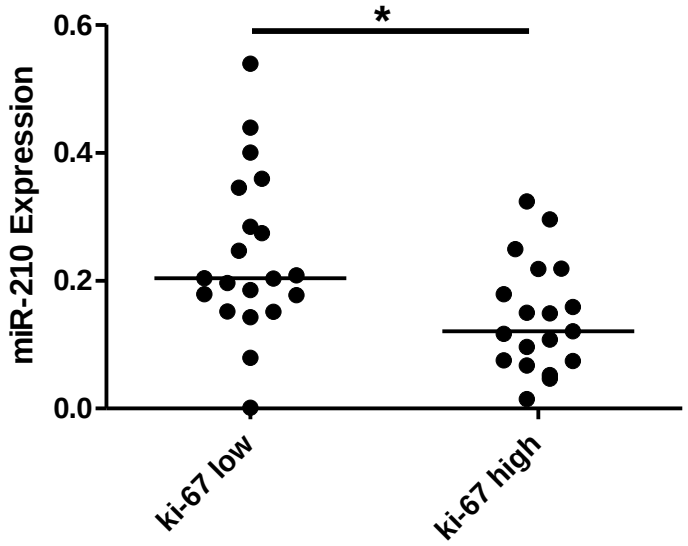


*Figure 6-20. Relationship of miR-210 expression to Ki67 expression determined by IHC in the CCRCC TMAs. miR-210 expression in the Ki-67 low tumours (N=20) was 1.7 fold higher than in the Ki-67 high tumours (N=19). Plotted = median. *p<0.05, Mann-Whitney test.*

6.4.7 miR-210 expression and mutation type and location

miR-210 expression was compared between the normal renal cortex, and tumours with mutations in exons 1, 2 or 3. No significant difference was found in median miR-210 expression among mutations in the three different exons. (Fig. 6-21)

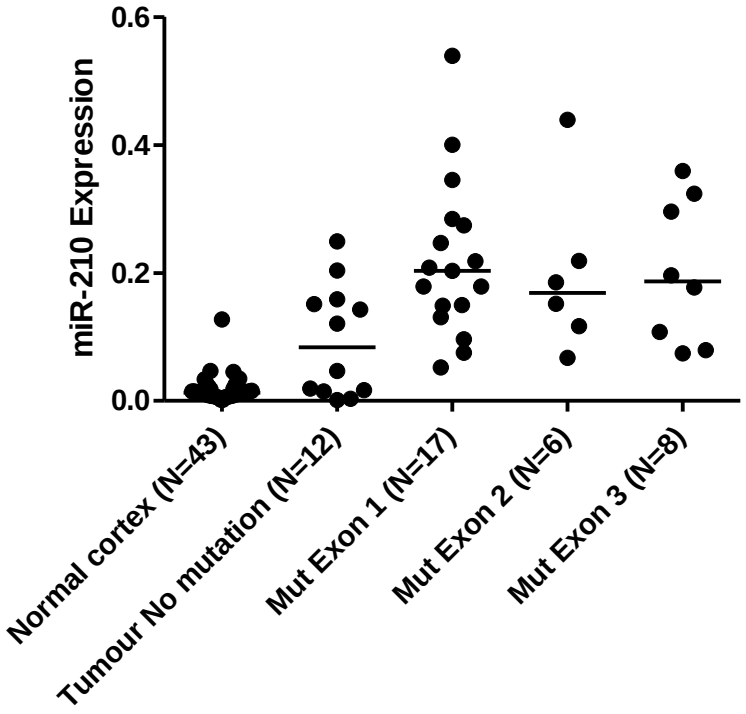


Figure 6-21. The relationship of miR-210 expression to exonic location of the VHL mutations. No difference was seen in median expression amongst mutations in the three exons. Plotted lines =median. No significant differences, Mann-Whitney test.

The tumours were also analysed for any potential differences between miR-210 expression based on mutation type – i.e. nonsense, missense or frameshift. Again, no significant difference was observed between the groups. (Fig. 6-22)

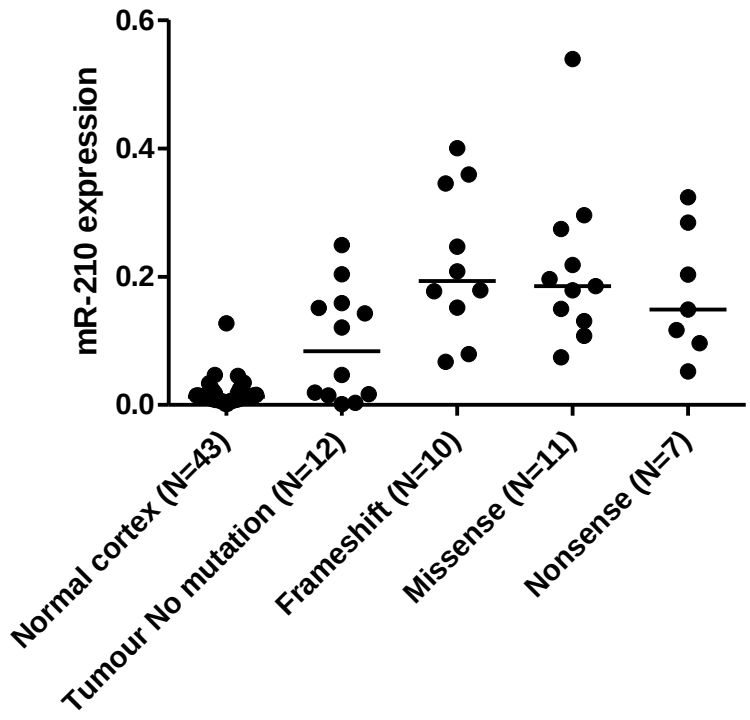


Figure 6-22. The relationship of VHL mutation type to miR-210 expression. No significant difference in median expression was seen between the mutation types. Plotted lines = median. No significant differences, Mann-Whitney test.

6.5 Expression of other VHL-regulated miRNAs in renal tumours

An experiment was carried out by colleagues in our research group to identify miRNAs differentially regulated by the presence or absence of VHL. This was achieved through the use of VHL-null RCC4 renal cancer cell lines. These were transfected with either an empty vector, or a vector containing the VHL coding region. Both VHL positive and VHL null RCC4 cell lines were expression profiled using three platforms. Two of these were microarray platforms (Illumina and Agilent), and the third was a Solexa deep-sequencing system. The Solexa system is able to sequence fragmented and size-fractionated cDNA in parallel, and is able to generate a 'copy number' of known miRNA sequences in experimental

samples. This novel and accurate method was applied used to help validate the microarray platforms. The results were collated to provide a table showing the genes most significantly up- or down-regulated in the absence of VHL. (Table 6-3)

RCC4 vs RCC4+VHL in normoxia (effect of the absence of VHL in normoxia)

	Agilent		Illumina		Solexa	
ID	logFC	adj.P.Val	logFC	adj.P.Val	logFC	logFC (without lines s3, s5)
hsa-miR-210	2.69	4.25E-14	1.23	0.01804	4.397557	4.605832335
hsa-miR-155	1.92	2.78E-12	1.32	3.55E-05	2.767768	2.981611147
hsa-miR-193b	0.6	3.39E-05	0.36	0.014496	1.848676	1.778463905
hsa-miR-152	0.5	3.95E-05	2.62	4.77E-05	not found	not found
hsa-miR-23b	-1.46	6.80E-09	-0.79	0.019525	not found	not found
hsa-miR-148a	-0.85	1.84E-06	-3.31	5.50E-07	-4.062984	-3.840892085
hsa-miR-145	-0.73	1.90E-05	-1.86	4.77E-05	-4.058838	-4.034820437
hsa-miR-503	-0.89	1.90E-05	-1.12	0.00496	-0.713028	-0.258970793
hsa-miR-143	-0.41	1.90E-05	-4.64	8.17E-08	not found	not found
hsa-miR-224	-0.68	0.015718	-1.1	0.014496	not found	not found
hsa-miR-9*	-0.09	0.027254	-1.17	0.038297	not found	not found
hsa-miR-100	-0.69	0.02102	-0.61	0.038297	-0.430145	-0.498263056
hsa-miR-424	-1.49	9.12E-07	-0.53	0.025486	-1.542905	-1.629143219

Table 6-3. miRNAs up- and down-regulated in the absence of VHL. Data from three platforms is displayed. miRNAs highlighted in red are up-regulated in the absence of VHL, while those in green are down-regulated. Data provided by Dr. Ioannis Ragoussis.

It was decided to investigate the expression of the highlighted miRNAs in the renal tumours, and compare expression to the matched normal controls. The hypothesis was that, if miR-210 as a HRM, is up-regulated in renal tumours, other HRMs identified here may also behave similarly in tumour tissue.

6.5.1 miR-148a is down-regulated in renal tumours

Pilot experiments on a small number of samples indicated that miR-148a was likely to be down-regulated in the renal tumour samples compared to the normal renal cortex. This miRNA was therefore pursued further with a greater number of samples. It was found that the miRNA was significantly down-regulated in the CCRCCs in the VHL mutation group. It also appeared down-regulated in the

papillary tumours, although this was not statistically significant due to the lower number of samples, and sample variation. (Fig. 6-23) There was no correlation with miR-148a expression and tumour grade or stage. (Fig. 6-24)

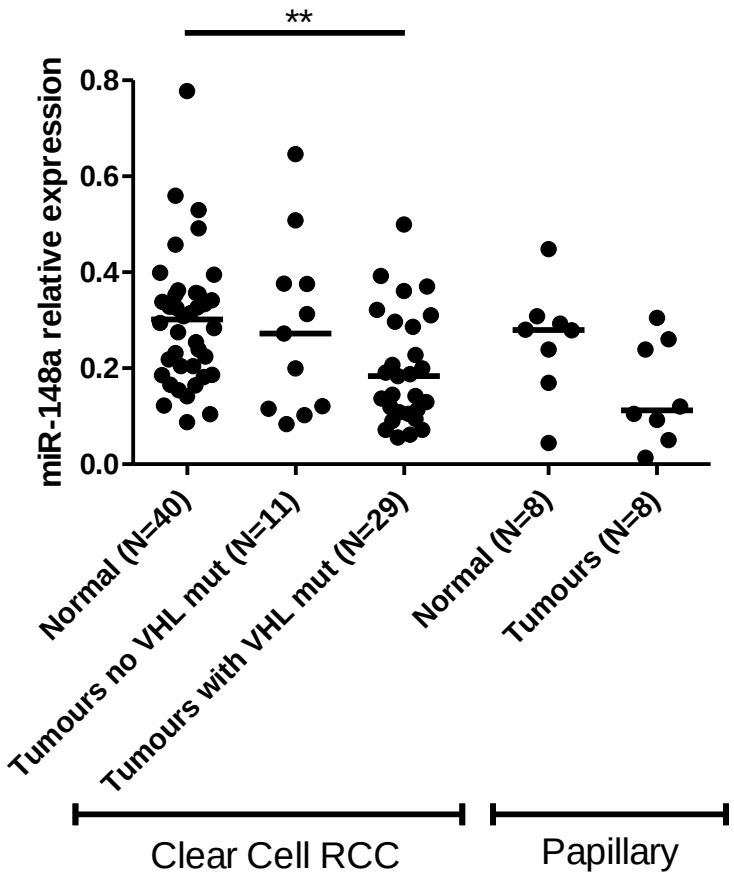


*Figure 6-23. miR-148a expression in CCRCC and papillary tumours. The was significant down-regulation of the miRNA in CCRCCs with VHL mutations. Papillary tumours also showed a downward trend, though this was not significant. Plotted lines = median. **p<0.01, Mann Whitney Test.*

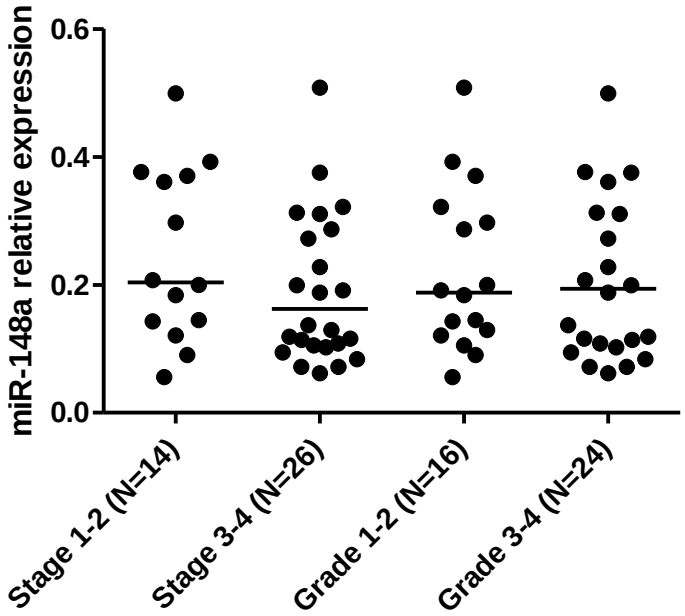


Figure 6-24. miR-148a expression and tumours stage/grade. There was no significant correlation. Plotted lines=median.

6.5.2 miR-100 is down-regulated in renal tumours

miR-100 was found to be down-regulated approximately two-fold in both CCRCCs and papillary tumours. The CCRCCs appeared to have slightly greater baseline miR-210 expression. (Fig. 6-25)

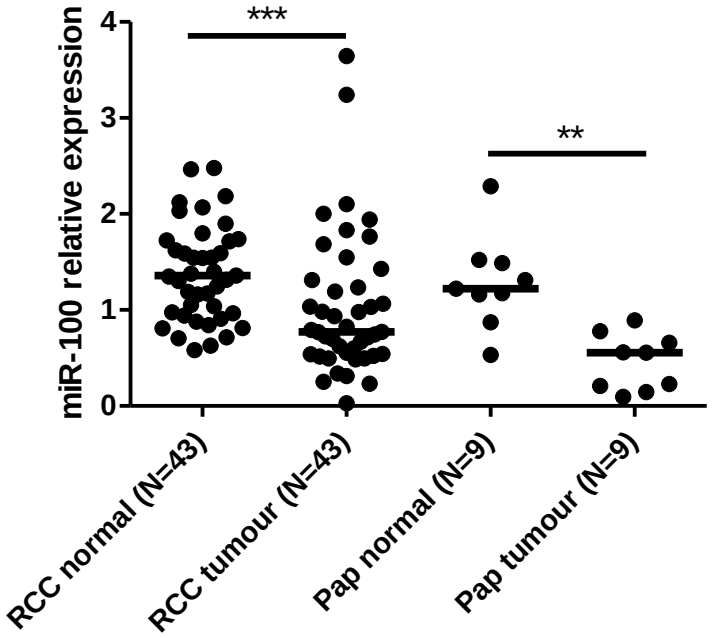


*Figure 6-25. miR-100 expression in CCRCCs and Papillary tumours, with matched normal controls. miR-100 expression was down-regulated 2-fold in CCRCCs and in papillary tumours. Plotted lines=median. **p<0.01, ***p<0.001, Mann Whitney test.*

There was no correlation of miR-100 expression with tumour stage or grade (Fig. 6-26).

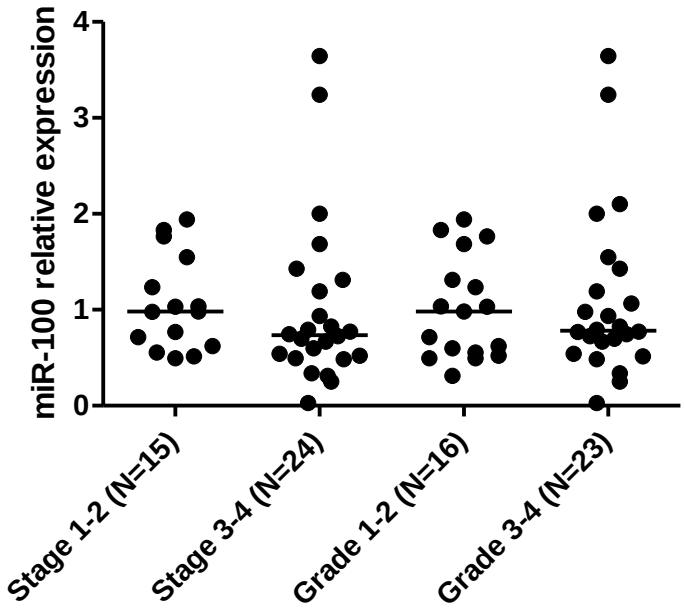


Figure 6-26. miR-100 expression in CCRCCs and tumour stage/grade. There were no significant differences between the groups. Mann-Whitney test.

6.5.3 Expression of other miRNAs in renal tumours

miR-503, miR-193, and miR-424 were detectable in the renal tumours, but there was no difference between the normal cortex and the renal tumours. (Fig. 6-27)

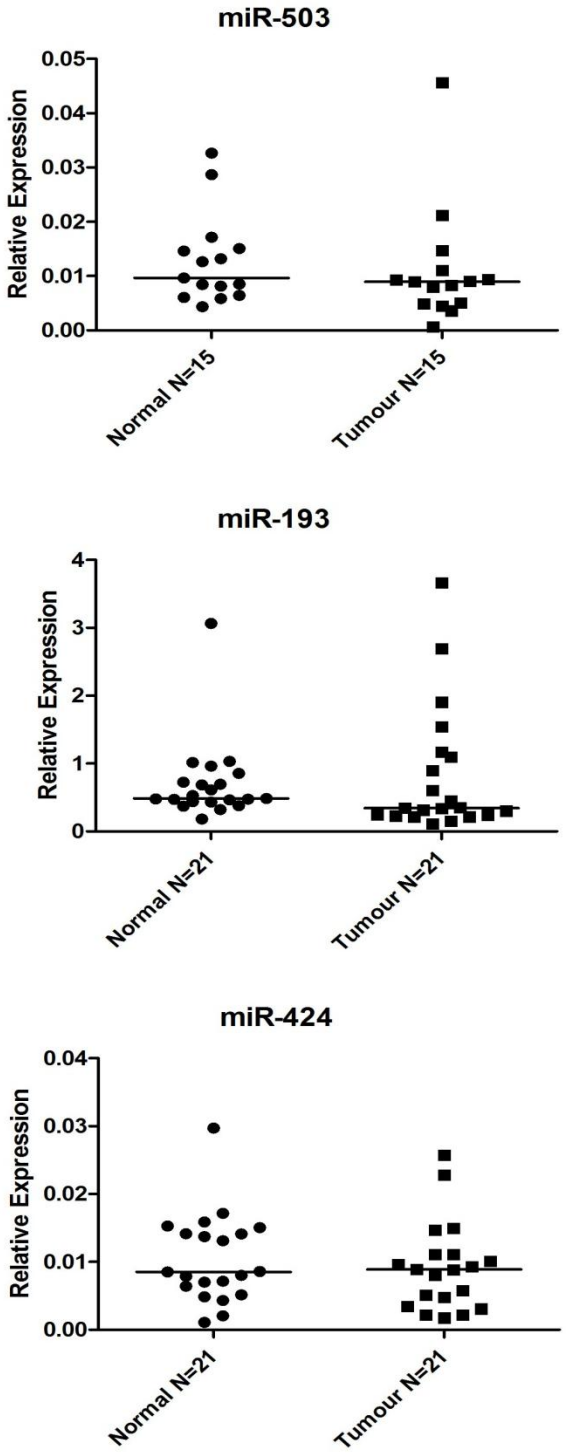


Figure 6-27. Expression of miR-503, -193 and -424 in renal cortex and tumours. All were detectable in the tissues, but there was no difference in expression between cortex and tumour. Mann-Whitney test.

miRs 145, 155 and 193b were not readily detected using the qPCR assay, and no conclusions as to their expression in these tissues could be drawn.

6.6 ISCU mRNA expression in renal tumours

miR-210 expression was measured in renal tumours and matched cortex, and normalised to two controls, GUSB and β-actin. The normalised data demonstrated a two-fold decrease in ISCU expression in the tumours, compared to the normal controls (Fig. 6-28)

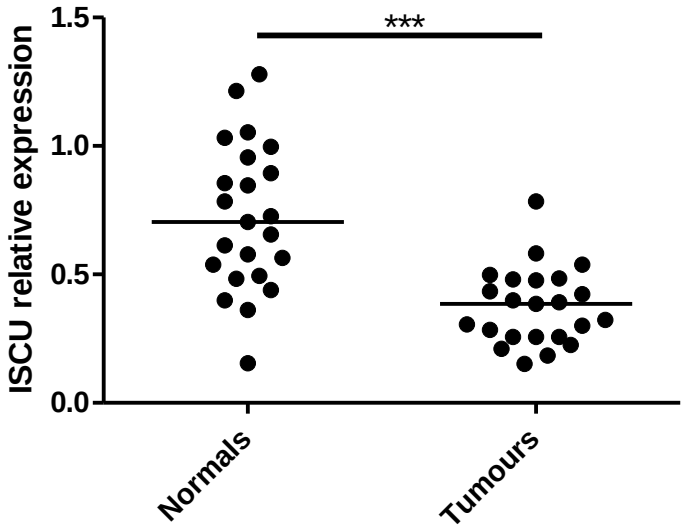


*Figure 6-28. ISCU expression in CCRCC renal tumours (N=40) and renal cortex (N=40), measured by qRT-PCR. There was a two-fold decrease in the tumours compared to the normal controls. Lines = median expression. ***p<0.001, Mann Whitney test*

ISCU expression was analysed comparing tumours with high and low stage or grade. No significant differences were found. (Fig. 6-29)

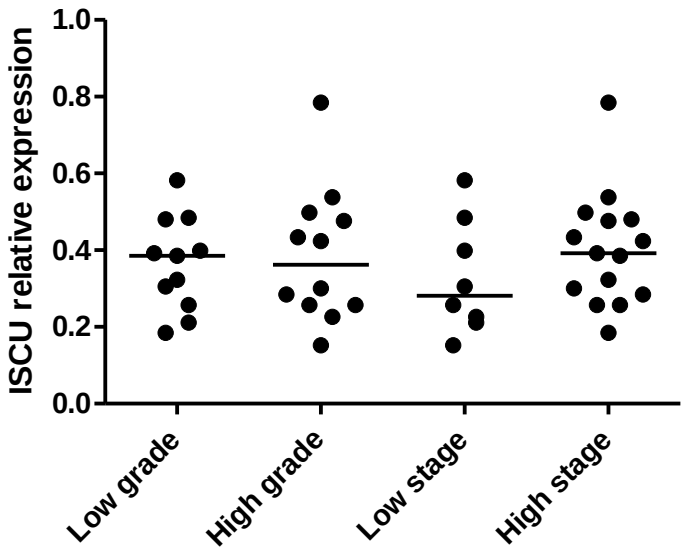


Figure 6-29. ISCU expression in low and high stage/grade tumours, measured by qRT-PCR. Plotted lines = median There were no significant differences, Mann-Whitney test.

6.6.1 ISCU protein is down-regulated in tumours and correlates with VHL mutation status

A tissue microarray was created based on tissues from the same tumours that were used for the miR-210 studies. Another array was made using the matched normal renal cortex controls. Using immunohistochemistry (IHC), they were stained for ISCU protein. Figure 6-30 shows typical appearances of normal and tumour tissues with percentage intensity scores of 0-8.

A comparison was made of the mean cytoplasmic percentage intensity score in the normal renal cortex, and the CCRCC tumours. The tumours expressed significantly less ISCU than the normal controls, with the percentage intensity score (PIS) being about 40% lower. (Fig. 6-31)

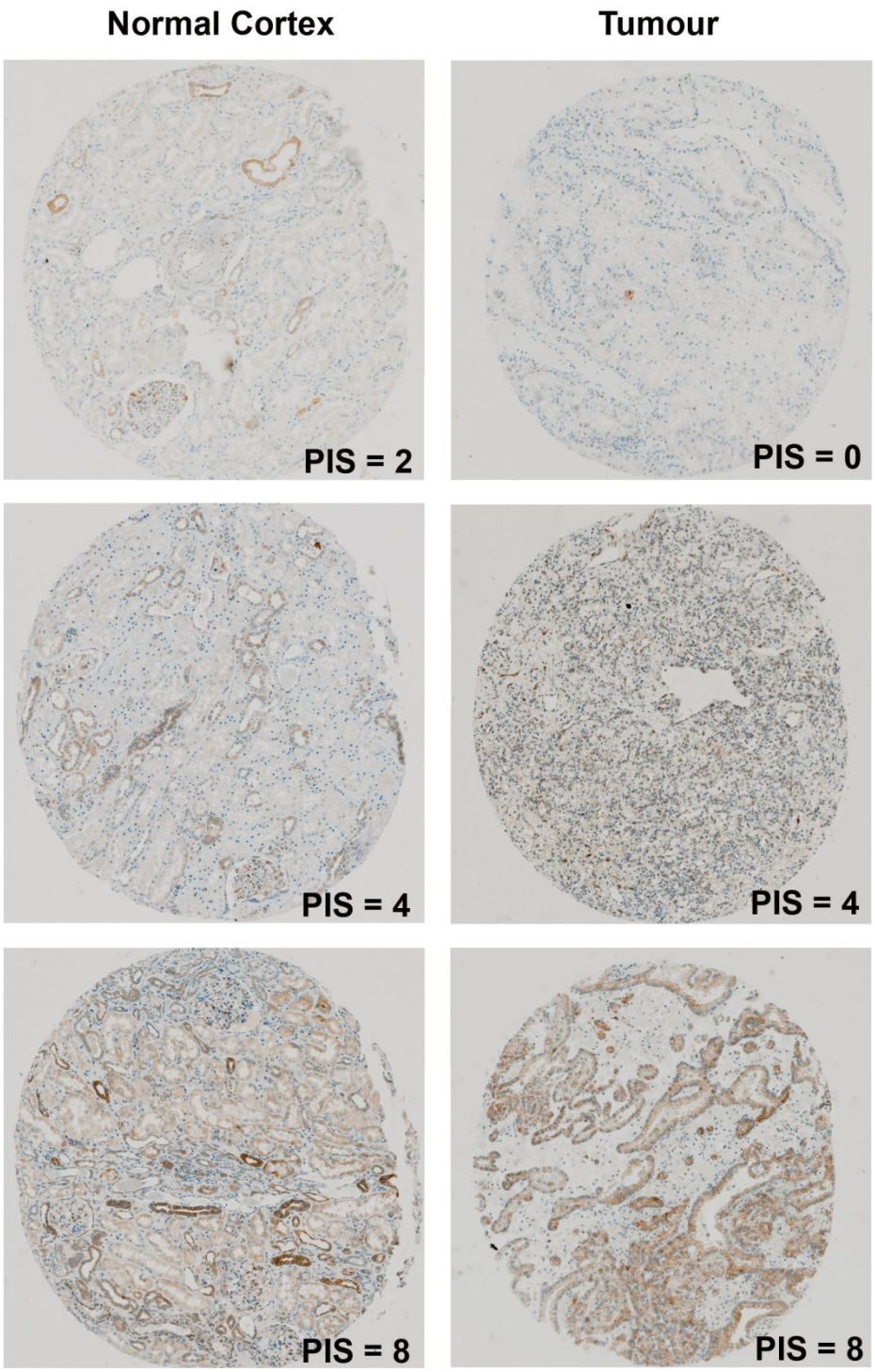


Figure 6-30. The histological appearances in normal renal cortex and CCRCC tumours of ISCU PIS scores of 0 – 8.

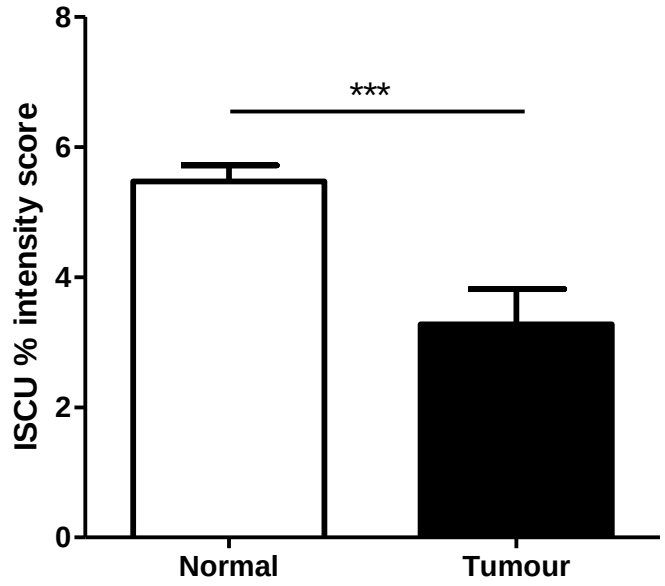


*Figure 6-31. Mean percentage intensity scores of ISCU in normal renal cortex (N=40) and tumours (N=40) in tissue microarrays. The tumours express 40% less ISCU. Plotted = mean + SEM, ***p<0.001, Wilcoxon matched-pairs signed rank test.*

The normal controls and the tumours were arranged on two separate arrays, one containing all the normal controls, and one containing all the tumours. The arrays were stained at the same time, using exactly the same reagents, batch and conditions. We investigated the correlation between ISCU protein and miR-210 levels. This would serve as evidence for a clinically significant mechanism for ISCU regulation.

The tumours were split in to two similar sized groups based on ISCU staining in the TMAs. The ISCU 'low' group had a PIS of 0-3 (N=23), and the ISCU 'high' group had a PIS of 4-12 (N=25). miR-210 expression was compared between high and low ISCU staining groups. It was observed that the median miR-210 expression in the low-staining group was 2.7 fold higher than in the high-ISCU staining group. The difference was highly significant ($p<0.001$, Mann-Whitney test (Fig. 6-32).

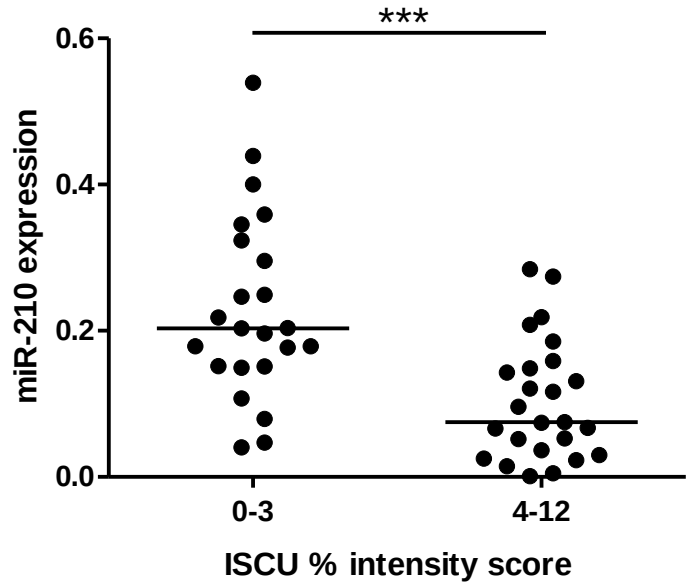


*Figure 6-32. Relationship of ISCU expression to miR-210 expression. CCRCCs were grouped in to low- and high- ISCU PIS groups, and compared for miR-210 expression. miR-210 expression was expressed 2.7-fold higher in the low ISCU-staining group. Lines=median. ***p<0.001, Mann Whitney test.*

The effect of VHL mutation on ISCU PIS was then examined. The CCRCC tumours were grouped in to those with, or without VHL mutations and the mean PIS for each group was calculated. It was found that only the tumours in the group with a VHL mutation had a significant lower ISCU expression than the respective normal controls. (Fig. 6-33)

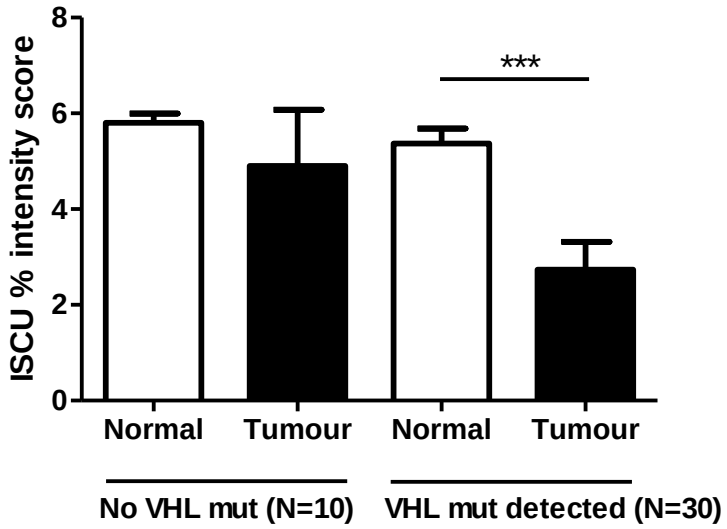


*Figure 6-33. ISCU expression in tumours with or without VHL mutations. Only the tumours in the VHL mutation group showed significantly lower ISCU levels than the normal controls. Plotted=mean + SEM. **p<0.01, unpaired t test.*

It was then decided to compare the mean ISCU PIS between the CCRCC tumours and the papillary tumours. It was found that the mean ISCU PIS was over 2-fold lower in the CCRCCs than the papillary tumours ($p<0.05$). (Fig 6-34)

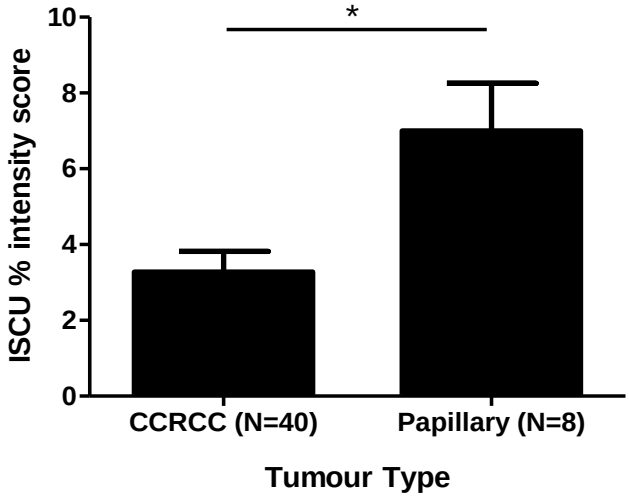


*Figure 6-34. ISCU PIS in CCRCCs and papillary tumours. Papillary tumours expressed greater than 2 fold more ISCU than CCRCCs. Shown=mean + SEM. *p<0.05, unpaired t test with Welch's correction.*

6.7 Characterization of CCRCCs using IHC and tissue microarrays

The TMA of the renal tumours was stained by IHC for HIF-1α and HIF-The purspose was to characterise the tumours by HIF expression, and to look for any correlations with HIF status and miR-210 expression.

It was found that the majority of tumours (64%) appeared to express no HIF-1α or 2α. Figure 6-35 shows the distribution of HIF staining amongst the 40 tumours on the TMA.

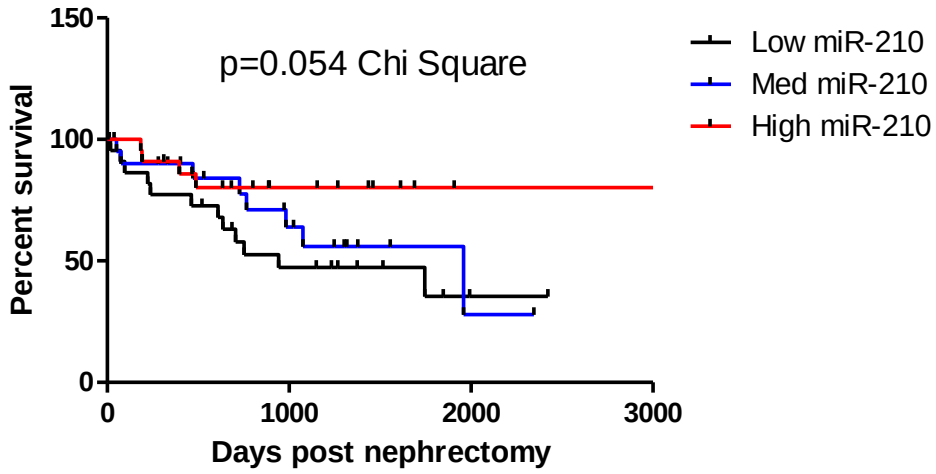


Figure 6-35. Distribution of HIF-1α and-2α staining in the CCRCC TMAs. VHL No HIF=no HIF staining (64% N=25); H1=HIF-1 only (21%, N=8); H1H2= HIF-1 and HIF-2 staining (15%, N=6); H2=HIF2 only staining (0%)

In the previous experience of this group, and other published studies, HIF staining has been found to be present in the majority of renal tumours. With this experiment (despite being repeated twice) not showing comparable results, it was decided that the data was likely to be unreliable. No attempts to correlate HIF status with other parameters were therefore attempted.

6.7.1 VHL protein expression

The PIS for VHL was calculated for all the CCRCCs on the TMA. This was then compared to the known VHL gene mutation status. There was no obvious correlation with VHL protein expression and VHL mutation status.

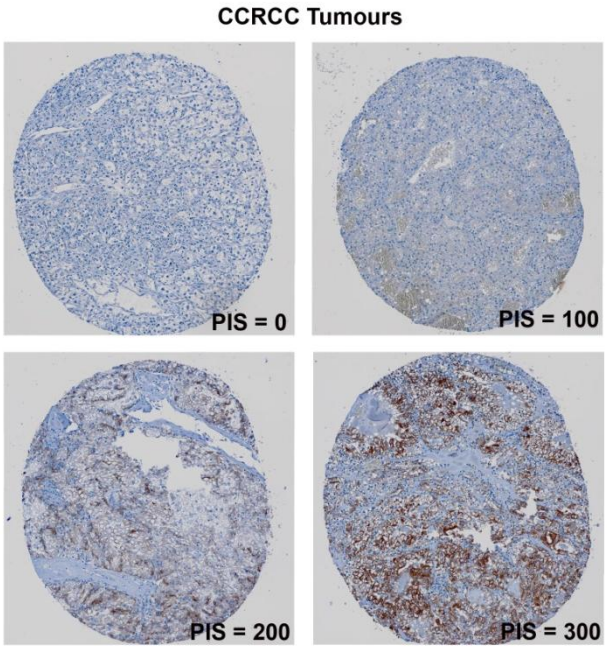


Figure 6-36. Representative TMA cores stained for VHL by IHC with PIS scores from 0 to 300.

The tumours were grouped in to CCRCCs with low (N=21) or high (N=18) cytoplasmic VHL expression as measured by PIS. miR-210 expression, and CA9 expression was plotted for each of these groups. No difference in CA9 or miR-210 expression was seen between the low or high VHL-expressing groups. (Fig. 6-37)

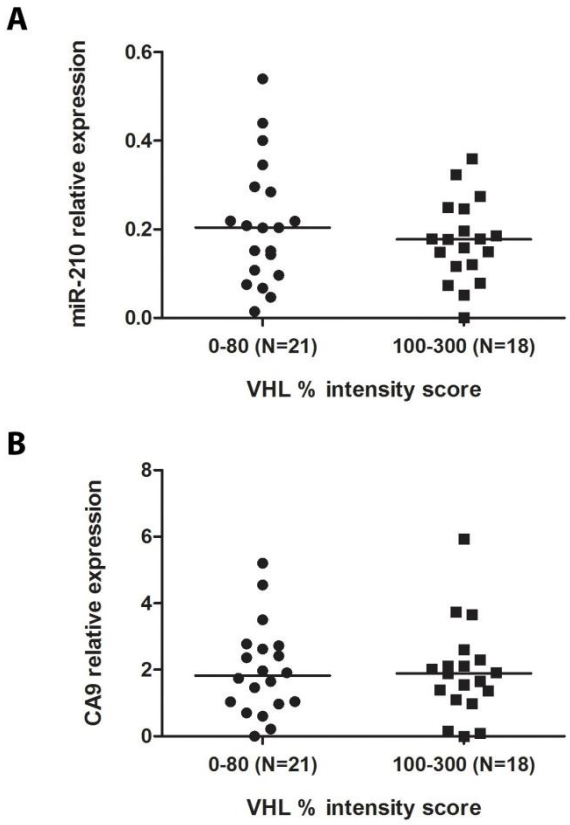


Figure 6-37. VHL protein expression and miR210/CA9 expression. A. VHL high- and low-PIS groups were compared for miR-210 expression. No significant difference was seen. B. VHL PIS compared for CA9 expression. No significant difference was seen. Lines=median. Mann-Whitney test.

CA9 IHC was performed on the TMAs. However, most tumours had maximal or near-maximal staining for CA9, and thus it was not possible to group them by expression of this protein.

6.7.2 TMA staining for E2F3 and GH2AX

E2F3 has been described as a potential miR-210 target (*145*); GH2AX is a DNA repair gene and is a marker of DNA damage from replications stress. Its expression has been shown to be lower in HIF-2α–exclusively expressing (H2) tumours, compared with H1, H1H2 or VHL WT tumours (*57*). In the HIF staining

experiment, no tumours in our TMA expressed HIF-2α exclusively, and thus it was impossible to directly compare the results of this study. However, miR-210 has been shown to target the DNA repair gene RAD52 (*158*). It was therefore decided to look for any correlation between GH2AX and miR-210 expression. However, as shown in figure 6-38 B, no correlation was seen.

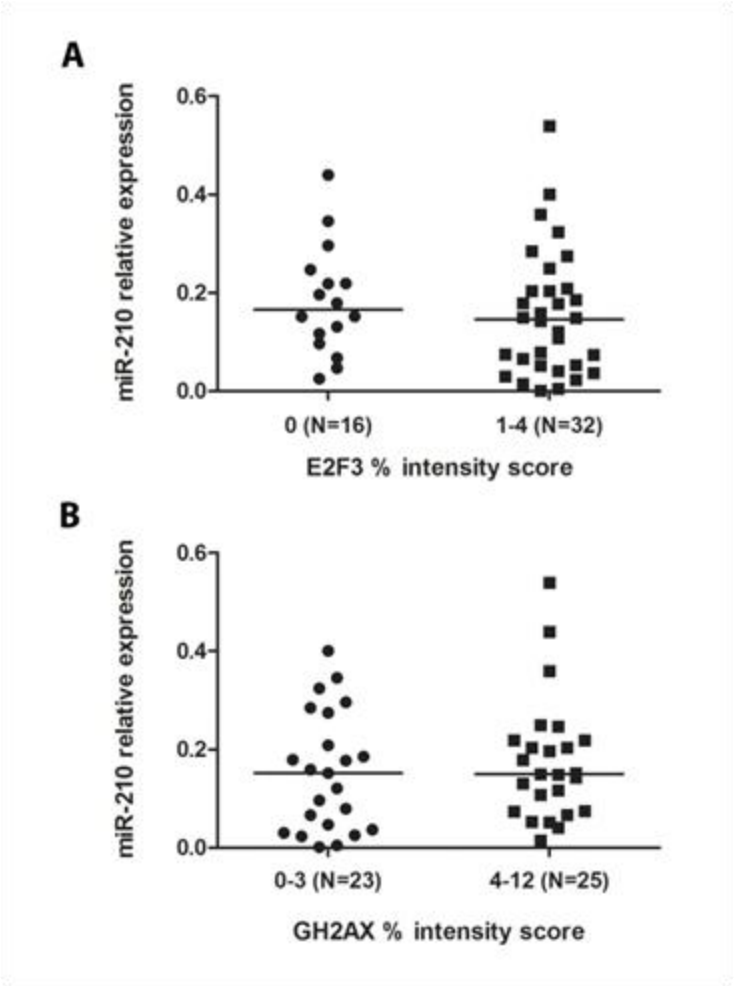


Figure 6-38. miR-210 expression and E2F3/GH2AX PIS. A. CCRCC tumours were separated in to two groups based on whether they expressed E2F3. No difference in miR-210 expression was seen between the groups. B. CCRCC tumours were separated in to low- and high- GH2AX expression. No difference in miR-210 expression was seen between the groups. Lines=median. Mann-Whitney test.

6.8 miR-210 expression in the serum of patients pre- and post nephrectomy

Following the finding that mice with miR-210 over-expression xenografts showed a trend towards expressing more miR-210 in their serum, it was hypothesized that patients with renal tumours may express higher levels of miR-210 than patients without them. This was based on the assumption that tumours are able to secrete miRNA in to the serum, and the finding that renal tumours express high levels of miR-210 compared to normal renal cortex controls.

17 archival serum samples were obtained. These had been collected in silicon-coated tubes, allowed to clot for one hour, centrifuged and the supernatant stored at -80°C. RNA was extracted from the serum as for cell line RNA extraction, except using Trizol LS reagent instead. cDNA was made, and miR-210 expression was measured by qRT-PCR, as previously described. The data were normalised to miR-16, based on findings from previous studies that this was a suitable control gene.(*159-161*) Comparison of the miR-210 expression in the serum pre- and post operation revealed no difference in the median expression. (Figure 4.5.1)

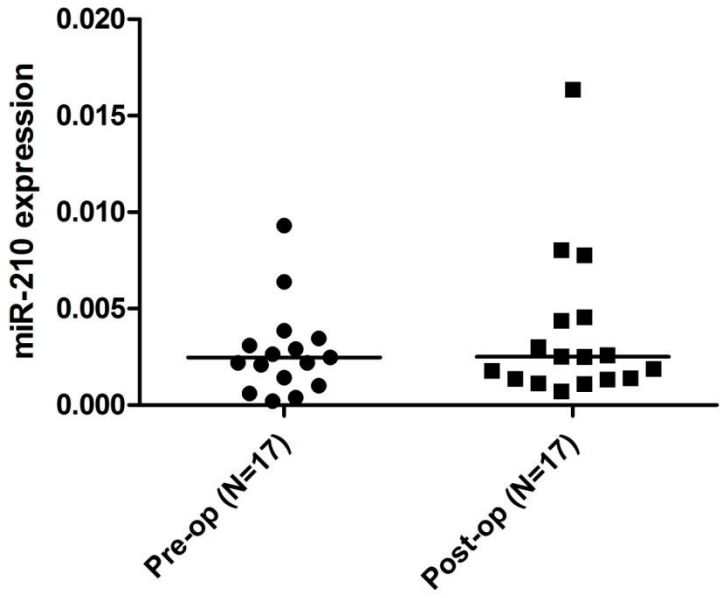


Figure 6-39. miR-210 expression pre- and post-nephrectomy. No difference was seen. Lines=median.

6.9 Discussion

There is a clear association with VHL protein dysfunction and the development of renal cancer, as evidenced by the development of renal tumours in VHL syndrome, and the high rate of somatic mutations in CCRCC.(*50*) In this study, only the clear cell subtype of renal cancers was found to have somatic VHL mutations, and of these, 72% had VHL mutations. The initial cell line experiments in this study were carried out with RCC4 and 786-O renal cancer cell lines, with the aim of demonstrating hypoxic and VHL-mediated regulation of miR-210 in renal cancer. Both cell lines harbour inactivating mutations of the VHL gene. They differ, however, in that RCC4s express both HIF-1α and -2α, whereas the 786-O

cells express HIF-2α only. RCC4 cells exhibited over-expression of miR-210 with VHL dysfunction, and in hypoxia in cells with functional VHL restored, as would be expected of a HIF-1α target. The 786-O cells, however, also demonstrated hypoxic and VHL-mediated regulation of miR-210, although to a lesser degree. This was unexpected, as miR-210 had previously been shown to be a HIF-1α target only.(*127*) Further proof of HIF-2α regulation of miR-210 in the 786-O cell line was found through HIF-2α knockdown experiments, and through identification of a HIF-2α binding site near the miR-210 gene locus. These experiments demonstrate that, although miR-210 is predominantly a HIF-1α target, HIF-2α is able to regulated it in its absence (in this cell line), albeit to a lesser degree.

In the human CCRCC tumours used in this study, VHL mutation status was initially demonstrated to be associated with miR-210 expression. It was noted, however, that there appeared to be a bimodal distribution of miR-210 expression in the CCRCCs with no VHL mutations (fig. 6-11). There was a cluster of tumours expressing similar miR-210 expression to the median values in the VHL mutation group, and another cluster with little or no miR-210 expression. The latter group may represent true wild-type VHL expression, with the higher miR-210 expressing miR-210 tumours representing VHL inactivation by another means, such as promoter hypermethylation (not measured in this study), which may affect 5-20% of tumours. Analysis of the miR-210 expression in combination with a second dataset (fig. 6-13) did not show a significant difference in miR-210 expression between the VHL-ve and VHL+ve tumours. It is worth noting that the collaborators who supplied the RNA for the additional tumours had analyzed the corresponding DNA for VHL promoter hypermethylation, in addition to VHL mutations and LOH. They found that all but one tumour in the dataset had VHL

inactivation by one of these means.(*162*) Reports of VHL gene mutation prevalence in sporadic CCRCC range from 18-82%.(*163*) Whatever the mechanism of VHL inactivation, this study clearly shows that miR-210 is significantly and highly up-regulated in renal tumours, compared to the normal renal cortex. Whether this is simply a reflection of VHL dysfunction, or a combinatorial effect with intrinsic tumour hypoxia contributing to overall miR-210 expression, is uncertain. In CCRCCs, a positive correlation of miR-210 expression with the HIF-1α target, CA9, was observed; this points to HIF as the likely mediator of its over-expression. (CA9 is not expressed in normal adult kidney(*164*), and the use of CA9 has been proposed as a biomarker for renal cancer). Reinforcing this statement is the finding that papillary tumours demonstrate much less miR-210 expression than the CCRCC group; an oncomine analysis of the Yusenko renal data shows that papillary tumours also express less CA9 at mRNA level.(*165*)

In the majority of cancers, high CA9 expression is correlated with increased levels of hypoxia and poor prognosis. However, in renal cell cancer, the opposite has been shown to be true,(*166*) and CA9 expression correlates negatively with survival, T-stage and Fuhrman grade. (*167*) This pattern might, therefore, be expected of miR-210 in cancer. It has been shown that miR-210 correlates with poor survival in breast, pancreatic and head and neck cancer.(*127, 168, 169*) In this study, miR-210 shows a statistically significant inverse relationship to tumour grade in CCRCCs, with higher grade tumours (grade 3-4) expressing 45% less miR-210 than lower grade (grade 1-2) tumours. There were similar findings with tumour stage, with the higher stage tumours expressing 24% less miR-210 than the lower stage tumours. Analysis of survival was carried out by dividing patients in to three equal size groups ranked on miR-210 expression levels. Patients with

tumours expressing the most miR-210 showed improved survival over the two groups with lower miR-210 expression.

The reason for high miR-210 expression being associated with good clinico-pathological parameters in CCRCC is unclear. One possibility is that, because the majority of CCRCCs will have VHL deficiency, the 'baseline' state of the tumours will be to have high expression of HIF-1α targets, including miR-210. Further de-differentiation of the tumours, with accumulating mutations and dysregulation of pathways, may manifest itself with reduction in the expression of genes such as miR-210. This would be supported in principle by the fact that miR-210 has an inverse relationship to tumour grade, a marker of differentiation. However, a more complex picture is likely to be occurring. It has been demonstrated that CCRCCs can express HIF-1α and -2α in combination, HIF-2α alone, or no HIF. Over-expression of HIF-2α, but not HIF-1α, has been shown to be necessary to overcome the tumours suppressor function of VHL in xenograft models.(*56, 170, 171*) Additionally, HIF-2α over-expression was necessary to form the clear cell phenotype in a mouse model of CCRCC.(*172*) HIF-2α has been associated with larger tumour size(*57*), and faster growth of xenografts.(*120*) The reason for low miR-210 (and CA9) correlating with poorer prognosis may reflect a predominance of HIF-2α activity (and reduced HIF-1α activity) in the CCRCC tumours. C-myc is known to be activated by HIF-2α, and inhibited by HIF-1α. C-myc activates cyclin D2 and E2F3 leading to the promotion of cell cycle progression, whilst leading to the repression of the pro-apopototic p27 and p21.(*173*) In this study, low miR-210 was associated with higher ki67 expression, a marker of proliferation, and would thus support the argument that its increased expression is associated with a pro-proliferative HIF-2α-predominant state. Although it was shown in this study that HIF-2α can sitll regulate miR-210 in HIF-1α-deficient 786-O cells, it is notable that

the hypoxia-mediated induction is much lower than in RCC4 cells, which express HIF-1α protein.

The association of VHL mutations with survival in renal cancer is not clear. One study of 100 patients with renal cancer found that VHL mutation status and CA9 expression in combination could be used to predict outcome. A combination of VHL mutation and high CA9 correlated with the most favourable outcome; either VHL mutation OR high CA9 correlated with intermediate outcome, and no VHL mutation with low CA9 was associated with the worst outcome. On multivariate analysis, however, only CA9 was an independent predictor of outcome.(*174*) In support of the fact that VHL mutations are associated with better prognosis are the observations that VHL disease-associated tumours grow more slowly than sporadic RCCs.(*175-177*) As the type and location of VHL mutation in VHL disease is predictive of the disease course and type of tumours encountered, one would predict that the characteristics of VHL mutation in somatic disease might confer prognostic information.(*50*) A review of thirteen studies commenting on VHL mutations and their relationship to clinicopathological variables found that in three studies VHL mutation correlated with favourable characteristics, four correlated with poor characteristics, and six found no correlation.(*163*) The variation in results may be explained by the lack of overall consensus for classifying VHL mutations in sporadic tumours, and the fact that some, but not all studies, incorporate hypermethylation data. Two recent studies have shown VHL inactivation by mutation, LOH or methylation in 91% (*178*) and 96.6% (*162*), and it has been suggested that VHL loss-of-function is probably not a feature of, but probably defines the clear cell subtype of renal cell cancer.(*162*)

In this study, no correlation of VHL mutation location or type was seen with miR-210 expression. This is perhaps not surprising, given the limited numbers of tumours examined, and the fact that many of the studies described above have conflicting results. However, it should be possible to measure the outcome of VHL mutations by downstream variations in proteins such as HIF-1α and HIF-2α. This approach was used by Gordan *et al*, who classified renal tumours by immunohistochemistry, in to those expressing no HIF-α (VHL WT, 12%), HIF-1α and HIF-2α (H1H2, 61%) and HIF-2α only (H2, 27%). They found no tumours exclusively expressing HIF-1α. It was found that the H2 tumours showed increased c-Myc activity, in that they expressed higher levels of c-Myc activated targets Cyclin D2 and E2F1 than VHL WT or H1H2 tumours. Additionally, expression of the c-Myc repressed targets p21 and p27 were reduced in the H2 tumours. Conversely, VHL WT tumours and H1H2 tumours showed increased expression of extracellular regulated kinase (ERK or mitogen activate protein kinase 1, MAPK) and ribosomal protein S6, a target of the mTOR substrate p70 S6 kinase. These proteins are important signalling molecules which are phosphorylated by several growth factor signal transduction pathways.(*57*) In our study, a TMA of the renal tumours which had been characterised for miR-210 expression, was stained for HIF-1α and HIF-2α. Like the Gordan study, we were able to detect different patterns of HIF-α expression among the tumours. However, the distribution of HIF staining was somewhat different, with 64% showing no HIF staining (WT), 15% showing HIF-1α and -2α staining (H1H2), and 21% showing HIF-1α staining exclusively (H1). No H2 tumours were found in this study and, unlike the Gordan study, H1 tumours were found to exist. The explanation for the major differences between the studies is uncertain. However, with the majority of tumours in this study harbouring a VHL mutation, and

significant CA9 expression, it would seem that the finding that 64% of the tumours express no HIF protein is probably inaccurate. Due to this, no further analysis based on HIF-α protein expression, as measured in this study, was carried out.

It is interesting that, although VHL protein expression in the TMAs did not show a correlation with miR-210 expression, the VHL mRNA as measured by qPCR did. The antibody to VHL used may target an epitope of the protein which is expressed in many tumours despite mutations of the gene. It is intriguing that the copy number of the VHL mRNA is associated with miR-210 expression. The primers to the gene were designed to the 3'UTR, which is the last part of the mRNA to be transcribed before addition of the poly-A tail. The mRNA level measured in this way may therefore provide a readout of potentially translated (though not necessarily fully functional) VHL mRNA which has not been stalled during transcription due to a mutation. The type of mutation may affect transcription, translation, or protein folding. Each may have different consequences for the cell, determining whether there is some functional VHL protein present, or none at all due to a failure of transcription.

Following work described in Chapter 4, which provided strong evidence that ISCU is a gene target of miR-210, it was decided to investigate the relevance of miR-210-medated repression in the tumour samples. The qRT-PCR analysis of ISCU expression showed that ISCU mRNA was down-regulated in the tumour samples compared to the normal controls. An oncomine search was carried out which demonstrated that it ISCU was down-regulated in tumours compared to normal controls in most data sets, in agreement with our normalised qRT-PCR data.(*165*) Use of the renal tumours and matched normal tissue TMAs provided further

evidence of ISCU down-regulation in CCRCCs. The tumours expressed about 60% of the ISCU staining of the normal controls. In addition, the fact that ISCU staining has an inverse relationship to miR-210 levels in the tumours, and the presence of higher ISCU staining in the low-miR-210-expressing papillary tumours than CCRCCs (which have much higher miR-210 expression), lends further evidence to miR-210 regulation of ISCU being relevant *in vivo*.

A number of miRNAs, which were found to be VHL-regulated in RCC4 renal cancer cells, were investigated in the renal tumour samples. miR-148a was significantly down-regulated in the VHL mutant CCRCCs, and showed a similar but non-significant trend in the papillary tumours. miR-100 was down-regulated in CCRCCs and papillary tumours. However, many of the other miRNAs identified as VHL-regulated in RCC4 cells did not demonstrate differential regulation in the tumours. This reflects the fact that some regulation of miRNAs is likely to be cell-line specific, and would perhaps not be seen on a more global scale. Additionally, care needs to be taken in interpreting small, two-fold changes in the expression of any gene in clinical material. This is due to the fact that, despite the use of multiple controls, it is not possible to be certain that an apparent gene regulation is not partly a result of variation in control gene expression between samples. This is likely to be particularly important when comparing different tissue, i.e. normal and tumours. This is perhaps less of an issue when comparing genes within a particular tissue type, e.g. gene expression within CCRCCs alone. Nevertheless, examination of the control gene data used in these experiments for miRNA analysis revealed that their average CT values in the tumours and normal controls were almost identical, allowing increased confidence in the data.

Following published data of the use of miRNAs as serum biomarkers (*161, 179*), and the trend towards increased miR-210 in the serum of mice harbouring miR-210 over-expressing xenografts, it was decided to look at the expression of miR-210 in the serum of patients. The hypothesis that miR-210 in the serum would fall following nephrectomy, however, was not proven. A comparison between miR-210 expression in the serum of healthy patients and those with renal tumours proved impossible. This was due to the huge variation in miR-210 expression in the serum samples. It is speculated that this will have been due to variation in extraction methodology, storage and age of the archival serum material. It highlights the need for prospective sample collection, with strict adherence to protocols for sample handling.

In conclusion, this chapter has demonstrated that miR-210, and other HRMs, are up-regulated in renal tumours. miR-210 expression is correlated negatively with VHL mRNA, and positively with CA9 mRNA. It has also been shown that expression of the miR-210 target, ISCU, correlates negatively with expression of the miRNA, providing evidence, though not proof, of the presence of functional miRNA-mediated regulation in the tumours. It has been shown that miR-210 can be detected in the serum, but its significance as a useful tumour marker is yet to be determined. Finally, miR-210 is associated with better prognosis and reduced tumour stage and grade in CCRCC, in contrast to other tumour types.

CHAPTER 7
Conclusions and future work

7.1 Conclusions

The first aim of this project was to identify whether miRNAs are differentially regulated in hypoxia. The efforts to use in-house manufactured microarray platforms met with limited success, due to the poor quality of the output. Data from other members of our research group, obtained using commercially available platforms, demonstrated that miR-210 was up-regulated in hypoxia in breast cancer cell lines. miR-210 was shown to be associated with a hypoxia metagene, and correlated with poor clinical outcome in breast cancer patients.(*127*) It was therefore decided to investigate the function of this miRNA further.

In Chapter 3, *in silico* algorithms were used to predict targets of miR-210. A number of targets were selected for investigation. The experiments using knock-down of miR-210 in hypoxia failed to show any convincing rescue of expression of a number of proteins predicted to be target of miR-210. However, subsequent analysis of mRNA profiles in MCF7 cells using commercial microarray platforms identified a new target. The mRNA expression of ISCU, which had not been predicted in the earlier builds of the *in-silico* algorithms, was found to be rescued by miR-210 knock-down in hypoxia, and was selected for further analysis.

In Chapter 4, miR-210 gain-of-function experiments (using miR-210 mimics), as well as knock-down, were carried out. These experiments provided strong evidence for ISCU being a target of miR-210. It was down-regulated by miR-210 over-expression in every cell line tested. Its expression was only partially rescued

by anti-210 in MCF7 cells, but not in other cell lines tested, suggesting that control of its expression is not mediated exclusively by miR-210 in hypoxia. It also highlights the fact that the effects of miRNAs are likely to vary between different cell lines and tissue types. This chapter discussed the consequences of miR-210-mediated knockdown of ISCU. ISCU down-regulation, and the subsequent loss of Fe-S cluster formation, resulted in reduced complex I activity in the mitochondria and increased ROS production, along with increased lactate production. Loss of the Fe-S cluster in aconitase led to activation of its function as IRP-1, with consequent increase in iron uptake in the cell.

In Chapter 5, constitutive over-expression of miR-210 in MCF7 and MDA-MB-231 cells was used to investigate the function of the miRNA. While the technique to produce the over-expression was successful, it did not lead to any firm conclusions with subsequent functional studies. Experiments on cell monolayer cultures did not demonstrate any difference in proliferation with miR-210 over-expression in normoxia, hypoxia, or with serum deprivation. *In vivo* models consisting of MCF7 or MDA-MB-231 xenografts with empty vector transfection or miR-210 over-expression produced contradicting data on the effect of miR-210 on tumour growth rate. Analysis of HIF, CA9 and Ki-67 expression by immunohistochemistry in the xenograft tumours failed to show any correlation with miR-210 expression status. Although analysis of miR-210 in the serum of the mice showed a trend towards increased expression in the mice harbouring miR-210 over-expressing xenografts, it was not statistically significant. The use of polysomal fractionation to look for miR-210 targets failed due to the great variability in the data, and the technical difficulties in getting enough good replicates for the experiment. In summary, the use of constitutive over-expression of miR-210 as an experimental tool did not lead to successful

identification of targets or functional implications of the miRNA, in contrast to the prior use of transient over-expression or down regulation (as seen in Chapter 4). The cause of this is unclear, but it may reflect the cells adjusting to the constitutive miR-210 over-expression by activation of alternative pathways. This may significantly dampen any effect of miR-210 that might otherwise be seen with transient over-expression.

In Chapter 6, the role of miR-210 in renal cancer was explored. It was established that miR-210 was constitutively up-regulated in VHL-defective RCC4 and 786-O cell lines, compared to those transfected with functional VHL. It was discovered that HIF-2α took over the regulation of miR-210 in HIF-1α-defective 786-O cells. The expression of miRNAs in renal cancer was investigated. It was found that miR-210 was highly over-expressed in CCRCC renal tumours compared to normal renal cortex controls. miR-210 appeared to be more highly expressed in CCRCC tumours with VHL mutations, but this was not statistically significant. However, with LOH and promoter hyper-methylation being additional sources of VHL inactivation or dysfunction, it is difficult to draw conclusions on gene mutation status alone. miR-210 did correlate with CA9, a well-described HIF-1α target. There was also a correlation with VHL mRNA, suggesting that its expression may relate to a gradient of VHL functionality. It is interesting that high miR-210 in renal cancer correlated with lower tumour grade and stage, in addition to correlating with improved survival. This is in contrast to studies in other tumour types, which show miR-210 to be associated hypoxic gene expression profiles and poorer prognosis. It is not possible to conclude from these experiments whether miR-210 is implicated directly in the prognosis of renal cancer. However, it may represent a marker of VHL function, and may reflect the balance of HIF-1α versus HIF-2α function within the cells. What was shown, however, was an inverse

correlation of miR-210 with its target, ISCU, suggesting that it does have functional significance *in vivo*.

7.2 Future work

Recent work by our group, and collaborators, has pooled data from expression profiling experiments and target prediction algorithms to generate a new list of potential miR-210 targets to investigate. Two of these targets involve mitochondrial function, and one is linked to tumour angiogenesis. Further investigation of these targets in both breast and renal cancer is planned.

The HIF expression data from the CCRCC TMAs did not show the levels of expression we would expect. Further experiments on thicker sections of the TMAs are planned to confirm the validity of the existing data. It is intended to use the TMAs to investigate further targets of miR-210, once they are confirmed *in vitro.*

The correlation of miR-210 with clinic-pathological variables in renal cancer suggests that it has potential as a marker for prediction of response to treatment. The departmental database contains clinical information on more than thirty patients with advanced renal cancer who were treated with anti-angiogenic agents, linked to archived pathological material. It is intended to look at the expression of miRNA and mRNA in this material, in order to look for markers (including miR-210) that could help to select suitable patients for anti-angiogenic therapies.

References

1. Statistics, O. o. N. (2008) Cancer.
2. Ahr, K., (Ed.) (2008) *Molecular Cell Biology*, 6th ed., W. H. Freeman.
3. Khosravi-Far, R., Campbell, S., Rossman, K. L., and Der, C. J. (1998) Increasing complexity of Ras signal transduction: involvement of Rho family proteins, *Adv Cancer Res 72*, 57-107.
4. Brazil, D. P., and Hemmings, B. A. (2001) Ten years of protein kinase B signalling: a hard Akt to follow, *Trends Biochem Sci 26*, 657-664.
5. Cotter, T. G. (2009) Apoptosis and cancer: the genesis of a research field, *Nat Rev Cancer 9*, 501-507.
6. Venkitaraman, A. R. (2002) Cancer susceptibility and the functions of BRCA1 and BRCA2, *Cell 108*, 171-182.
7. Knudson, A. G., Jr. (1971) Mutation and cancer: statistical study of retinoblastoma, *Proc Natl Acad Sci U S A 68*, 820-823.
8. Fearon, E. R., and Vogelstein, B. (1990) A genetic model for colorectal tumorigenesis, *Cell 61*, 759-767.
9. Hanahan, D., and Weinberg, R. A. (2000) The hallmarks of cancer, *Cell 100*, 57-70.
10. Lopez-Lazaro, M. (2006) Hypoxia-inducible factor 1 as a possible target for cancer chemoprevention, *Cancer Epidemiol Biomarkers Prev 15*, 2332-2335.
11. Semenza, G. L. Oxygen homeostasis, *Wiley Interdiscip Rev Syst Biol Med 2*, 336-361.
12. Vaupel, P., Schlenger, K., Knoop, C., and Hockel, M. (1991) Oxygenation of human tumors: evaluation of tissue oxygen distribution in breast cancers by computerized O2 tension measurements, *Cancer Res 51*, 3316-3322.
13. Hockel, M., Schlenger, K., Knoop, C., and Vaupel, P. (1991) Oxygenation of carcinomas of the uterine cervix: evaluation by computerized O2 tension measurements, *Cancer Res 51*, 6098-6102.
14. Vaupel, P., Thews, O., and Hoeckel, M. (2001) Treatment resistance of solid tumors: role of hypoxia and anemia, *Med Oncol 18*, 243-259.
15. Gray, L. H., Conger, A. D., Ebert, M., Hornsey, S., and Scott, O. C. (1953) The concentration of oxygen dissolved in tissues at the time of irradiation as a factor in radiotherapy, *Br J Radiol 26*, 638-648.
16. Hockel, M., and Vaupel, P. (2001) Tumor hypoxia: definitions and current clinical, biologic, and molecular aspects, *J Natl Cancer Inst 93*, 266-276.
17. Teicher, B. A., Holden, S. A., al-Achi, A., and Herman, T. S. (1990) Classification of antineoplastic treatments by their differential toxicity toward putative oxygenated and hypoxic tumor subpopulations in vivo in the FSaIIC murine fibrosarcoma, *Cancer Res 50*, 3339-3344.
18. Wouters, A., Pauwels, B., Lardon, F., and Vermorken, J. B. (2007) Review: implications of in vitro research on the effect of radiotherapy and chemotherapy under hypoxic conditions, *Oncologist 12*, 690-712.
19. Hockel, M., Schlenger, K., Aral, B., Mitze, M., Schaffer, U., and Vaupel, P. (1996) Association between tumor hypoxia and malignant progression in advanced cancer of the uterine cervix, *Cancer Res 56*, 4509-4515.
20. Generali, D., Berruti, A., Brizzi, M. P., Campo, L., Bonardi, S., Wigfield, S., Bersiga, A., Allevi, G., Milani, M., Aguggini, S., Gandolfi, V., Dogliotti, L.,

Bottini, A., Harris, A. L., and Fox, S. B. (2006) Hypoxia-inducible factor-1alpha expression predicts a poor response to primary chemoendocrine therapy and disease-free survival in primary human breast cancer, *Clin Cancer Res 12*, 4562-4568.

21. Jubb, A. M., Buffa, F. M., and Harris, A. L. (2009) Assessment of tumor hypoxia for prediction of response to therapy and cancer prognosis, *J Cell Mol Med*.
22. Holmgren, L., O'Reilly, M. S., and Folkman, J. (1995) Dormancy of micrometastases: balanced proliferation and apoptosis in the presence of angiogenesis suppression, *Nat Med 1*, 149-153.
23. Becker, A., Stadler, P., Lavey, R. S., Hansgen, G., Kuhnt, T., Lautenschlager, C., Feldmann, H. J., Molls, M., and Dunst, J. (2000) Severe anemia is associated with poor tumor oxygenation in head and neck squamous cell carcinomas, *Int J Radiat Oncol Biol Phys 46*, 459-466.
24. Dewhirst, M. W., Cao, Y., and Moeller, B. (2008) Cycling hypoxia and free radicals regulate angiogenesis and radiotherapy response, *Nat Rev Cancer 8*, 425-437.
25. Wang, G. L., Jiang, B. H., Rue, E. A., and Semenza, G. L. (1995) Hypoxia-inducible factor 1 is a basic-helix-loop-helix-PAS heterodimer regulated by cellular O2 tension, *Proc Natl Acad Sci U S A 92*, 5510-5514.
26. Schuster, S. J., Wilson, J. H., Erslev, A. J., and Caro, J. (1987) Physiologic regulation and tissue localization of renal erythropoietin messenger RNA, *Blood 70*, 316-318.
27. Beck, I., Ramirez, S., Weinmann, R., and Caro, J. (1991) Enhancer element at the 3'-flanking region controls transcriptional response to hypoxia in the human erythropoietin gene, *J Biol Chem 266*, 15563-15566.
28. Pugh, C. W., Tan, C. C., Jones, R. W., and Ratcliffe, P. J. (1991) Functional analysis of an oxygen-regulated transcriptional enhancer lying 3' to the mouse erythropoietin gene, *Proc Natl Acad Sci U S A 88*, 10553-10557.
29. Madan, A., and Curtin, P. T. (1993) A 24-base-pair sequence 3' to the human erythropoietin gene contains a hypoxia-responsive transcriptional enhancer, *Proc Natl Acad Sci U S A 90*, 3928-3932.
30. Semenza, G. L., Nejfelt, M. K., Chi, S. M., and Antonarakis, S. E. (1991) Hypoxia-inducible nuclear factors bind to an enhancer element located 3' to the human erythropoietin gene, *Proc Natl Acad Sci U S A 88*, 5680-5684.
31. Semenza, G. L., and Wang, G. L. (1992) A nuclear factor induced by hypoxia via de novo protein synthesis binds to the human erythropoietin gene enhancer at a site required for transcriptional activation, *Mol Cell Biol 12*, 5447-5454.
32. Wang, G. L., and Semenza, G. L. (1993) Characterization of hypoxia-inducible factor 1 and regulation of DNA binding activity by hypoxia, *J Biol Chem 268*, 21513-21518.
33. Jiang, B. H., Semenza, G. L., Bauer, C., and Marti, H. H. (1996) Hypoxia-inducible factor 1 levels vary exponentially over a physiologically relevant range of O2 tension, *Am J Physiol 271*, C1172-1180.
34. Wood, S. M., Gleadle, J. M., Pugh, C. W., Hankinson, O., and Ratcliffe, P. J. (1996) The role of the aryl hydrocarbon receptor nuclear translocator (ARNT) in hypoxic induction of gene expression. Studies in ARNT-deficient cells, *J Biol Chem 271*, 15117-15123.

35. Tian, H., McKnight, S. L., and Russell, D. W. (1997) Endothelial PAS domain protein 1 (EPAS1), a transcription factor selectively expressed in endothelial cells, *Genes Dev 11*, 72-82.
36. Jiang, B. H., Zheng, J. Z., Leung, S. W., Roe, R., and Semenza, G. L. (1997) Transactivation and inhibitory domains of hypoxia-inducible factor 1alpha. Modulation of transcriptional activity by oxygen tension, *J Biol Chem 272*, 19253-19260.
37. Schofield, C. J., and Ratcliffe, P. J. (2004) Oxygen sensing by HIF hydroxylases, *Nat Rev Mol Cell Biol 5*, 343-354.
38. Appelhoff, R. J., Tian, Y. M., Raval, R. R., Turley, H., Harris, A. L., Pugh, C. W., Ratcliffe, P. J., and Gleadle, J. M. (2004) Differential function of the prolyl hydroxylases PHD1, PHD2, and PHD3 in the regulation of hypoxia-inducible factor, *J Biol Chem 279*, 38458-38465.
39. Epstein, A. C., Gleadle, J. M., McNeill, L. A., Hewitson, K. S., O'Rourke, J., Mole, D. R., Mukherji, M., Metzen, E., Wilson, M. I., Dhanda, A., Tian, Y. M., Masson, N., Hamilton, D. L., Jaakkola, P., Barstead, R., Hodgkin, J., Maxwell, P. H., Pugh, C. W., Schofield, C. J., and Ratcliffe, P. J. (2001) C. elegans EGL-9 and mammalian homologs define a family of dioxygenases that regulate HIF by prolyl hydroxylation, *Cell 107*, 43-54.
40. Minamishima, Y. A., Moslehi, J., Bardeesy, N., Cullen, D., Bronson, R. T., and Kaelin, W. G., Jr. (2008) Somatic inactivation of the PHD2 prolyl hydroxylase causes polycythemia and congestive heart failure, *Blood 111*, 3236-3244.
41. Tian, Y. M., Mole, D. R., Ratcliffe, P. J., and Gleadle, J. M. (2006) Characterization of different isoforms of the HIF prolyl hydroxylase PHD1 generated by alternative initiation, *Biochem J 397*, 179-186.
42. Knowles, H. J., Raval, R. R., Harris, A. L., and Ratcliffe, P. J. (2003) Effect of ascorbate on the activity of hypoxia-inducible factor in cancer cells, *Cancer Res 63*, 1764-1768.
43. Selak, M. A., Armour, S. M., MacKenzie, E. D., Boulahbel, H., Watson, D. G., Mansfield, K. D., Pan, Y., Simon, M. C., Thompson, C. B., and Gottlieb, E. (2005) Succinate links TCA cycle dysfunction to oncogenesis by inhibiting HIF-alpha prolyl hydroxylase, *Cancer Cell 7*, 77-85.
44. Doege, K., Heine, S., Jensen, I., Jelkmann, W., and Metzen, E. (2005) Inhibition of mitochondrial respiration elevates oxygen concentration but leaves regulation of hypoxia-inducible factor (HIF) intact, *Blood 106*, 2311-2317.
45. Hagen, T., Taylor, C. T., Lam, F., and Moncada, S. (2003) Redistribution of intracellular oxygen in hypoxia by nitric oxide: effect on HIF1alpha, *Science 302*, 1975-1978.
46. Kaelin, W. G., Jr., and Thompson, C. B. Q&A: Cancer: clues from cell metabolism, *Nature 465*, 562-564.
47. Hon, W. C., Wilson, M. I., Harlos, K., Claridge, T. D., Schofield, C. J., Pugh, C. W., Maxwell, P. H., Ratcliffe, P. J., Stuart, D. I., and Jones, E. Y. (2002) Structural basis for the recognition of hydroxyproline in HIF-1 alpha by pVHL, *Nature 417*, 975-978.
48. Min, J. H., Yang, H., Ivan, M., Gertler, F., Kaelin, W. G., Jr., and Pavletich, N. P. (2002) Structure of an HIF-1alpha -pVHL complex: hydroxyproline recognition in signaling, *Science 296*, 1886-1889.

49. Schoenfeld, A. R., Davidowitz, E. J., and Burk, R. D. (2000) Elongin BC complex prevents degradation of von Hippel-Lindau tumor suppressor gene products, *Proc Natl Acad Sci U S A 97*, 8507-8512.
50. Richards, F. M. (2001) Molecular pathology of von HippelLindau disease and the VHL tumour suppressor gene, *Expert Rev Mol Med 2001*, 1-27.
51. Hershko, A., and Ciechanover, A. (1998) The ubiquitin system, *Annu Rev Biochem 67*, 425-479.
52. Ohh, M., Yauch, R. L., Lonergan, K. M., Whaley, J. M., Stemmer-Rachamimov, A. O., Louis, D. N., Gavin, B. J., Kley, N., Kaelin, W. G., Jr., and Iliopoulos, O. (1998) The von Hippel-Lindau tumor suppressor protein is required for proper assembly of an extracellular fibronectin matrix, *Mol Cell 1*, 959-968.
53. Semenza, G. L. (2003) Targeting HIF-1 for cancer therapy, *Nat Rev Cancer 3*, 721-732.
54. Dang, C. V., Le, A., and Gao, P. (2009) MYC-induced cancer cell energy metabolism and therapeutic opportunities, *Clin Cancer Res 15*, 6479-6483.
55. Harris, A. L. (2002) Hypoxia--a key regulatory factor in tumour growth, *Nat Rev Cancer 2*, 38-47.
56. Raval, R. R., Lau, K. W., Tran, M. G., Sowter, H. M., Mandriota, S. J., Li, J. L., Pugh, C. W., Maxwell, P. H., Harris, A. L., and Ratcliffe, P. J. (2005) Contrasting properties of hypoxia-inducible factor 1 (HIF-1) and HIF-2 in von Hippel-Lindau-associated renal cell carcinoma, *Mol Cell Biol 25*, 5675-5686.
57. Gordan, J. D., Lal, P., Dondeti, V. R., Letrero, R., Parekh, K. N., Oquendo, C. E., Greenberg, R. A., Flaherty, K. T., Rathmell, W. K., Keith, B., Simon, M. C., and Nathanson, K. L. (2008) HIF-alpha effects on c-Myc distinguish two subtypes of sporadic VHL-deficient clear cell renal carcinoma, *Cancer Cell 14*, 435-446.
58. Pasqualini, R., Bourdoulous, S., Koivunen, E., Woods, V. L., Jr., and Ruoslahti, E. (1996) A polymeric form of fibronectin has antimetastatic effects against multiple tumor types, *Nat Med 2*, 1197-1203.
59. Clifford, S. C., Cockman, M. E., Smallwood, A. C., Mole, D. R., Woodward, E. R., Maxwell, P. H., Ratcliffe, P. J., and Maher, E. R. (2001) Contrasting effects on HIF-1alpha regulation by disease-causing pVHL mutations correlate with patterns of tumourigenesis in von Hippel-Lindau disease, *Hum Mol Genet 10*, 1029-1038.
60. Tang, N., Mack, F., Haase, V. H., Simon, M. C., and Johnson, R. S. (2006) pVHL function is essential for endothelial extracellular matrix deposition, *Mol Cell Biol 26*, 2519-2530.
61. Stickle, N. H., Chung, J., Klco, J. M., Hill, R. P., Kaelin, W. G., Jr., and Ohh, M. (2004) pVHL modification by NEDD8 is required for fibronectin matrix assembly and suppression of tumor development, *Mol Cell Biol 24*, 3251-3261.
62. Grosfeld, A., Stolze, I. P., Cockman, M. E., Pugh, C. W., Edelmann, M., Kessler, B., Bullock, A. N., Ratcliffe, P. J., and Masson, N. (2007) Interaction of hydroxylated collagen IV with the von hippel-lindau tumor suppressor, *J Biol Chem 282*, 13264-13269.
63. von Toerne, C., Schmidt, C., Adams, J., Kiss, E., Bedke, J., Porubsky, S., Gretz, N., Lindenmeyer, M. T., Cohen, C. D., Grone, H. J., and Nelson, P. J.

(2009) Wnt pathway regulation in chronic renal allograft damage, *Am J Transplant 9*, 2223-2239.
64. Esteban, M. A., Tran, M. G., Harten, S. K., Hill, P., Castellanos, M. C., Chandra, A., Raval, R., O'Brien T, S., and Maxwell, P. H. (2006) Regulation of E-cadherin expression by VHL and hypoxia-inducible factor, *Cancer Res 66*, 3567-3575.
65. Evans, A. J., Russell, R. C., Roche, O., Burry, T. N., Fish, J. E., Chow, V. W., Kim, W. Y., Saravanan, A., Maynard, M. A., Gervais, M. L., Sufan, R. I., Roberts, A. M., Wilson, L. A., Betten, M., Vandewalle, C., Berx, G., Marsden, P. A., Irwin, M. S., Teh, B. T., Jewett, M. A., and Ohh, M. (2007) VHL promotes E2 box-dependent E-cadherin transcription by HIF-mediated regulation of SIP1 and snail, *Mol Cell Biol 27*, 157-169.
66. Brembeck, F. H., Rosario, M., and Birchmeier, W. (2006) Balancing cell adhesion and Wnt signaling, the key role of beta-catenin, *Curr Opin Genet Dev 16*, 51-59.
67. Peruzzi, B., and Bottaro, D. P. (2006) Beta-catenin signaling: linking renal cell carcinoma and polycystic kidney disease, *Cell Cycle 5*, 2839-2841.
68. Cohen, H. T., Zhou, M., Welsh, A. M., Zarghamee, S., Scholz, H., Mukhopadhyay, D., Kishida, T., Zbar, B., Knebelmann, B., and Sukhatme, V. P. (1999) An important von Hippel-Lindau tumor suppressor domain mediates Sp1-binding and self-association, *Biochem Biophys Res Commun 266*, 43-50.
69. Yuen, J. S., Cockman, M. E., Sullivan, M., Protheroe, A., Turner, G. D., Roberts, I. S., Pugh, C. W., Werner, H., and Macaulay, V. M. (2007) The VHL tumor suppressor inhibits expression of the IGF1R and its loss induces IGF1R upregulation in human clear cell renal carcinoma, *Oncogene 26*, 6499-6508.
70. Wightman, B., Ha, I., and Ruvkun, G. (1993) Posttranscriptional regulation of the heterochronic gene lin-14 by lin-4 mediates temporal pattern formation in C. elegans, *Cell 75*, 855-862.
71. Lee, R. C., Feinbaum, R. L., and Ambros, V. (1993) The C. elegans heterochronic gene lin-4 encodes small RNAs with antisense complementarity to lin-14, *Cell 75*, 843-854.
72. Reinhart, B. J., Slack, F. J., Basson, M., Pasquinelli, A. E., Bettinger, J. C., Rougvie, A. E., Horvitz, H. R., and Ruvkun, G. (2000) The 21-nucleotide let-7 RNA regulates developmental timing in Caenorhabditis elegans, *Nature 403*, 901-906.
73. Hayashita, Y., Osada, H., Tatematsu, Y., Yamada, H., Yanagisawa, K., Tomida, S., Yatabe, Y., Kawahara, K., Sekido, Y., and Takahashi, T. (2005) A polycistronic microRNA cluster, miR-17-92, is overexpressed in human lung cancers and enhances cell proliferation, *Cancer Res 65*, 9628-9632.
74. Pillai, R. S., Bhattacharyya, S. N., and Filipowicz, W. (2007) Repression of protein synthesis by miRNAs: how many mechanisms?, *Trends Cell Biol 17*, 118-126.
75. Lee, Y., Kim, M., Han, J., Yeom, K. H., Lee, S., Baek, S. H., and Kim, V. N. (2004) MicroRNA genes are transcribed by RNA polymerase II, *EMBO J 23*, 4051-4060.
76. Borchert, G. M., Lanier, W., and Davidson, B. L. (2006) RNA polymerase III transcribes human microRNAs, *Nat Struct Mol Biol 13*, 1097-1101.

77. Lee, Y., Ahn, C., Han, J., Choi, H., Kim, J., Yim, J., Lee, J., Provost, P., Radmark, O., Kim, S., and Kim, V. N. (2003) The nuclear RNase III Drosha initiates microRNA processing, *Nature 425*, 415-419.
78. Han, J., Lee, Y., Yeom, K. H., Nam, J. W., Heo, I., Rhee, J. K., Sohn, S. Y., Cho, Y., Zhang, B. T., and Kim, V. N. (2006) Molecular basis for the recognition of primary microRNAs by the Drosha-DGCR8 complex, *Cell 125*, 887-901.
79. Zeng, Y., and Cullen, B. R. (2003) Sequence requirements for micro RNA processing and function in human cells, *Rna 9*, 112-123.
80. Zeng, Y., and Cullen, B. R. (2005) Efficient processing of primary microRNA hairpins by Drosha requires flanking nonstructured RNA sequences, *J Biol Chem 280*, 27595-27603.
81. Han, J., Lee, Y., Yeom, K. H., Kim, Y. K., Jin, H., and Kim, V. N. (2004) The Drosha-DGCR8 complex in primary microRNA processing, *Genes Dev 18*, 3016-3027.
82. Yi, R., Qin, Y., Macara, I. G., and Cullen, B. R. (2003) Exportin-5 mediates the nuclear export of pre-microRNAs and short hairpin RNAs, *Genes Dev 17*, 3011-3016.
83. Lund, E., Guttinger, S., Calado, A., Dahlberg, J. E., and Kutay, U. (2004) Nuclear export of microRNA precursors, *Science 303*, 95-98.
84. Bernstein, E., Caudy, A. A., Hammond, S. M., and Hannon, G. J. (2001) Role for a bidentate ribonuclease in the initiation step of RNA interference, *Nature 409*, 363-366.
85. Winter, J., Jung, S., Keller, S., Gregory, R. I., and Diederichs, S. (2009) Many roads to maturity: microRNA biogenesis pathways and their regulation, *Nat Cell Biol 11*, 228-234.
86. Doench, J. G., and Sharp, P. A. (2004) Specificity of microRNA target selection in translational repression, *Genes Dev 18*, 504-511.
87. Brennecke, J., Stark, A., Russell, R. B., and Cohen, S. M. (2005) Principles of microRNA-target recognition, *PLoS Biol 3*, e85.
88. Grimson, A., Farh, K. K., Johnston, W. K., Garrett-Engele, P., Lim, L. P., and Bartel, D. P. (2007) MicroRNA targeting specificity in mammals: determinants beyond seed pairing, *Mol Cell 27*, 91-105.
89. Kapp, L. D., and Lorsch, J. R. (2004) The molecular mechanics of eukaryotic translation, *Annu Rev Biochem 73*, 657-704.
90. Pillai, R. S., Bhattacharyya, S. N., Artus, C. G., Zoller, T., Cougot, N., Basyuk, E., Bertrand, E., and Filipowicz, W. (2005) Inhibition of translational initiation by Let-7 MicroRNA in human cells, *Science 309*, 1573-1576.
91. Petersen, C. P., Bordeleau, M. E., Pelletier, J., and Sharp, P. A. (2006) Short RNAs repress translation after initiation in mammalian cells, *Mol Cell 21*, 533-542.
92. Nottrott, S., Simard, M. J., and Richter, J. D. (2006) Human let-7a miRNA blocks protein production on actively translating polyribosomes, *Nat Struct Mol Biol 13*, 1108-1114.
93. Wakiyama, M., Takimoto, K., Ohara, O., and Yokoyama, S. (2007) Let-7 microRNA-mediated mRNA deadenylation and translational repression in a mammalian cell-free system, *Genes Dev 21*, 1857-1862.
94. Kiriakidou, M., Tan, G. S., Lamprinaki, S., De Planell-Saguer, M., Nelson, P. T., and Mourelatos, Z. (2007) An mRNA m7G cap binding-like motif within human Ago2 represses translation, *Cell 129*, 1141-1151.

95. Kinch, L. N., and Grishin, N. V. (2009) The human Ago2 MC region does not contain an eIF4E-like mRNA cap binding motif, *Biol Direct 4*, 2.
96. Filipowicz, W., Bhattacharyya, S. N., and Sonenberg, N. (2008) Mechanisms of post-transcriptional regulation by microRNAs: are the answers in sight?, *Nat Rev Genet 9*, 102-114.
97. Lim, L. P., Lau, N. C., Garrett-Engele, P., Grimson, A., Schelter, J. M., Castle, J., Bartel, D. P., Linsley, P. S., and Johnson, J. M. (2005) Microarray analysis shows that some microRNAs downregulate large numbers of target mRNAs, *Nature 433*, 769-773.
98. Bartel, D. P., and Chen, C. Z. (2004) Micromanagers of gene expression: the potentially widespread influence of metazoan microRNAs, *Nat Rev Genet 5*, 396-400.
99. Bagga, S., Bracht, J., Hunter, S., Massirer, K., Holtz, J., Eachus, R., and Pasquinelli, A. E. (2005) Regulation by let-7 and lin-4 miRNAs results in target mRNA degradation, *Cell 122*, 553-563.
100. Eulalio, A., Behm-Ansmant, I., and Izaurralde, E. (2007) P bodies: at the crossroads of post-transcriptional pathways, *Nat Rev Mol Cell Biol 8*, 9-22.
101. Liu, J., Rivas, F. V., Wohlschlegel, J., Yates, J. R., 3rd, Parker, R., and Hannon, G. J. (2005) A role for the P-body component GW182 in microRNA function, *Nat Cell Biol 7*, 1261-1266.
102. Jakymiw, A., Lian, S., Eystathioy, T., Li, S., Satoh, M., Hamel, J. C., Fritzler, M. J., and Chan, E. K. (2005) Disruption of GW bodies impairs mammalian RNA interference, *Nat Cell Biol 7*, 1267-1274.
103. Meister, G. (2007) miRNAs get an early start on translational silencing, *Cell 131*, 25-28.
104. Chu, C. Y., and Rana, T. M. (2006) Translation repression in human cells by microRNA-induced gene silencing requires RCK/p54, *PLoS Biol 4*, e210.
105. Anderson, P., and Kedersha, N. (2006) RNA granules, *J Cell Biol 172*, 803-808.
106. Vasudevan, S., Tong, Y., and Steitz, J. A. (2008) Cell-cycle control of microRNA-mediated translation regulation, *Cell Cycle 7*, 1545-1549.
107. Vasudevan, S., Tong, Y., and Steitz, J. A. (2007) Switching from repression to activation: microRNAs can up-regulate translation, *Science 318*, 1931-1934.
108. Vasudevan, S., and Steitz, J. A. (2007) AU-rich-element-mediated upregulation of translation by FXR1 and Argonaute 2, *Cell 128*, 1105-1118.
109. Alvarez-Garcia, I., and Miska, E. A. (2005) MicroRNA functions in animal development and human disease, *Development 132*, 4653-4662.
110. Grosshans, H., Johnson, T., Reinert, K. L., Gerstein, M., and Slack, F. J. (2005) The temporal patterning microRNA let-7 regulates several transcription factors at the larval to adult transition in C. elegans, *Dev Cell 8*, 321-330.
111. Giraldez, A. J., Mishima, Y., Rihel, J., Grocock, R. J., Van Dongen, S., Inoue, K., Enright, A. J., and Schier, A. F. (2006) Zebrafish MiR-430 promotes deadenylation and clearance of maternal mRNAs, *Science 312*, 75-79.
112. Wienholds, E., Kloosterman, W. P., Miska, E., Alvarez-Saavedra, E., Berezikov, E., de Bruijn, E., Horvitz, H. R., Kauppinen, S., and Plasterk, R. H. (2005) MicroRNA expression in zebrafish embryonic development, *Science 309*, 310-311.

113. Hwang, H. W., and Mendell, J. T. (2006) MicroRNAs in cell proliferation, cell death, and tumorigenesis, *Br J Cancer 94*, 776-780.
114. Lu, J., Getz, G., Miska, E. A., Alvarez-Saavedra, E., Lamb, J., Peck, D., Sweet-Cordero, A., Ebert, B. L., Mak, R. H., Ferrando, A. A., Downing, J. R., Jacks, T., Horvitz, H. R., and Golub, T. R. (2005) MicroRNA expression profiles classify human cancers, *Nature 435*, 834-838.
115. Thomson, J. M., Newman, M., Parker, J. S., Morin-Kensicki, E. M., Wright, T., and Hammond, S. M. (2006) Extensive post-transcriptional regulation of microRNAs and its implications for cancer, *Genes Dev 20*, 2202-2207.
116. Volinia, S., Calin, G. A., Liu, C. G., Ambs, S., Cimmino, A., Petrocca, F., Visone, R., Iorio, M., Roldo, C., Ferracin, M., Prueitt, R. L., Yanaihara, N., Lanza, G., Scarpa, A., Vecchione, A., Negrini, M., Harris, C. C., and Croce, C. M. (2006) A microRNA expression signature of human solid tumors defines cancer gene targets, *Proc Natl Acad Sci U S A 103*, 2257-2261.
117. Yanaihara, N., Caplen, N., Bowman, E., Seike, M., Kumamoto, K., Yi, M., Stephens, R. M., Okamoto, A., Yokota, J., Tanaka, T., Calin, G. A., Liu, C. G., Croce, C. M., and Harris, C. C. (2006) Unique microRNA molecular profiles in lung cancer diagnosis and prognosis, *Cancer Cell 9*, 189-198.
118. Takamizawa, J., Konishi, H., Yanagisawa, K., Tomida, S., Osada, H., Endoh, H., Harano, T., Yatabe, Y., Nagino, M., Nimura, Y., Mitsudomi, T., and Takahashi, T. (2004) Reduced expression of the let-7 microRNAs in human lung cancers in association with shortened postoperative survival, *Cancer Res 64*, 3753-3756.
119. He, L., Thomson, J. M., Hemann, M. T., Hernando-Monge, E., Mu, D., Goodson, S., Powers, S., Cordon-Cardo, C., Lowe, S. W., Hannon, G. J., and Hammond, S. M. (2005) A microRNA polycistron as a potential human oncogene, *Nature 435*, 828-833.
120. Biswas, S., Troy, H., Leek, R., Chung, Y. L., Li, J. L., Raval, R. R., Turley, H., Gatter, K., Pezzella, F., Griffiths, J. R., Stubbs, M., and Harris, A. L. Effects of HIF-1alpha and HIF2alpha on Growth and Metabolism of Clear-Cell Renal Cell Carcinoma 786-0 Xenografts, *J Oncol 2010*, 757908.
121. Pastorekova, S., Zavadova, Z., Kostal, M., Babusikova, O., and Zavada, J. (1992) A novel quasi-viral agent, MaTu, is a two-component system, *Virology 187*, 620-626.
122. Li, L., Xu, J., Yang, D., Tan, X., and Wang, H. Computational approaches for microRNA studies: a review, *Mamm Genome 21*, 1-12.
123. Lewis, B. P., Shih, I. H., Jones-Rhoades, M. W., Bartel, D. P., and Burge, C. B. (2003) Prediction of mammalian microRNA targets, *Cell 115*, 787-798.
124. Grun, D., Wang, Y. L., Langenberger, D., Gunsalus, K. C., and Rajewsky, N. (2005) microRNA target predictions across seven Drosophila species and comparison to mammalian targets, *PLoS Comput Biol 1*, e13.
125. Baek, D., Villen, J., Shin, C., Camargo, F. D., Gygi, S. P., and Bartel, D. P. (2008) The impact of microRNAs on protein output, *Nature 455*, 64-71.
126. Selbach, M., Schwanhausser, B., Thierfelder, N., Fang, Z., Khanin, R., and Rajewsky, N. (2008) Widespread changes in protein synthesis induced by microRNAs, *Nature 455*, 58-63.
127. Camps, C., Buffa, F. M., Colella, S., Moore, J., Sotiriou, C., Sheldon, H., Harris, A. L., Gleadle, J. M., and Ragoussis, J. (2008) hsa-miR-210 Is induced by hypoxia and is an independent prognostic factor in breast cancer, *Clin Cancer Res 14*, 1340-1348.

128. Hossain, M. A. (2008) Hypoxic-ischemic injury in neonatal brain: involvement of a novel neuronal molecule in neuronal cell death and potential target for neuroprotection, *Int J Dev Neurosci 26*, 93-101.
129. Xia, Y., and Schneyer, A. L. (2009) The biology of activin: recent advances in structure, regulation and function, *J Endocrinol 202*, 1-12.
130. Johnson, D. C., Dean, D. R., Smith, A. D., and Johnson, M. K. (2005) Structure, function, and formation of biological iron-sulfur clusters, *Annu Rev Biochem 74*, 247-281.
131. Rouault, T. A., and Tong, W. H. (2008) Iron-sulfur cluster biogenesis and human disease, *Trends Genet 24*, 398-407.
132. Rudolf, J., Makrantoni, V., Ingledew, W. J., Stark, M. J., and White, M. F. (2006) The DNA repair helicases XPD and FancJ have essential iron-sulfur domains, *Mol Cell 23*, 801-808.
133. Rouault, T. A., and Tong, W. H. (2005) Iron-sulphur cluster biogenesis and mitochondrial iron homeostasis, *Nat Rev Mol Cell Biol 6*, 345-351.
134. Bencze, K. Z., Kondapalli, K. C., Cook, J. D., McMahon, S., Millan-Pacheco, C., Pastor, N., and Stemmler, T. L. (2006) The structure and function of frataxin, *Crit Rev Biochem Mol Biol 41*, 269-291.
135. Lill, R., and Muhlenhoff, U. (2008) Maturation of iron-sulfur proteins in eukaryotes: mechanisms, connected processes, and diseases, *Annu Rev Biochem 77*, 669-700.
136. Campuzano, V., Montermini, L., Molto, M. D., Pianese, L., Cossee, M., Cavalcanti, F., Monros, E., Rodius, F., Duclos, F., Monticelli, A., Zara, F., Canizares, J., Koutnikova, H., Bidichandani, S. I., Gellera, C., Brice, A., Trouillas, P., De Michele, G., Filla, A., De Frutos, R., Palau, F., Patel, P. I., Di Donato, S., Mandel, J. L., Cocozza, S., Koenig, M., and Pandolfo, M. (1996) Friedreich's ataxia: autosomal recessive disease caused by an intronic GAA triplet repeat expansion, *Science 271*, 1423-1427.
137. Rotig, A., de Lonlay, P., Chretien, D., Foury, F., Koenig, M., Sidi, D., Munnich, A., and Rustin, P. (1997) Aconitase and mitochondrial iron-sulphur protein deficiency in Friedreich ataxia, *Nat Genet 17*, 215-217.
138. Camaschella, C., Campanella, A., De Falco, L., Boschetto, L., Merlini, R., Silvestri, L., Levi, S., and Iolascon, A. (2007) The human counterpart of zebrafish shiraz shows sideroblastic-like microcytic anemia and iron overload, *Blood 110*, 1353-1358.
139. Mochel, F., Knight, M. A., Tong, W. H., Hernandez, D., Ayyad, K., Taivassalo, T., Andersen, P. M., Singleton, A., Rouault, T. A., Fischbeck, K. H., and Haller, R. G. (2008) Splice mutation in the iron-sulfur cluster scaffold protein ISCU causes myopathy with exercise intolerance, *Am J Hum Genet 82*, 652-660.
140. Olsson, A., Lind, L., Thornell, L. E., and Holmberg, M. (2008) Myopathy with lactic acidosis is linked to chromosome 12q23.3-24.11 and caused by an intron mutation in the ISCU gene resulting in a splicing defect, *Hum Mol Genet 17*, 1666-1672.
141. Murphy, M. P. (2009) How mitochondria produce reactive oxygen species, *Biochem J 417*, 1-13.
142. Guzy, R. D., Hoyos, B., Robin, E., Chen, H., Liu, L., Mansfield, K. D., Simon, M. C., Hammerling, U., and Schumacker, P. T. (2005) Mitochondrial complex III is required for hypoxia-induced ROS production and cellular oxygen sensing, *Cell Metab 1*, 401-408.

143. Solaini, G., Baracca, A., Lenaz, G., and Sgarbi, G. Hypoxia and mitochondrial oxidative metabolism, *Biochim Biophys Acta 1797*, 1171-1177.
144. Tong, W. H., and Rouault, T. (2000) Distinct iron-sulfur cluster assembly complexes exist in the cytosol and mitochondria of human cells, *EMBO J 19*, 5692-5700.
145. Giannakakis, A., Sandaltzopoulos, R., Greshock, J., Liang, S., Huang, J., Hasegawa, K., Li, C., O'Brien-Jenkins, A., Katsaros, D., Weber, B. L., Simon, C., Coukos, G., and Zhang, L. (2008) miR-210 links hypoxia with cell cycle regulation and is deleted in human epithelial ovarian cancer, *Cancer Biol Ther 7*, 255-264.
146. Favaro, E., Ramachandran, A., McCormick, R., Gee, H., Blancher, C., Crosby, M., Devlin, C., Blick, C., Buffa, F., Li, J. L., Vojnovic, B., Pires das Neves, R., Glazer, P., Iborra, F., Ivan, M., Ragoussis, J., and Harris, A. L. MicroRNA-210 regulates mitochondrial free radical response to hypoxia and krebs cycle in cancer cells by targeting iron sulfur cluster protein ISCU, *PLoS One 5*, e10345.
147. Wouters, B. G., and Koritzinsky, M. (2008) Hypoxia signalling through mTOR and the unfolded protein response in cancer, *Nat Rev Cancer 8*, 851-864.
148. Guzy, R. D., Sharma, B., Bell, E., Chandel, N. S., and Schumacker, P. T. (2008) Loss of the SdhB, but Not the SdhA, subunit of complex II triggers reactive oxygen species-dependent hypoxia-inducible factor activation and tumorigenesis, *Mol Cell Biol 28*, 718-731.
149. Gimenez-Roqueplo, A. P., Favier, J., Rustin, P., Mourad, J. J., Plouin, P. F., Corvol, P., Rotig, A., and Jeunemaitre, X. (2001) The R22X mutation of the SDHD gene in hereditary paraganglioma abolishes the enzymatic activity of complex II in the mitochondrial respiratory chain and activates the hypoxia pathway, *Am J Hum Genet 69*, 1186-1197.
150. Pollard, P., Wortham, N., Barclay, E., Alam, A., Elia, G., Manek, S., Poulsom, R., and Tomlinson, I. (2005) Evidence of increased microvessel density and activation of the hypoxia pathway in tumours from the hereditary leiomyomatosis and renal cell cancer syndrome, *J Pathol 205*, 41-49.
151. Chan, S. Y., Zhang, Y. Y., Hemann, C., Mahoney, C. E., Zweier, J. L., and Loscalzo, J. (2009) MicroRNA-210 controls mitochondrial metabolism during hypoxia by repressing the iron-sulfur cluster assembly proteins ISCU1/2, *Cell Metab 10*, 273-284.
152. Koritzinsky, M., and Wouters, B. G. (2007) Hypoxia and regulation of messenger RNA translation, *Methods Enzymol 435*, 247-273.
153. Esquela-Kerscher, A., and Slack, F. J. (2006) Oncomirs - microRNAs with a role in cancer, *Nat Rev Cancer 6*, 259-269.
154. Calin, G. A., Ferracin, M., Cimmino, A., Di, L. G., Shimizu, M., Wojcik, S. E., Iorio, M. V., Visone, R., Sever, N. I., Fabbri, M., Iuliano, R., Palumbo, T., Pichiorri, F., Roldo, C., Garzon, R., Sevignani, C., Rassenti, L., Alder, H., Volinia, S., Liu, C. G., Kipps, T. J., Negrini, M., and Croce, C. M. (2005) A MicroRNA signature associated with prognosis and progression in chronic lymphocytic leukemia, *N.Engl.J.Med. 353*, 1793-1801.
155. Xi, Y., Nakajima, G., Gavin, E., Morris, C. G., Kudo, K., Hayashi, K., and Ju, J. (2007) Systematic analysis of microRNA expression of RNA extracted from

fresh frozen and formalin-fixed paraffin-embedded samples, *RNA 13*, 1668-1674.
156. Li, J., Smyth, P., Flavin, R., Cahill, S., Denning, K., Aherne, S., Guenther, S. M., O'Leary, J. J., and Sheils, O. (2007) Comparison of miRNA expression patterns using total RNA extracted from matched samples of formalin-fixed paraffin-embedded (FFPE) cells and snap frozen cells, *BMC Biotechnol 7*, 36.
157. Mitchell, P. S., Parkin, R. K., Kroh, E. M., Fritz, B. R., Wyman, S. K., Pogosova-Agadjanyan, E. L., Peterson, A., Noteboom, J., O'Briant, K. C., Allen, A., Lin, D. W., Urban, N., Drescher, C. W., Knudsen, B. S., Stirewalt, D. L., Gentleman, R., Vessella, R. L., Nelson, P. S., Martin, D. B., and Tewari, M. (2008) Circulating microRNAs as stable blood-based markers for cancer detection, *Proc Natl Acad Sci U S A 105*, 10513-10518.
158. Crosby, M. E., Kulshreshtha, R., Ivan, M., and Glazer, P. M. (2009) MicroRNA regulation of DNA repair gene expression in hypoxic stress, *Cancer Res 69*, 1221-1229.
159. Mattie, M. D., Benz, C. C., Bowers, J., Sensinger, K., Wong, L., Scott, G. K., Fedele, V., Ginzinger, D., Getts, R., and Haqq, C. (2006) Optimized high-throughput microRNA expression profiling provides novel biomarker assessment of clinical prostate and breast cancer biopsies, *Mol Cancer 5*, 24.
160. Zhang, L., Huang, J., Yang, N., Greshock, J., Megraw, M. S., Giannakakis, A., Liang, S., Naylor, T. L., Barchetti, A., Ward, M. R., Yao, G., Medina, A., O'Brien-Jenkins, A., Katsaros, D., Hatzigeorgiou, A., Gimotty, P. A., Weber, B. L., and Coukos, G. (2006) microRNAs exhibit high frequency genomic alterations in human cancer, *Proc Natl Acad Sci U S A 103*, 9136-9141.
161. Lawrie, C. H., Gal, S., Dunlop, H. M., Pushkaran, B., Liggins, A. P., Pulford, K., Banham, A. H., Pezzella, F., Boultwood, J., Wainscoat, J. S., Hatton, C. S., and Harris, A. L. (2008) Detection of elevated levels of tumour-associated microRNAs in serum of patients with diffuse large B-cell lymphoma, *Br J Haematol 141*, 672-675.
162. Young, A. C., Craven, R. A., Cohen, D., Taylor, C., Booth, C., Harnden, P., Cairns, D. A., Astuti, D., Gregory, W., Maher, E. R., Knowles, M. A., Joyce, A., Selby, P. J., and Banks, R. E. (2009) Analysis of VHL Gene Alterations and their Relationship to Clinical Parameters in Sporadic Conventional Renal Cell Carcinoma, *Clin Cancer Res 15*, 7582-7592.
163. Gossage, L., and Eisen, T. Alterations in VHL as potential biomarkers in renal-cell carcinoma, *Nat Rev Clin Oncol 7*, 277-288.
164. Ivanov, S., Liao, S. Y., Ivanova, A., Danilkovitch-Miagkova, A., Tarasova, N., Weirich, G., Merrill, M. J., Proescholdt, M. A., Oldfield, E. H., Lee, J., Zavada, J., Waheed, A., Sly, W., Lerman, M. I., and Stanbridge, E. J. (2001) Expression of hypoxia-inducible cell-surface transmembrane carbonic anhydrases in human cancer, *Am J Pathol 158*, 905-919.
165. Rhodes, D. R., Kalyana-Sundaram, S., Mahavisno, V., Varambally, R., Yu, J., Briggs, B. B., Barrette, T. R., Anstet, M. J., Kincead-Beal, C., Kulkarni, P., Varambally, S., Ghosh, D., and Chinnaiyan, A. M. (2007) Oncomine 3.0: genes, pathways, and networks in a collection of 18,000 cancer gene expression profiles, *Neoplasia 9*, 166-180.
166. Bui, M. H., Seligson, D., Han, K. R., Pantuck, A. J., Dorey, F. J., Huang, Y., Horvath, S., Leibovich, B. C., Chopra, S., Liao, S. Y., Stanbridge, E., Lerman, M. I., Palotie, A., Figlin, R. A., and Belldegrun, A. S. (2003) Carbonic

anhydrase IX is an independent predictor of survival in advanced renal clear cell carcinoma: implications for prognosis and therapy, *Clin Cancer Res 9*, 802-811.

167. Bui, M. H., Visapaa, H., Seligson, D., Kim, H., Han, K. R., Huang, Y., Horvath, S., Stanbridge, E. J., Palotie, A., Figlin, R. A., and Belldegrun, A. S. (2004) Prognostic value of carbonic anhydrase IX and KI67 as predictors of survival for renal clear cell carcinoma, *J Urol 171*, 2461-2466.
168. Greither, T., Grochola, L., Udelnow, A., Lautenschlager, C., Wurl, P., and Taubert, H. (2009) Elevated expression of microRNAs 155, 203, 210 and 222 in pancreatic tumours associates with poorer survival, *Int J Cancer*.
169. Gee, H. E., Camps, C., Buffa, F. M., Patiar, S., Winter, S. C., Betts, G., Homer, J., Corbridge, R., Cox, G., West, C. M., Ragoussis, J., and Harris, A. L. hsa-mir-210 is a marker of tumor hypoxia and a prognostic factor in head and neck cancer, *Cancer 116*, 2148-2158.
170. Maranchie, J. K., Vasselli, J. R., Riss, J., Bonifacino, J. S., Linehan, W. M., and Klausner, R. D. (2002) The contribution of VHL substrate binding and HIF1-alpha to the phenotype of VHL loss in renal cell carcinoma, *Cancer Cell 1*, 247-255.
171. Covello, K. L., Simon, M. C., and Keith, B. (2005) Targeted replacement of hypoxia-inducible factor-1alpha by a hypoxia-inducible factor-2alpha knock-in allele promotes tumor growth, *Cancer Res 65*, 2277-2286.
172. Kondo, K., Klco, J., Nakamura, E., Lechpammer, M., and Kaelin, W. G., Jr. (2002) Inhibition of HIF is necessary for tumor suppression by the von Hippel-Lindau protein, *Cancer Cell 1*, 237-246.
173. Gordan, J. D., Bertout, J. A., Hu, C. J., Diehl, J. A., and Simon, M. C. (2007) HIF-2alpha promotes hypoxic cell proliferation by enhancing c-myc transcriptional activity, *Cancer Cell 11*, 335-347.
174. Patard, J. J., Fergelot, P., Karakiewicz, P. I., Klatte, T., Trinh, Q. D., Rioux-Leclercq, N., Said, J. W., Belldegrun, A. S., and Pantuck, A. J. (2008) Low CAIX expression and absence of VHL gene mutation are associated with tumor aggressiveness and poor survival of clear cell renal cell carcinoma, *Int J Cancer 123*, 395-400.
175. Suzuki, H., Ueda, T., Komiya, A., Okano, T., Isaka, S., Shimazaki, J., and Ito, H. (1997) Mutational state of von Hippel-Lindau and adenomatous polyposis coli genes in renal tumors, *Oncology 54*, 252-257.
176. Choyke, P. L., Glenn, G. M., Walther, M. M., Zbar, B., Weiss, G. H., Alexander, R. B., Hayes, W. S., Long, J. P., Thakore, K. N., and Linehan, W. M. (1992) The natural history of renal lesions in von Hippel-Lindau disease: a serial CT study in 28 patients, *AJR Am J Roentgenol 159*, 1229-1234.
177. Neumann, H. P., Bender, B. U., Berger, D. P., Laubenberger, J., Schultze-Seemann, W., Wetterauer, U., Ferstl, F. J., Herbst, E. W., Schwarzkopf, G., Hes, F. J., Lips, C. J., Lamiell, J. M., Masek, O., Riegler, P., Mueller, B., Glavac, D., and Brauch, H. (1998) Prevalence, morphology and biology of renal cell carcinoma in von Hippel-Lindau disease compared to sporadic renal cell carcinoma, *J Urol 160*, 1248-1254.
178. Nickerson, M. L., Jaeger, E., Shi, Y., Durocher, J. A., Mahurkar, S., Zaridze, D., Matveev, V., Janout, V., Kollarova, H., Bencko, V., Navratilova, M., Szeszenia-Dabrowska, N., Mates, D., Mukeria, A., Holcatova, I., Schmidt, L. S., Toro, J. R., Karami, S., Hung, R., Gerard, G. F., Linehan, W. M., Merino, M., Zbar, B., Boffetta, P., Brennan, P., Rothman, N., Chow, W. H.,

Waldman, F. M., and Moore, L. E. (2008) Improved identification of von Hippel-Lindau gene alterations in clear cell renal tumors, *Clin Cancer Res 14*, 4726-4734.

179. Wang, K., Zhang, S., Marzolf, B., Troisch, P., Brightman, A., Hu, Z., Hood, L. E., and Galas, D. J. (2009) Circulating microRNAs, potential biomarkers for drug-induced liver injury, *Proc Natl Acad Sci U S A*.